FINAL REPORT

PRODUCTION OF ELEMENTAL SULFUR FROM SPENT SORBENT AND CO_2

Grantee:

The Department of Civil and Environmental Engineering
University of Cincinnati
Cincinnati, Ohio 45221

Project Number CDO/D-90/2-04
Period of Performance: April 1, 1992 - October 31, 1994
Expiration Date: October 31, 1994

Project Manager:
Tim C. Keener, Ph.D
Telephone: 513/556-2518

This Project Was Funded in Part by The Ohio Coal Development Office

Department of Development, State of Ohio

October 31, 1994

Contributing Project Investigators:

Soon-Jai Khang

Deborah Soriano

Lingqing Zhao

DISCLAIMER

DISCLAIMER

Portions of this document may be illegible in electronic image products. Images are produced from the best available original document.

TABLE OF CONTENTS

LIST OF FIGURES

LIST OF TABLES

EXECUTIVE SUMMARY

This proof of concept project studied the feasibility of producing elemental sulfur from a spent solid sorbent and carbon dioxide (CO_2) gas. The objectives were to research 1) producing H_2S gas from an aqueous solution produced from spent sorbent solid consisting of primarily CaS, and 2) research the potential of producing elemental sulfur at temperatures below 600°C by means of a novel reaction between H_2S with CO_2. The spent sorbent derives from a novel coal desulfurization process currently under development by the Ohio Coal Development Office (OCDO) and the U.S. DOE that provides for up to 80% desulfurization of the coal before combustion. The spent sorbent consists mainly of calcium sulfide with minor quantities of unreacted lime (CaO) and limestone ($CaCO_3$). In this study, CaS is dissolved in a solution of acetic acid forming a solution containing primarily hydrogen sulfide, calcium ions and acetate ions. The hydrogen sulfide is subsequently stripped from the solution by carbon dioxide (available from stack gas) and the H_2S-CO_2 mixture is catalytically converted to form elemental sulfur. This conversion is aided by the reaction between CO_2 and H_2 (water-gas shift reaction) to produce water vapor and carbon monoxide. This is according to the following reactions;

$$2\ H_2S \rightleftharpoons 2\ H_2 + S_2$$

$$CO_2 + H_2 \rightleftharpoons CO + H_2O$$

Advantages of this scheme are 1) Production of low cost elemental sulfur at reasonable temperatures rather than sulfuric acid which is preferable from a storage and resource recovery standpoint, 2) Regeneration of the calcium based sorbent for reuse in the coal

desulfurization unit, and 3) Consumption of CO_2, a gas which has been found to affect global warming.

This project provides the basic design data for large scale applications of the technology.

The project was carried out in three phases.

Phase #1: Basic Studies

This phase of work focused on the fundamental nature of the project. The following three separate tasks were performed; *Task 1: CaS Solubility Studies*, *Task 2: H_2S Stripping Studies* and *Task 3: $CaCO_3$ Regeneration Studies.*

This phase focused on the solubility of CaS in solutions containing various acid buffers. Acetic acid was found to be a suitable acid for further studies and the solubility of CaS in acetic acid solutions with different concentrations at different temperatures were measured.

Stripping experiments were conducted in a batch stripping column. A mathematical model was derived to calculate mass transfer coefficients at different stripper operating conditions. These conditions include acid concentration, liquid temperature and CO_2 flow rate. The theoretically calculated mass transfer coefficient was compared with the experimental measured data, and the agreement was found to be reasonable.

The liquid solution from the stripper outlet was investigated in terms of regenerating $CaCO_3$. Particle formation and growth as a function of residence time and pH were measured by a Coulter Counter Particle Size Analyzer and observed under a microscope. An analysis of the amount of Calcium recovered was performed and found to be highly dependant on pH.

Phase #2: Elemental Sulfur Production Studies

A thorough review of the literature concerning the production of elemental sulfur was performed. An experimental investigation was performed at different operating conditions for the reaction:

$$2\ H_2S \rightleftharpoons 2\ H_2 + S_2$$

$$CO_2 + H_2 \rightleftharpoons CO + H_2O$$

The following three separate tasks were performed; *Task 1: Thermodynamic Analysis, Task 2: Catalyst Preparation* and *Task 3: Testing of Packed Bed Catalytic Reactor.*

The theoretical equilibrium conversions were calculated using the Stanjan program. The analysis was done to determine the effect of three different parameters: temperature, pressure, and H_2S:CO_2 ratio. This analysis indicated that conversion wold be increased by the addition of CO_2 due to the water-gas shift reaction.

A suitable method of preparation for Co-Mo sulfide catalyst was obtained using a thermogravimetric analyzer. This technique was found to be suitable for a commercial catalyst which was used in subsequent tests.

Experiments were conducted in the tube reactor packed with the sulfided Co-Mo catalyst at temperatures from 465 - 575°C. The lower temperature was chosen due to kinetic limitations of the H_2S decomposition reaction, and the upper temperature chosen so as not to sinter the catalyst. The results showed that higher sulfur conversions can be obtained by using an equimolar mixture of H_2S and CO_2 instead of H_2S alone. The results also show that sulfur conversion increases with increasing temperature. The Arrhenius equation for the specific rate constant for the temperature range studied was found to have the following form:

$$\kappa = 3776e^{\frac{-118}{RT}}$$

where the activation energy has the units of kJ/mol.

Phase #3: Integrated System Design

The results from the previous two phases were integrated into a small scale production unit suitable for long term studies. Both the stripping and the reacting process were conducted continuously. The results showed that the conversion of H_2S to elemental sulfur decreases with increasing gas flowrate but the equilibrium was never reached for the gas flowrate range tested.

INTRODUCTION

The passage of acid rain legislation will undoubtedly result in the implementation of SO_2 control technologies on an increasing number of power plants, both existing and new, in the United States. These control technologies will be primarily of the "throw-away" type which result in large volumes of waste product which must be disposed. Conceivably, these systems may be further regulated to minimize these large volumes of waste materials, and pollution prevention measures may be instituted whereby utilities are encouraged to recover their sulfur in a more useable form.

Utilization of high sulfur feed stocks in sour natural gas, residual crude oils and high sulfur coal in power plants is increasing today. The sulfur removed from crude oil is usually in the form of gaseous hydrogen sulfide (West, 1984). In most situations, H_2S must be removed from crude oil before combustion or utilization to comply with environmental regulations, as well as to prevent contamination on the catalysts used in downstream processes. The processes for removing hydrogen sulfide from gas streams are generally both capital and energy intensive. It is possible to partially offset the cost of sulfur removal by recovering sulfur in a marketable form if catalytic reaction based processes are used. Additionally, the production of sulfur in the United States is at its lowest point since 1965 while consumption is anticipated to be 19 million metric tons per year by the year 2000.

This study has as its general objective the production of elemental sulfur from the reaction of H_2S and CO_2 gases across a catalyst. Specifically, the hydrogen sulfide can be derived from the spent sorbent of a unique coal desulfurization process described below. The

spent sorbent stems from a novel coal desulfurization process (mild pyrolysis) which has been shown[1] to provide up to 80% desulfurization of high sulfur coals before combustion. The spent sorbent consists mainly of calcium sulfide (CaS) with minor quantities of unreacted lime and limestone.

The feasibility of desulfurization by a mild pyrolysis of coal has been well established in the literature. During coal pyrolysis, sulphur release is mainly in the form of H_2S and COS. In a reducing environment, sulphur release is primarily in the form of H_2S. For example, FeS_2 is reduced to produce H_2S.

$$FeS_2 + H_2 \text{ ----> } FeS + H_2S$$

Studies have shown that the pyrolysis of Illinois No. 6 coal releases up to 87% of total sulphur between 500 - 600°C which includes both inorganic and organic sulfur compounds. However, tests have shown that at low pyrolysis temperatures (i.e.< 600 ^{0}C) the predominant form of the sulfur which is evolved is the organic fraction[2].

When CaO particles are added into the system, the pyrolyized H_2S with trace quantities of COS react according to the following:

$$CaO + H_2S \text{ ----> } CaS + H_2O$$

$$CaO + COS \text{ ----> } CaS + CO_2$$

These desulfurization reactions can be carried out at moderate temperatures below about 600°C. Typical reaction data is shown[3] in Figure 1 for the conversion of CaO with H_2S. At 764°C with 0.83% of H_2S, it is possible to reach above 90% conversion in 30 minutes (Refer to the open circles in Figure 1). Since this reaction is known to follow first order kinetics with respect to the H_2S concentration, the reaction time will be much shorter with an

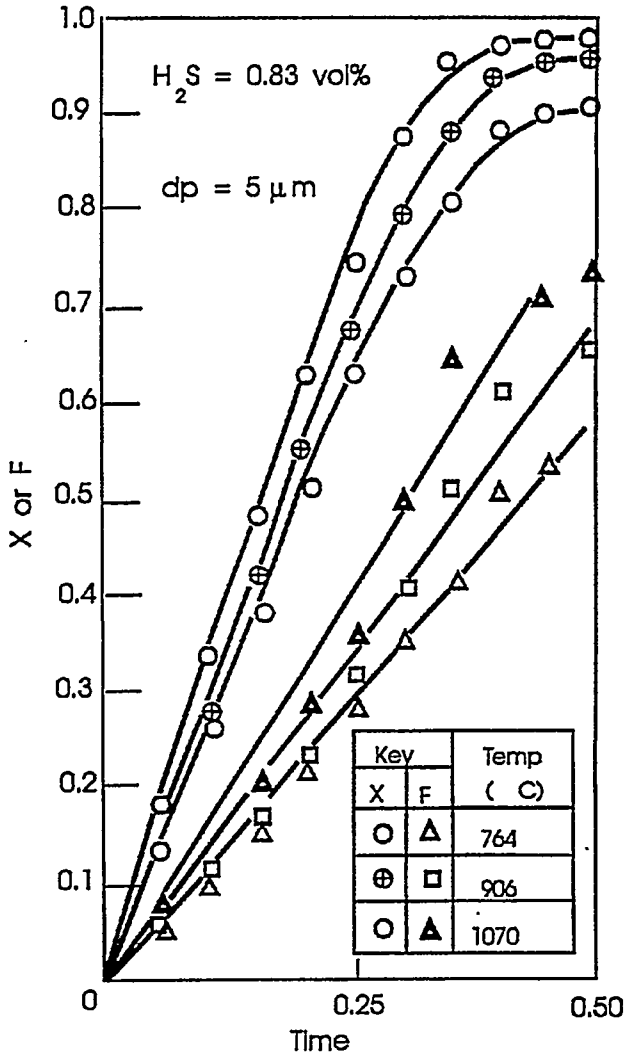

Figure 1-1. Conversion vs. Time for the Reaction of CaO with H_2S [Reference: Hasatani, M. et al., 1983.]

increased concentration of H_2S.

These two basic steps have been combined into a novel coal feeder device which concomitantly releases hydrogen sulfide and hydrocarbon gases from the coal by low temperature pyrolysis, and scrubs the H_2S by means of a bed of calcium oxide/calcium carbonate. The devolatilized gases are scrubbed of H_2S so that they may be directed to the combustion zone for oxidation and heat release. Thus, the sulfur is captured in a most convenient form and is not introduced into the boiler.

The novel coal feeder has been built and evaluated with a high volatile bituminous coal (Ohio #8). The sulfur containing gases evolved during pyrolysis have been shown[1] to be predominately H_2S and to have been derived from the decomposition of the organic sulfur fraction of the parent coal. Additional tests have also shown that the H_2S is essentially completely reacted with a bed of CaO at temperatures of 650°C to form CaS. Therefore, this mild pyrolysis desulfurization process produces a calcium sulfide solid which can become the feed material for a sulfur recovery system. The recovery of sulfur in its elemental form has many advantages including storage volume savings and its market value.

Therefore, a research project was initiated to investigate the feasibility of recovering elemental sulfur from the CaS solid. A unique process was envisioned after consideration of the physical and chemical constraints of the materials involved which consisted of a method of releasing the sulfur (in the form of H_2S) from the calcium at low temperatures in an acidic solution, stripping of the H_2S gas by means of CO_2 (generally considered a waste gas) and subsequent formation of elemental sulfur by reaction of these gases across a catalyst. This project was further subdivided into the following objectives:

1) Investigate the formation of hydrogen sulfide from CaS in an acidic solution,
2) Investigate the release of hydrogen sulfide from a stripping column using CO_2 gas,
3) Investigate the production and precipitation of $CaCO_3$ from the stripping operation,
4) Investigate the production of elemental sulfur from the reaction of CO_2 and H_2S across a suitable catalyst.

The project was carried out in three phases.

Phase #1: Basic Studies

This phase of work focused on the fundamental nature of the project. The following three separate tasks were performed.

Task 1: CaS Solubility Studies

This study focused on the solubility of CaS in solutions containing the various acid buffers. Solubility of CaS in acetic acid solutions with different concentrations at different temperatures were measured.

Task 2: H_2S Stripping Studies

Stripping experiments were conducted in a batch stripping column. A mathematical model was derived to calculate mass transfer coefficients at different stripper operating conditions. These conditions include acid concentration, liquid temperature and CO_2 flow rate. The theoretically calculated mass transfer coefficient was compared with the experimental measured data, and the agreement was found to be reasonable.

Task 3: $CaCO_3$ Regeneration Studies

The liquid solution from the stripper outlet was investigated in terms of regenerating

$CaCO_3$. Particle formation and growth as a function of residence time and pH were measured by means of a particle size analyzer and observed under a microscope. An analysis of the amount of calcium recovered versus pH was performed.

Phase #2: Elemental Sulfur Production Studies

A review of the literature concerning the production of elemental sulfur was performed. An experimental investigation was performed at different operating conditions for the set of reactions:

$$2\ H_2S \rightleftharpoons 2\ H_2 + S_2$$

$$CO_2 + H_2 \rightleftharpoons CO + H_2O$$

The following three separate tasks were performed.

Task 1: Thermodynamic Analysis

Theoretical equilibrium conversions were calculated. The analysis was done to determine the effect of three different parameters: temperature, pressure, and H_2S:CO_2 ratio.

Task 2: Catalyst Preparation

A suitable method of preparation for a Co-Mo sulfide catalyst was obtained using a thermogravimetric analyzer.

Task 3: Testing of Packed Bed Catalytic Reactor

Experiments were conducted in a tube reactor packed with a Co-Mo catalyst. The

results show that sulfur conversions are a function of the mixture ratio of H_2S to CO_2 and the reactor temperature.

Phase #3: Integrated System Design

The results from the previous two phases were integrated into a small scale production unit suitable for longer term studies. Both the stripping and the reacting process were conducted continuously. The results showed that the conversion of H_2S to elemental sulfur decreases with increasing gas flowrate.

PHASE 1: BASIC STUDIES

The objectives of this phase were to 1) determine the optimal conditions for the solubility of the sorbent i.e. calcium sulfide (CaS) in a buffered solution, 2) investigate hydrogen sulfide (H_2S) gas stripping from the resulting solution with carbon dioxide (CO_2) gas, and 3) study calcium carbonate ($CaCO_3$) regeneration from the solution.

Task #1 - CaS Solubility Studies

For these studies, the following parameters were varied: type of acid, acid concentration, and temperature. The two acids that were tested were formic acid (HCOOH) and acetic acid (CH_3COOH). The acid concentration for both acids was varied from 0.01N to 2.0N. This variation in concentration resulted in a range of initial pH values from 1.4 to 3.4. Solubility measurements were made at temperatures of 20, 40, and 60°C.

Reagent grade calcium sulfide (CaS) powder (stock # C-1046, lot # 95008-A-1, CERAC Chemical Co., Milwaukee, WI, <325 mesh) with a purity of 99% was used which was stored in a desiccator in order to prevent it from absorbing moisture. As only one size of this grade was available, and as this size represents a powder of maximum surface area, no CaS size dependent studies were conducted. The formic acid solution (prepared from the concentrated formic acid, assay min. as HCOOH=88.0%) and the acetic acid solution (prepared from concentrated acetic acid, assay min. as CH_3COOH=99.7%) were both prepared by diluting the acid with CO_2-free deionized water. The following chemical reactions take

place when the CaS is dissolved in the acid solutions:

$$CaS(s) + 2CH_3COOH(l) \rightleftharpoons Ca^{+2} + 2CH_3COOH^- + H_2S(l) \quad \text{Eq. 1}$$

$$CaS(s) + 2HCOOH(l) \rightleftharpoons Ca^{+2} + 2HCOO^- + H_2S(l) \quad \text{Eq. 2}$$

Some dissociation of the H_2S will occur as follows:

$$H_2S(l) \rightleftharpoons H^+ + HS^- \quad \text{Eq. 3}$$

The solubility of CaS was determined from the difference in weight between the excess CaS solid added into 50.0 ml of the solution and the total suspended solid left in the mixture after 30 minutes of mixing. The mixing period of 30 minutes was chosen based on the experiments done at 10 and 60 minutes of mixing time which showed no difference in the solubility value. The total suspended solids were measured using the standard method (2540D) from the "Standard Methods for the Examination of Water and Wastewater" by APHA-AWWA-WPCF, 17th Edition, 1989. The results for solubility as a function of acid concentration for formic acid and acetic acid at 20°C are shown in Table 1-1 and Table 1-2 respectively.

From Tables 1-1 and 1-2, one can see that the solubility of CaS increases with increasing concentration while the pH of the saturated solution decreases for both acid solutions. The solubility of CaS in the solution of HCOOH at 20°C is slightly less than that of CH_3COOH as shown in Figures 1-2 and 1-3. The pH of the saturated acid solutions as a function of acid concentration are shown in Figure 1-3.

Table 1-1. Solubility of 99% Pure CaS in the Formic Acid (HCOOH) Solution

HCOOH solution characteristics			Solubility (g/100 ml)	Saturated solution characteristics	
Concentration (% by vol)	pH	Temperature (°C)		pH	Temperature (°C)
0.04	2.9	25.3	0.080	11.0	27.2
0.38	2.4	25.0	0.353	8.0	25.7
0.75	2.3	17.7	0.597	5.2	17.9
1.13	2.1	22.2	0.795	4.6	22.8
1.89	1.9	21.7	1.311	4.4	21.4
3.77	1.7	21.7	1.565	3.4	21.5
5.66	1.6	20.6	1.747	3.1	21.0
11.32	1.4	20.5	2.082	2.7	21.0

Table 1-2. Solubility of 99% Pure CaS in the Acetic Acid (CH_3COOH) Solution

CH_3COOH solution characteristics			Solubility (g/100 ml)	Saturated solution characteristics	
Concentration (% by vol)	pH	Temperature (°C)		pH	Temperature (°C)
0.06	3.4	24.5	0.071	11.3	24.4
0.57	2.9	21.7	0.620	11.3	21.2
1.14	2.8	21.4	1.217	11.1	21.0
1.72	2.6	24.2	1.548	9.6	24.3
2.29	2.6	20.9	1.688	8.2	20.7
3.43	2.5	21.0	1.700	5.8	20.8
5.72	2.3	20.1	1.991	4.7	19.3
11.45	2.2	20.5	2.229	4.2	21.4

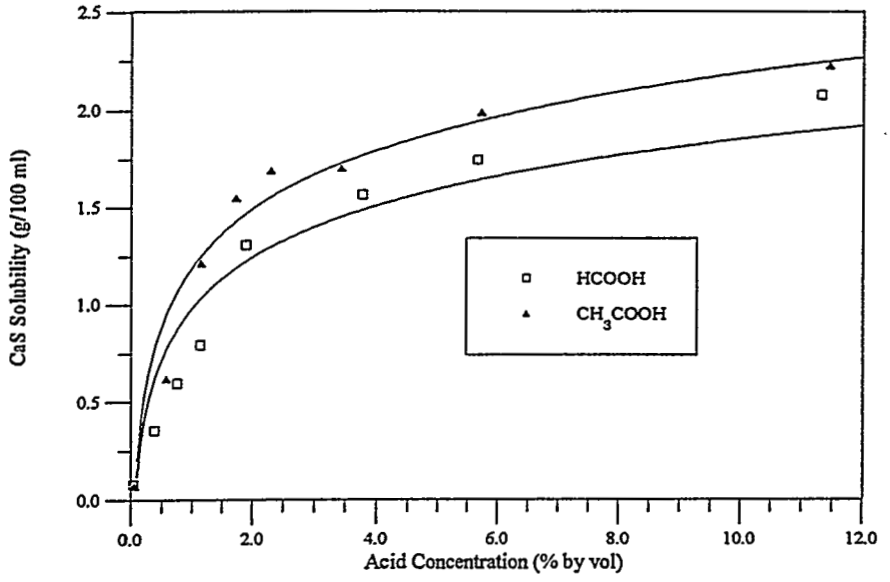

Figure 1-2. Solubility of CaS in HCOOH and CH_3COOH Solutions vs. Acid Concentration (@ room temperature)

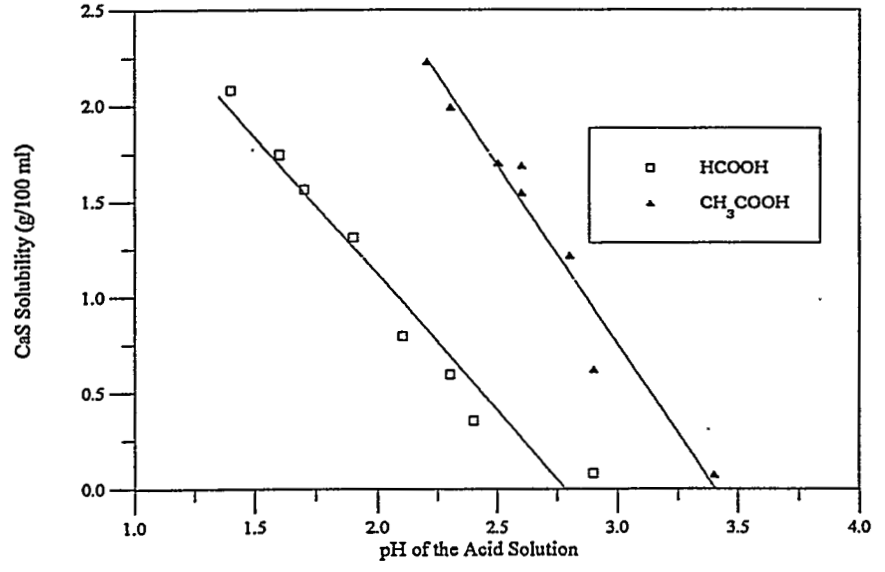

Figure 1-3. Solubility of CaS in HCOOH and CH_3COOH Solutions vs. pH

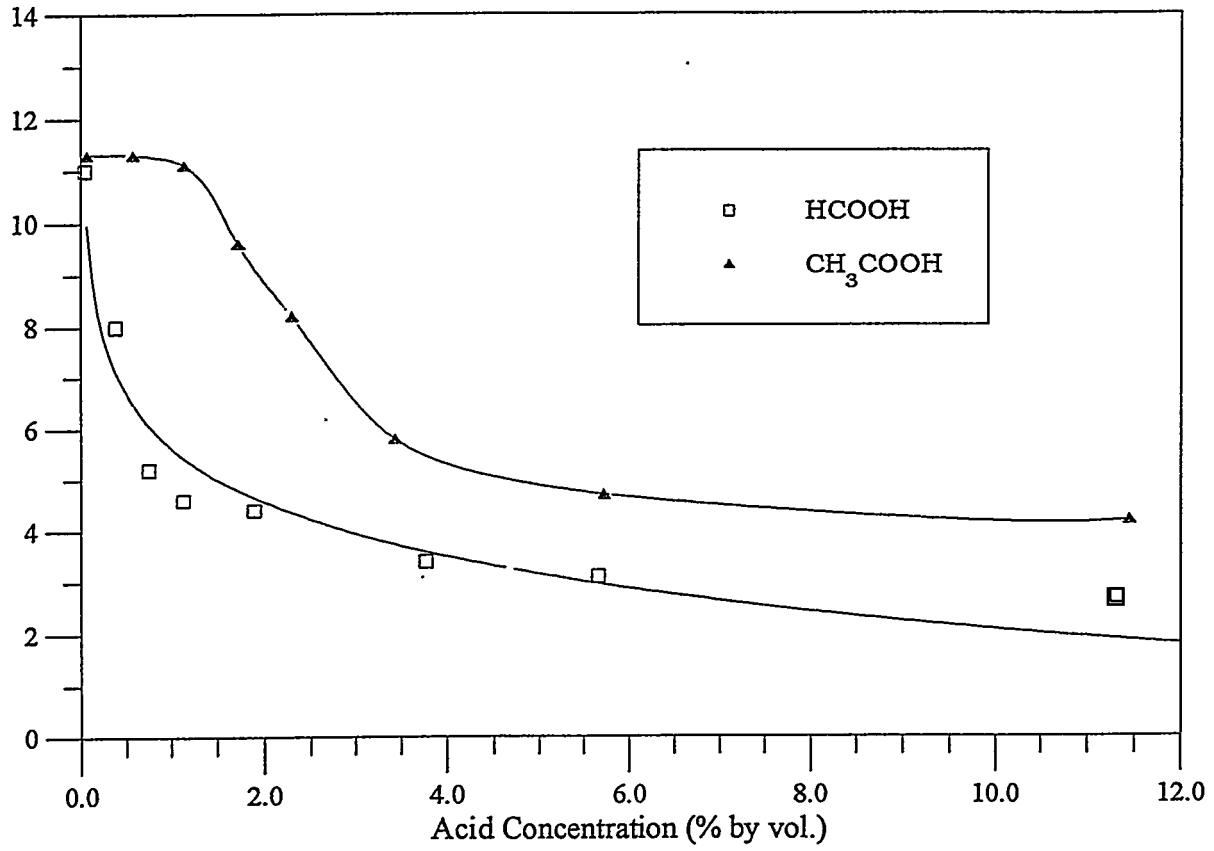

Figure 1-4. pH of HCOOH and CH_3COOH Solutions Saturated with CaS

CH_3COOH solution was chosen to be used as the solution for the stripping studies since it has a slightly higher solubility of CaS than the HCOOH solution at 20°C. Solubility of CaS only in CH_3COOH solution at higher temperature was studied. The results for solubility as a function of CH_3COOH concentration at different temperatures are shown in Table 1-3 and Figure 1-4. One can see that the solubility of CaS increases with both increasing acid concentration and increasing solution temperature. The pH of the CaS saturated solution as a function of acid concentration are shown in Figure 1-5. The pH decreases with increasing acid concentration.

Table 1-3. Solubility of 99% Pure CaS in Acetic Acid (CH_3COOH) Solution

acid concentration		solubility of CaS (g/100ml)			pH of solution		
N	% vol	20°C	40°C	60°C	20°C	40°C	60°C
0.05	0.29	-	0.3220	0.3374	11.3	11.52	11.19
0.1	0.57	0.3092	0.6042	0.5684	11.3	11.52	11.28
0.2	1.14	1.1078	1.0530	1.1494	11.2	11.22	11.19
0.3	1.72	1.6664	1.5490	1.6428	8.30	9.28	10.06
0.4	2.29	1.7676	2.1104	2.1026	7.70	8.66	9.34
0.5	2.86	1.7750	2.0526	2.2686	7.12	8.54	8.68
0.7	4.01	1.9834	2.4036	3.3092	5.95	7.87	8.02
1.0	5.72	1.9148	3.3678	3.8714	4.78	7.01	8.35
1.5	8.59	2.5120	3.9364	4.9390	4.65	5.41	7.99
2.0	11.45	2.7572	6.2002	6.7280	4.29	4.42	7.82

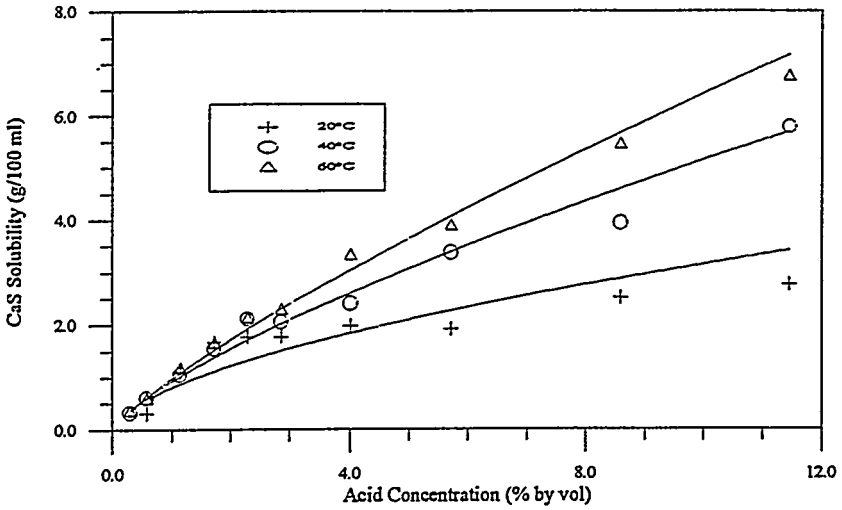

Figure 1-5. Solubility of CaS in CH3COOH Solutions vs. Acid Concentration at Different Temperatures

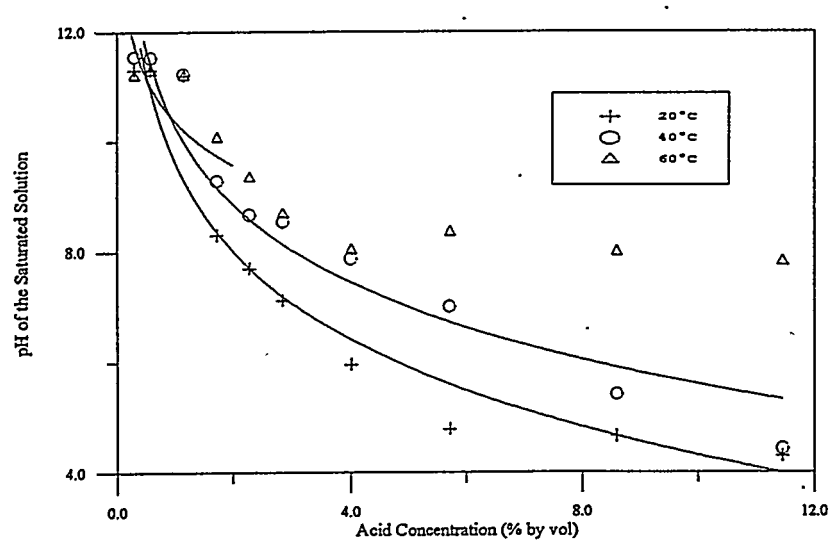

Figure 1-6. pH of the Saturated Solution vs. the Acid Concentration

Task #2 - H_2S Stripping Studies

The parameters that were varied for these studies were: acid concentration, CO_2 flow rate, and temperature. The test matrix shown in Table 1-4 shows how these parameters were varied to give the different experimental conditions.

Experimental Apparatus

A schematic diagram of the experimental apparatus is shown in Figure 1-7. The stripping experiments were conducted in a batch stripping column made of glass. The flow of CO_2 from a compressed gas cylinder tank was bubbled through the stripping column from the bottom through a glass frit to strip out the H_2S in the solution. The concentration of H_2S in the exit gas stream was measured by an H_2S analyzer (Western Research H_2S Analyzer model 721A). Due to the high outlet H_2S concentration, nitrogen (N_2) was used to dilute a slipstream from the stripping column in order to measure the H_2S concentration within the range of the H_2S analyzer. The H_2S analyzer was calibrated within this range using two H_2S concentrations, 1.98% and 0.10% by volume. A hole was made on the side of the stripping column where an electrode, connected to a pH meter (Fisher Accument Model 950), was inserted. Heating tape was used to heat the stripping column for the high temperature experiments and the temperature of the solution was measured by a K-type thermocouple. The concentration of H_2S, the pH value and the temperature of the solution were recorded throughout the experiment by a data acquisition system.

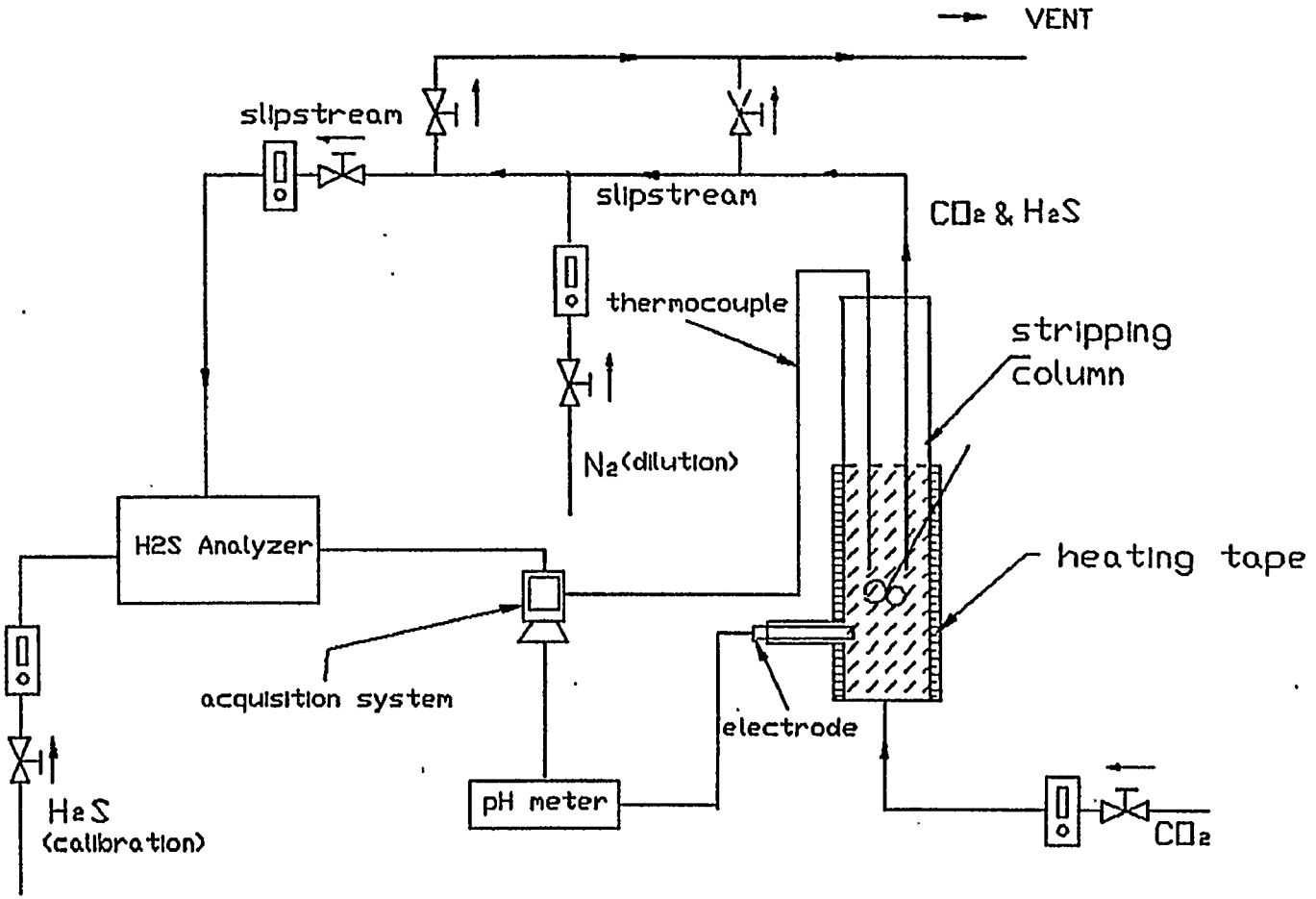

Figure 1-7. Experimental Apparatus for Stripping Experiments

Table 1-4. Stripping Experimental Matrix

variables: acid concentration (0.1, 0.2, 0.3 N)

CO_2 flowrate (1, 2, 3 lpm)

temperature (20, 40, 60 °C)

Acid Concentration	CO_2 flowrate	Temperature		
		20°C	40°C	60°C
0.1 N	1 lpm	1	10	19
	2 lpm	2	11	20
	3 lpm	3	12	21
0.2 N	1 lpm	4	13	22
	2 lpm	5	14	23
	3 lpm	6	15	24
0.3 N	1 lpm	7	16	25
	2 lpm	8	17	26
	3 lpm	9	18	27

Experimental Procedure

First, a known amount of solid CaS was added to the stripping column containing 300ml of acetic acid with a given concentration at a given temperature. Since the amount of CaS added to the acetic acid solution was much less than the amount required to reach the saturation limit (normally, only 30% of saturation limit was used), it was assumed that all the CaS dissolved and reacted with the acetic acid. According to equation 1, the solution primarily contained calcium ions (Ca^{+2}), acetate ions (CH_3COO^-) and dissolved H_2S. Once the CaS was completely dissolved, the flow of CO_2 was started. The pH was measured throughout the experiment in order to calculate the mass transfer coefficient. In order to check the mass balance of sulfur of the system, a LECO total sulfur analyzer was used to measure the amount of total sulfur in the remaining solution after stripping.

The theoretical mass transfer coefficient for the stripping experiments were calculated using a mathematical model. These values were then used to calculate theoretical values for the H_2S exit concentrations and these calculated concentrations were compared with the actual measured data from the H_2S analyzer. The derivation of the mathematical model is outlined below.

Mathematic Model for the Mass Transfer Coefficient

The two film theory was employed to derive a mathematical model to calculate the mass transfer coefficients. The model was based on the following assumptions:

- These is no chemical reaction between H_2S and CO_2 within the temperature range of the stripping experiments.
- The difference of concentration is the only driving force for mass transfer.
- Pseudo-steady-state conditions existed in the liquid with respect to H_2S concentration changes in a single bubble (i.e. the concentration of H_2S in the liquid was a constant over the time it took one bubble to rise from the bottom to the top of the cylinder)
- The Henry's constant of H_2S in water was used as the Henry's constant of H_2S in the acetic acid solution due to the lack of more specific data.

The derivation of the mass transfer coefficient is as follows:

$$-r_A = -\frac{1}{S_T}\frac{dN_A}{dt} = k_{Ag}(P_{Ai} - P_A) = k_{Al}(C_A - C_{Ai}) = k_{Al}(\frac{H_A C_A - P_{Ai}}{H_A})$$

where, r_A--the rate of mass transfer;

S_T-- the total surface area for mass transfer ;

N_A-- the amount of H_2S in the liquid;

k_{Ag}-- mass transfer coefficient in gas phase;

k_{Al}-- mass transfer coefficient in liquid phase;

P_A-- partial pressure of H_2S in the gas;

P_{Ai}-- partial pressure of H_2S at the gas/liquid interface;

C_A-- the concentration of H_2S in the liquid;

C_{Ai}-- the concentration of H_2S at the interface;

H_A-- Henry's constant;

$$C_{Ai} = \frac{P_{Ai}}{H_A}$$

$$-r_A = -\frac{1}{S_T}\frac{dN_A}{dt} = \frac{H_A C_A - P_A}{\frac{1}{k_{Ag}} + \frac{H_A}{k_{Al}}} = K_{AG}(H_A C_A - P_A)$$

where, K_{AG}-- overall mass transfer coefficient

$$-\frac{dC_A}{dt} = -\frac{1}{V_l}\frac{dN_A}{dt} = -\frac{S_T}{V_l}\frac{1}{S_T}\frac{dN_A}{dt} = a_i K_{AG}(H_A C_A - P_A)$$

Eq. 4

where, V_l-- the volume of liquid in the cylinder;

a_i-- the surface area per unit volume;

In Eq. 4, the partial pressure of H_2S, P_A, at any given time is a function of the residence time of the bubble. Therefore, the average partial pressure along the cylinder--P_{averg} was used to substitute for P_A. Thus, a mass balance on H_2S was written for one bubble rising in the cylinder. It was assumed that pseudo-steady-state conditions existed (i.e. the concentration of H_2S in the liquid, C_A, was a constant over the time it took for one bubble to rise from the bottom to the top of the cylinder).

Mass balance on one bubble is:

$$V_b \frac{P_A}{RT}\Big|_x - \left[V_b \frac{P_A}{RT}\Big|_{x+\Delta x} + \frac{\Delta x}{L} S_b K_{AG}(H_A C_A - P_A)\right] = 0$$

thus,

$$V_b \frac{dP_A}{RTdx} = \frac{S_b}{L} K_{AG}(H_A C_A - P_A)$$

$$\frac{dP}{dx} = \frac{S_b}{V_b L} RTK_{AG}(H_A C_A - P_A)$$

where, S_b-- the surface area of one bubble;

V_b-- the volume of one bubble;

L-- the height of liquid in the cylinder;

Multiply and divide the right hand side of the equation by n V_l and let $nS_b/V_l=a_i$,

$$\frac{dP}{dx/L} = V_l a_i \frac{RT}{nV_b} K_{AG}(H_A C_A - P_A)$$

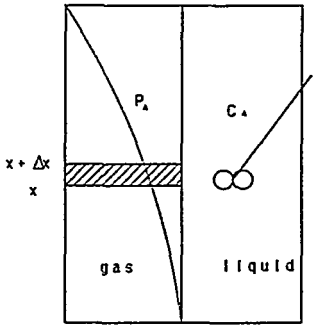

let Z=x/L (normalization)

$$\frac{dP}{dZ} = V_l \frac{RT}{nV_b} K_{AG} a_i (H_A C_A - P_A)$$

@ Z=0, P=0

$$\int_0^{P_i} \frac{dP}{H_A C_A - P_A} = \int_0^z V_l \frac{RT}{nV_b} K_{AG} a_i dZ$$

$$\ln \frac{H_A C_A - P_i}{H_A C_A} = V_l \frac{RT}{V} K_{AG} a_i Z$$

let

$$C_1 = V_l \frac{RT}{nV_b} K_{AG} a_i$$

thus,

$$P_i = H_A C_A (1 - e^{-C_1 Z})$$

$$P_{averg} = \int_0^1 H_A C_A dZ - \int_0^1 H_A C_A e^{-C_1 Z} dZ = H_A C_A + \left(H_A C_A \frac{1}{C_1} e^{-C_1 Z}\right)\Big|_0^1 = H_A C_A + H_A C_A \frac{e^{-C_1}}{C_1} - H_A C_A \frac{1}{C_1} = H_A C_A \left(1 - \frac{1}{C_1} + \frac{e^{-C_1}}{C_1}\right)$$

let $P_{averg} = P_A$ and substitute into Eq. 4

$$-\frac{dC_A}{dt} = K_{AG} a_i \left(\frac{1}{C_1} - \frac{e^{-C_1}}{C_1}\right) H_A C_A = K_{AG} a_i H_A C_A C_2$$

where,

$$C_2 = \frac{1}{C_1} - \frac{e^{-C_1}}{C_1}$$

@ t=0, $C_A = C_i$

@ t=t, $C_A = C_A$

$$\int_{C_i}^{C_A} \frac{dC_A}{C_A} = \int_0^t K_{AG} a_i H_A C_2 dt$$

$$\ln \frac{C_i}{C_A} = a_i K_{AG} H_A C_2 t$$

$$\ln C_A = \ln C_i - K_{AG} a_i H_A C_2 t \qquad \text{Eq. 5}$$

Thus, if the concentration of H_2S in the liquid at a given time is known, the value of K_{AG} can be obtained from Eq. 5.

Calculation of H_2S Concentration

The mass balance of sulfur of the system is:

$$[H_2S] + [HS^-] + [S^{2-}] = [S_{rest}] \qquad \text{Eq. 6}$$

for sulfur, there are two reactions:

$$H_2S \rightleftharpoons HS^- + H^+ \qquad (K_1)$$

$$HS^- \rightleftharpoons S^{2-} + H^+ \qquad (K_2)$$

$$K_1 = \frac{[HS^-][H^+]}{[H_2S]}$$

$$[HS^-] = \frac{K_1[H_2S]}{[H^+]}$$

$$K_2 = \frac{[S^{2-}][H^+]}{[HS^-]}$$

$$[S^{2-}] = \frac{K_2[HS^-]}{[H^+]} = \frac{K_1K_2[H_2S]}{[H^+]^2}$$

substituting $[HS^-]$ and $[S^{2-}]$ into Eq. 6,

$$[H_2S] + \frac{K_1[H_2S]}{[H^+]} + \frac{K_1k_2[H_2S]}{[H^+]^2} = [S_{rest}]$$

Thus,

$$C_A = [H_2S] = \frac{[S_{rest}]}{1 + \frac{K_1}{[H^+]} + \frac{K_1K_2}{[H^+]^2}}$$

Eq. 7

Knowing the amount of sulfur added to the cylinder in the form of CaS and the mass of sulfur stripped out in the form of H_2S, the amount of sulfur remaining in the solution, S_{rest}, can be calculated. From Eq. 7, C_A can be calculated. By combining Eq. 7 and Eq. 5, the theoretical overall mass transfer coefficient, K_{AG}, can be calculated.

It is important to note that when calculating the mass of sulfur stripped out in the form of H_2S, which is the integration of the concentration of H_2S just stripped out from the solution

at different time, some non-negligible factors must be considered. The concentration of H_2S measured by the H_2S analyzer is not the same with and should be converted to that just comes out from the solution. To do so, both the space above the solution in the stripping column and retention time for H_2S to travel from the stripping column to the H_2S analyzer were taken into account. The space above the solution in the stripping column, which is 200 ml (compare to 300 ml solution), is treated as a CSTR in the model. The retention time for H_2S to travel from the stripping column to the H_2S analyzer is 60, 24 and 18 seconds when the CO_2 flowrate is 1, 2 and 3 lpm respectively. The correction of the concentrations is shown below:

P-- the H_2S concentration just above the solution;

P_1-- the H_2S concentration comes out from the stripping column;

P_2-- the H_2S concentration measured by H_2S analyzer;

F-- the CO_2 flowrate;

V-- the volume of space above the solution in the stripping column.

The space above the solution in the stripping column is treated as a CSTR. The relationship of P and P_1 is (mass balance):

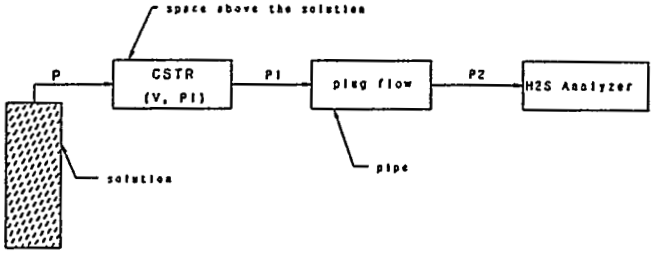

$$P\,F = P_1\,F + \frac{d(P_1 V)}{dt}$$

then,

$$P = P_1 + \frac{\Delta P_1}{\Delta t}\frac{V}{F}$$

The magnitude of P_1 is equal to P_2. The difference between them is the retention time of the H_2S in the tubing.

Work Performed/Results Obtained

In all, 27 stripping experiments were performed. The mass balance on sulfur of the system for all the experiments was closed. It has been found that the mass of sulfur in the remaining solution after the stripping is negligible compared to the total amount of sulfur added, indicating that almost all the H_2S can be stripped out by CO_2 in the stripping column. The maximum concentration of H_2S output from the stripping column varied from 16% to 53.5% depending on the amount of CaS dissolved in the acid. The data analysis of these experiments was performed in order to calculate the mass transfer coefficient for the stripping experiments using the mathematic model outlined previously. These values were used to calculate theoretical values for the H_2S exit concentrations. For example, Figure 1-8 shows the calculated concentrations compared with the actual measured data from the H_2S analyzer for stripping experiment #16 to #18. The H_2S concentrations shown are the ones that have been diluted by N_2 with 19 times flow rate in order to measure them within the range of the H_2S

analyzer. The theoretical concentrations have also been corrected by taking into account the retention time of the H_2S in the tubing and sampling system. One can see that the calculated concentration profile is parallel to the actual measured concentration profile, which indicates that the mathematic model is accurate enough to predict the output from the stripping experiment. The calculated concentrations compared with the actual measured data from the H_2S analyzer for all 27 stripping experiments can be found in Appendix A.

The calculated mass transfer coefficients are shown in Table 1-5. Figures 1-8 to 1-10 show the relationship between the mass transfer coefficient and the temperature of the solution while Figures 1-11 to 1-13 show the relationship between the mass transfer coefficient and the CO_2 flow rate. One can see from these figures that the mass transfer coefficient increases with increasing CO_2 flow rate, however it decreases with increasing temperature of the solution. From Table 1-5 one can conclude that there is no obvious trend for the effect of acid concentration on the mass transfer coefficient.

Table 1-5. Mass Transfer Coefficients of the Stripping Experiments (10^{-3} mol H_2S/L-atm-sec)

Acid Concentration	CO_2 flow rate (lpm)	Temperature 20°C	40°C	60°C
0.1	1	1.40	1.55	1.21
	2	2.04	2.53	1.66
	3	2.73	3.29	1.78
0.2	1	1.59	1.07	0.95
	2	3.06	2.38	1.58
	3	4.68	4.10	3.44
0.3	1	1.33	1.10	0.66
	2	3.45	2.87	2.27
	3	4.09	3.06	3.50

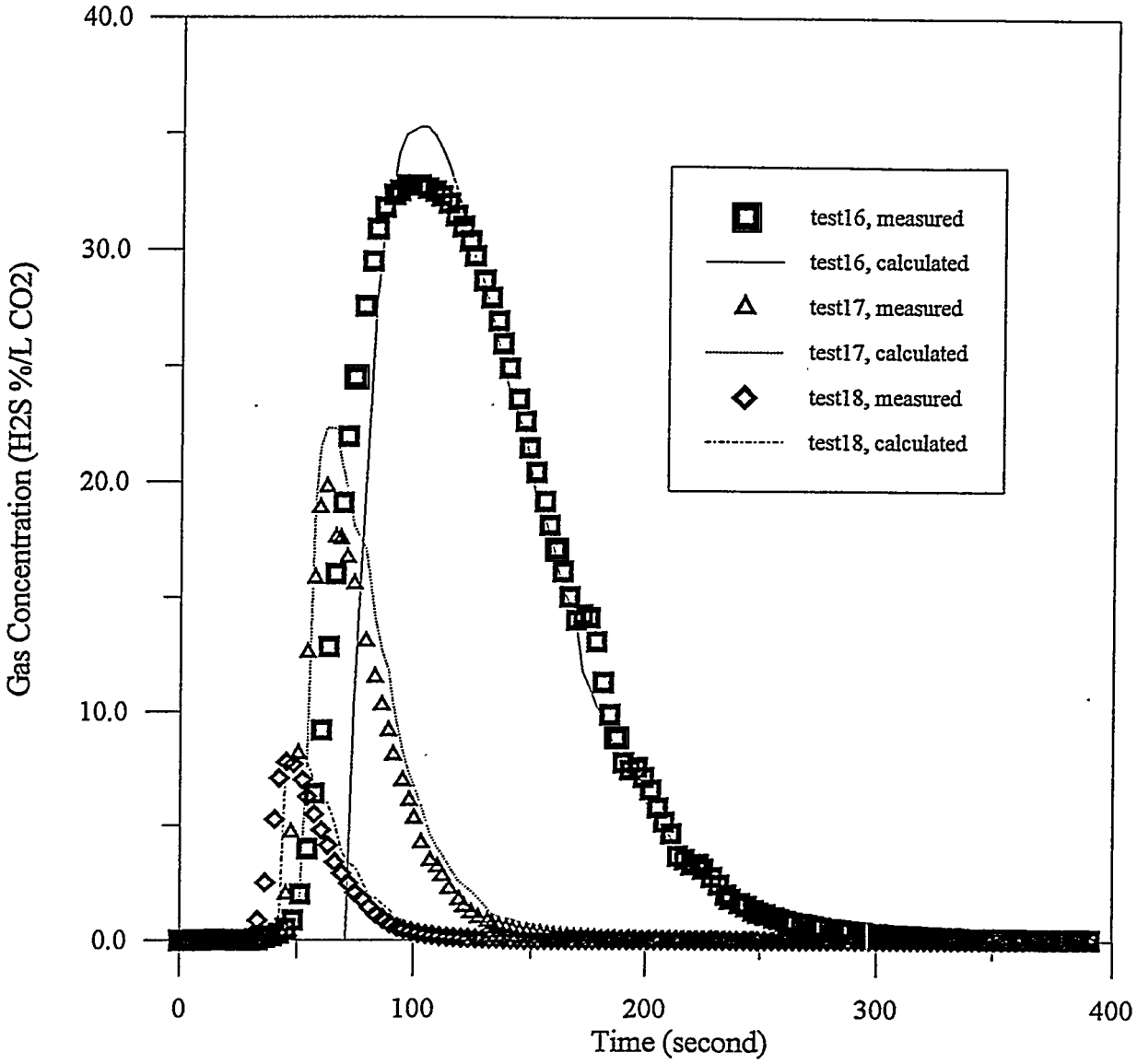

Figure 1-8. Measured vs. Calculated H_2S Concentration (test no. 16 to no. 18)

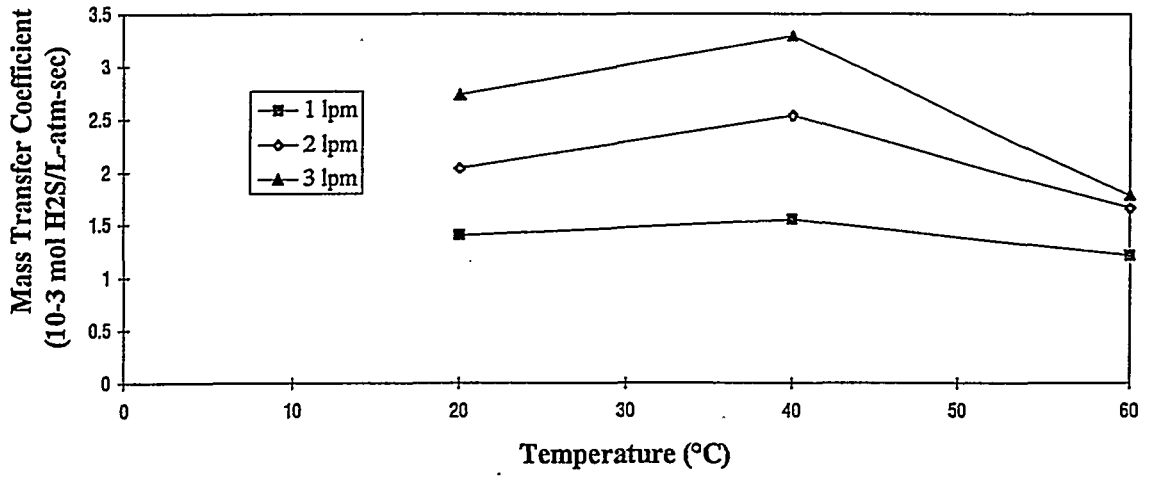

Figure 1-9. Mass Transfer Coefficient vs. Temperature (acid concentration = 0.1N)

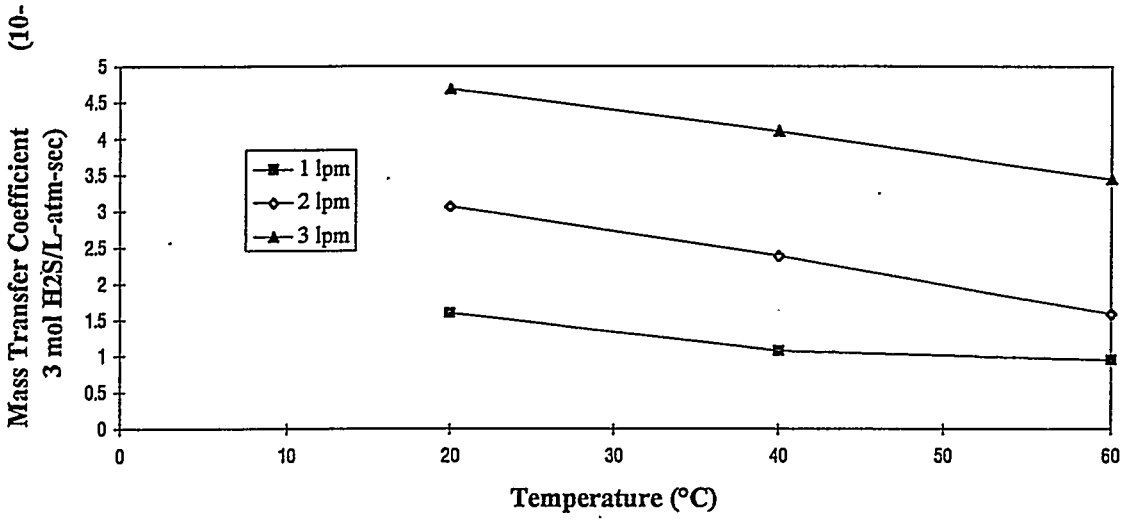

Figure 1-10. Mass Transfer Coefficient vs. Temperature (acid concentration = 0.2N)

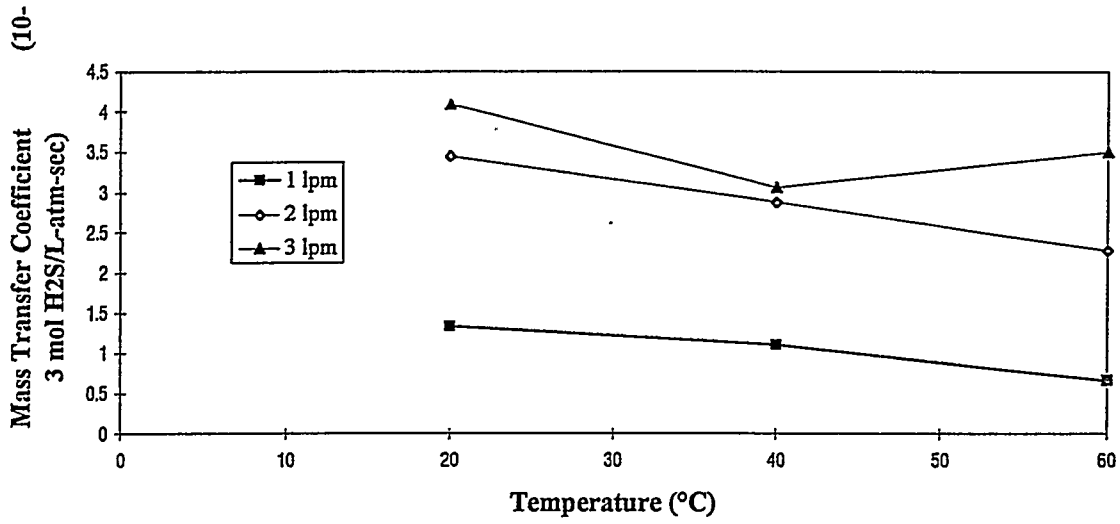

Figure 1-11. Mass Transfer Coefficient vs. Temperature (acid concentration = 0.3N)

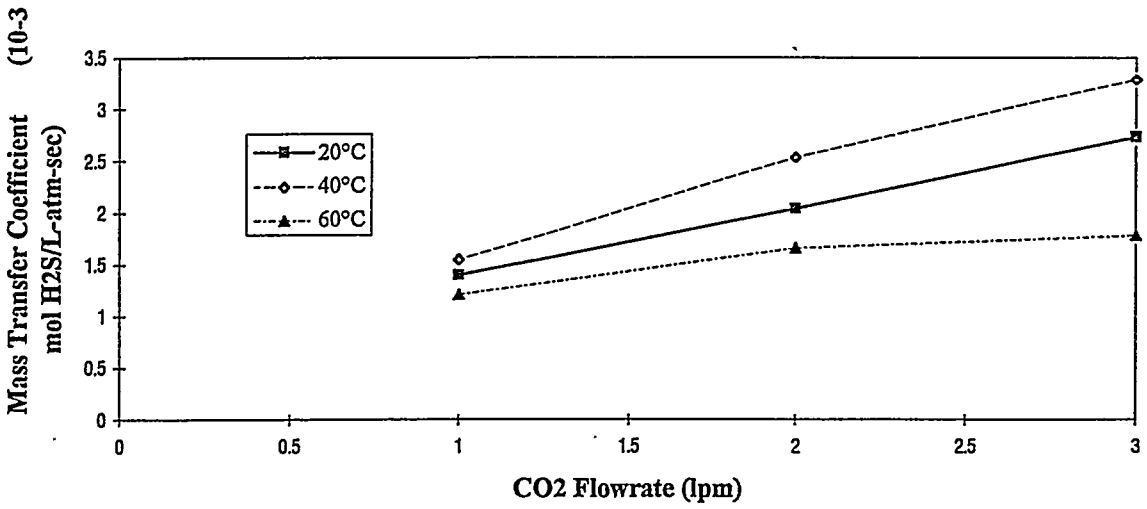

Figure 1-12. Mass Transfer Coefficient vs. CO_2 Flow Rate (acid concentration = 0.1N)

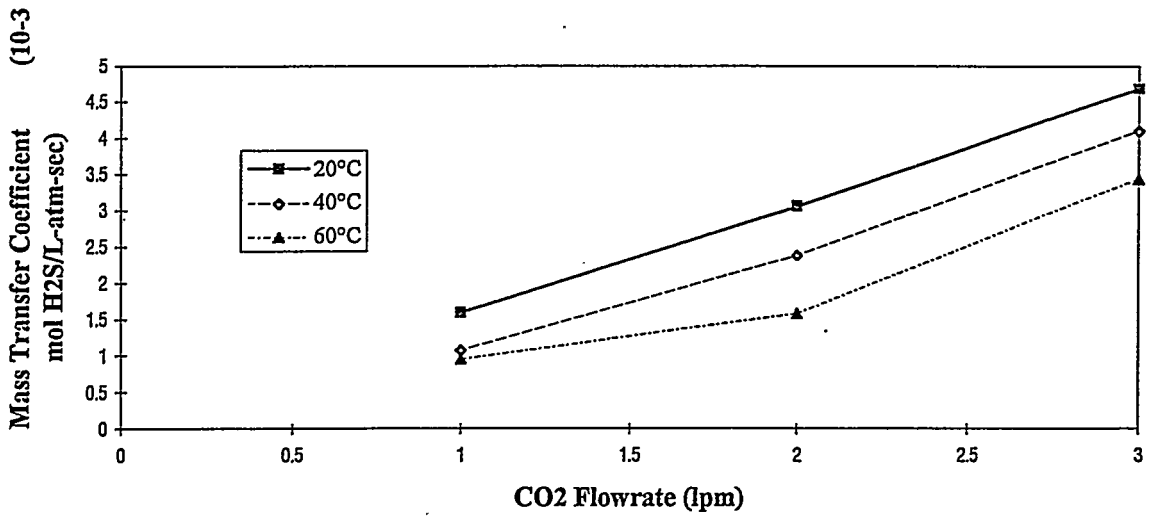

Figure 1-13. Mass Transfer Coefficient vs. CO_2 Flow Rate (acid concentration = 0.2N)

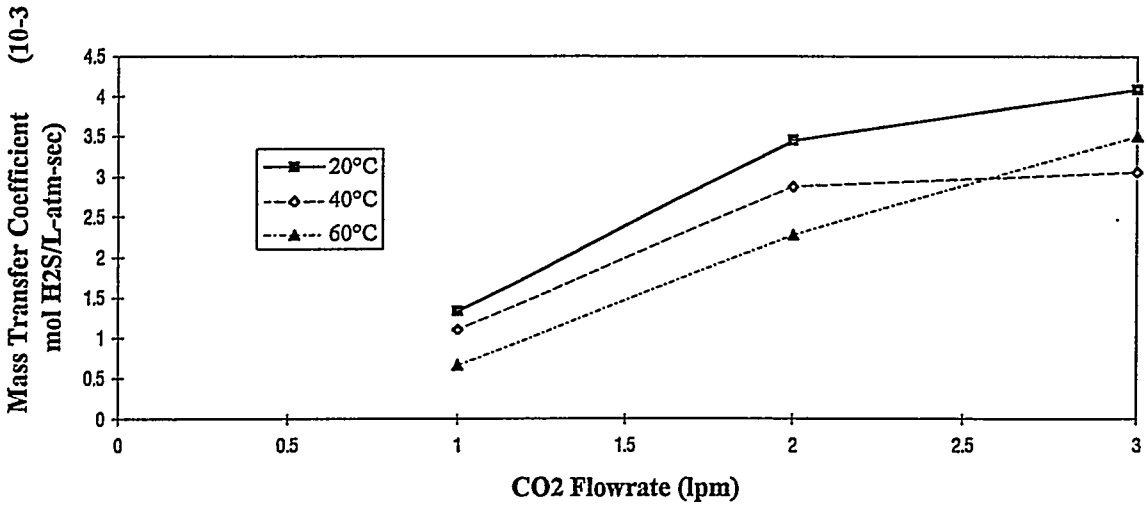

Figure 1-14. Mass Transfer Coefficient vs. CO_2 Flow Rate (acid concentration = 0.3N)

In order to study the effect of initial H_2S concentration on the mass transfer coefficient, a set of stripping experiments were performed at room temperature. The temperature of the solution, the acetic acid concentration and the CO_2 flowrate were held constant throughout these experiments. The acetic acid concentration and the CO_2 flow rate were 0.1 N and 1 lpm respectively. The initial H_2S concentrations in the solution were varied by dissolving different amounts (i.e. 10, 20, 50, 70 and 90 percent of the saturation of CaS at room temperature) of CaS in the stripping column. The initial H_2S concentrations were calculated knowing the pH and assuming that the CaS added had all dissolved before CO_2 was bubbled into the stripping column. It was assumed that the remaining sulfur in the solution after stripping is negligible since this was shown to be the case in all previous experiments. Therefore, the mass balances on sulfur for these experiments were also closed. The results are shown in Table 1-6. They showed that the initial H_2S concentration in the solution does not affect the mass transfer coefficient if everything else is held constant. However, the maximum peak of the H_2S concentration of the exit stream increases with increasing initial H_2S concentration in the solution (see Figure 1-15).

Table 1-6. Effect of Initial H_2S Concentration on the Mass Transfer Coefficient

CaS saturation (%)	10	20	50	70	90
amount of CaS added (g)	0.1881	0.3762	0.9328	1.3130	1.6783
initial pH	3.73	4.12	4.47	5.17	6.23
initial H_2S conc. in the solution (mol/L)	0.0087	0.017	0.043	0.060	0.066
maximum peak of H_2S conc. in exit stream (%)	5.70	10.07	22.61	29.45	31.16
finial pH	3.73	4.11	4.47	5.11	5.71
amount of H_2S stripped out (g)	0.086	0.173	0.476	0.689	0.937
amount of S stripped out (%)	96.86	103.64	108.16	111.13	118.17
mass transfer coefficient (10^{-3} mol/atm-L-sec)	1.86	1.93	1.86	1.62	1.41

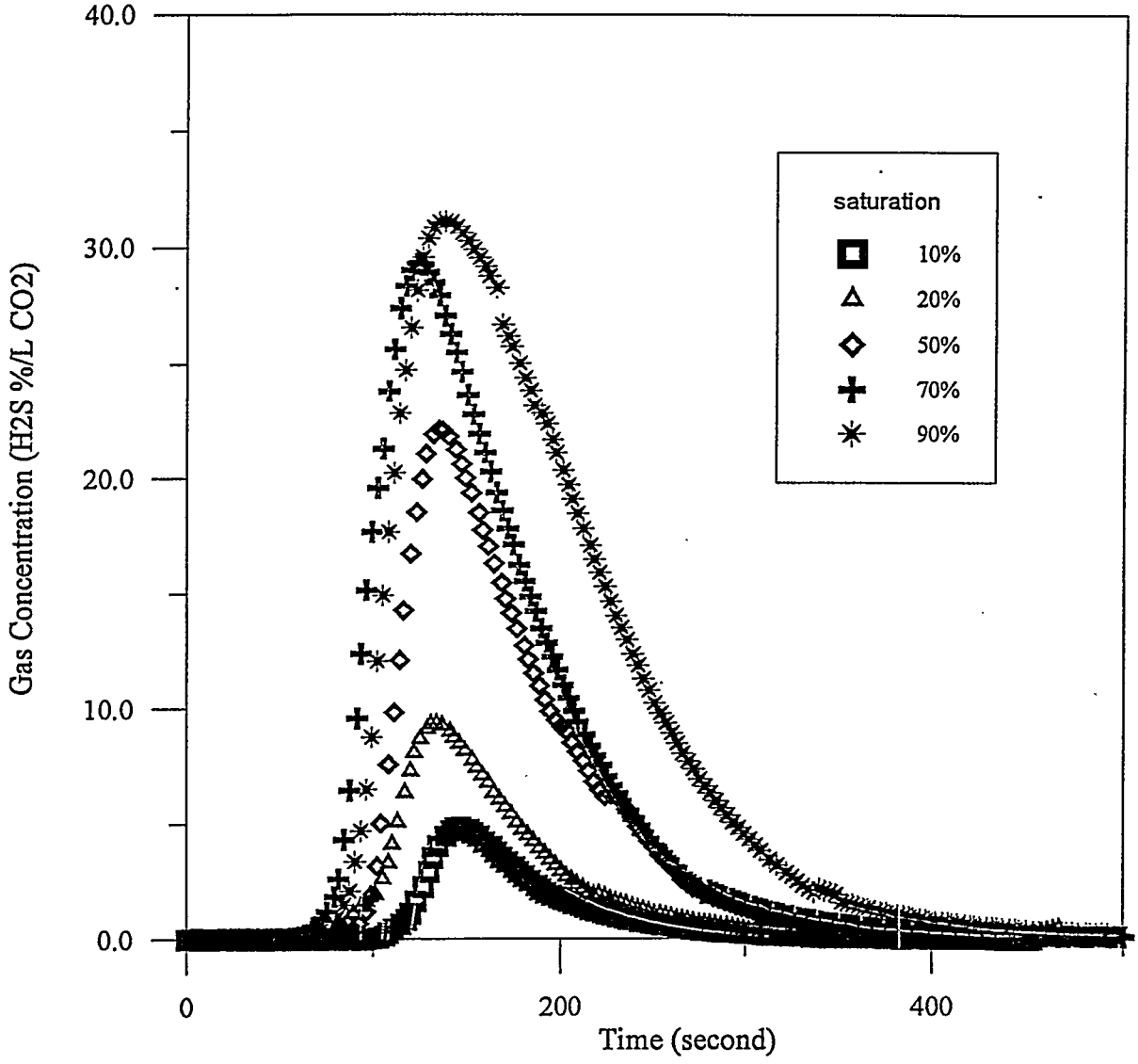

Figure 1-15. H_2S Concentration vs. Initial Saturation Limit

Accuracy and Precision of the Data

The mass balance on sulfur has been checked by comparing the amount of sulfur (as CaS) added into the cylinder and the sum of the amount of sulfur (as H_2S) being stripped and the total sulfur remaining in the liquid upon completion of each experiment. The results are shown in Appendix B. The maximum error of these experiments with respect to the sulfur balance has been calculated as 38%. The following factors most likely contributed to this error:

- The sulfur added into the cylinder was in the form of CaS. CaS powder of 325 mesh with a purity of 99% was used which was kept in a desiccator in order to prevent it from absorbing moisture. Purity of CaS and moisture content might cause error.
- The instrument error of the Analytical Balance to measure the weight of CaS;
- The amount of sulfur (as H_2S) being stripped was obtained by integrating the H_2S concentration recorded by the data acquisition system with experimental time. The accuracy of the data acquisition system might cause some error although it was calibrated.
- The concentration of H_2S record was measured by an H_2S analyzer with an accuracy of ± 1% fullscale reading (5% by volume). The H_2S analyzer was calibrated by H_2S calibration gas with concentrations of 0, 0.1% and 1.98%.
- Several experiments were performed to measure the amount of sulfur remaining in the liquid upon the completion of stripping by a total sulfur analyzer. The results of these experiments showed that the amount of sulfur remaining in the liquid was negligible comparing to the amount of sulfur added into the cylinder and these results were expanded to all 27 experiments.
- The experimental error caused by the investigator.
- An identical bubble size was used in all 27 experiments without taking into account the effect of the temperature of the solution or the concentration of acetic acid. The calculation of bubble size is listed in **Appendix B**.

- The amount of sulfur remaining in the liquid upon the completion of the stripping experiments was considered negligible.
- The Henry's constant of H_2S in water was used as the Henry's constant of H_2S in the acetic acid solution due to the lack of more specific data.

Task #3 - $CaCO_3$ Regeneration Studies

The parameters that were varied for these studies were pH, type of base and time. The pH was varied by adding different amounts of the base. The types of base that were tested were NaOH and $Ca(OH)_2$. The time was varied after the addition of the base. The growth of the particles were analyzed quantitatively by using a Coulter Counter particle size analyzer and qualitatively by using a microscope.

The precipitation of $CaCO_3$ from the solution saturated with CO_2 occurs according to the following overall reaction:

$$Ca^{+2} + 2CH_3COO^- + CO_2(l) + H_2O(l) \rightleftharpoons CaCO_3(s) + 2CH_3COOH(l) \qquad \text{Eq.8}$$

Calcium acetate ($Ca(C_2H_2O_2)_2$) is not expected to precipitate out of the solution because of its high solubility compared to that of $CaCO_3$. The solubilities of $Ca(C_2H_2O_2)_2$ and $CaCO_3$ in cold water are 37.4 gm/100cc and 0.00153 gm/100cc respectively.

The regeneration of $CaCO_3$ was studied qualitatively using the liquid solution from the stripping experiment #19 from the experimental matrix in Table 1-4. The solution was divided equally into four 50ml quantities. The pH value of these solutions were adjusted by adding 0.2 N NaOH solution in order to precipitate the $CaCO_3$ out of the solution. The initial pH value of the solution was 5.30. The pH value were adjusted to the values listed in Table 1-7. The precipitate from each solution was filtered and weighed. It was found by looking at the crystals under the microscope that the size of the $CaCO_3$ crystals increased with increasing

pH (see Figures 1-16 and 1-17). The crystals were also observed after time periods of 1.5hr, and 19hr. It was found that the particle size also increased with time (see Figures 1-18 and 1-19). It was concluded from Table 1-7 that more precipitate can be obtained with higher pH values.

Table 1-7. The Amount of Precipitate at Different pH

	#1	#2	#3	#4
pH value	9.63	10.93	12.01	12.48
initial wt of filter paper (gm)	0.0781	0.0777	0.0798	0.0756
finial wt of filter paper (gm)	0.0791	0.0805	0.0971	0.1045
wt of the precipitate(gm)	0.0010	0.0028	0.0173	0.0289

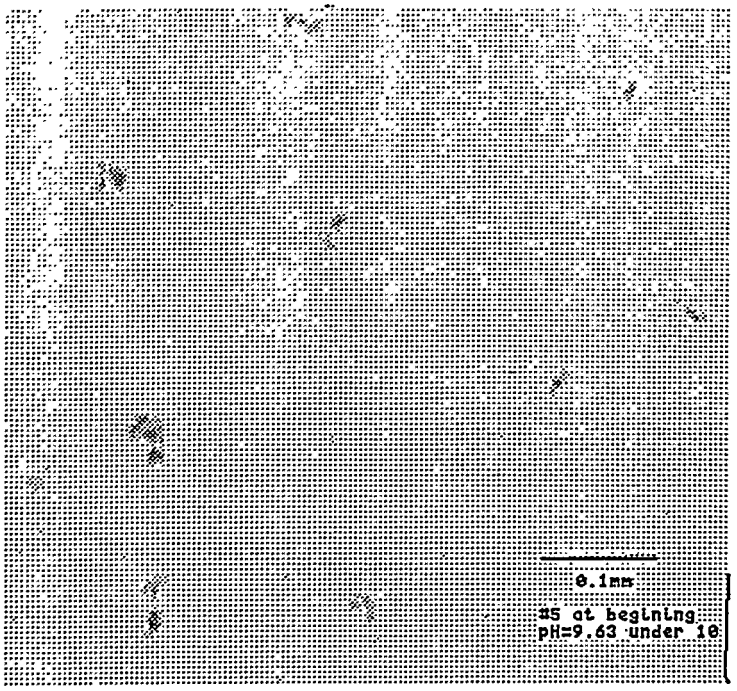

Figure 1-16. $CaCO_3$ crystal under microscope at the time that NaOH was just added (pH=9.63)

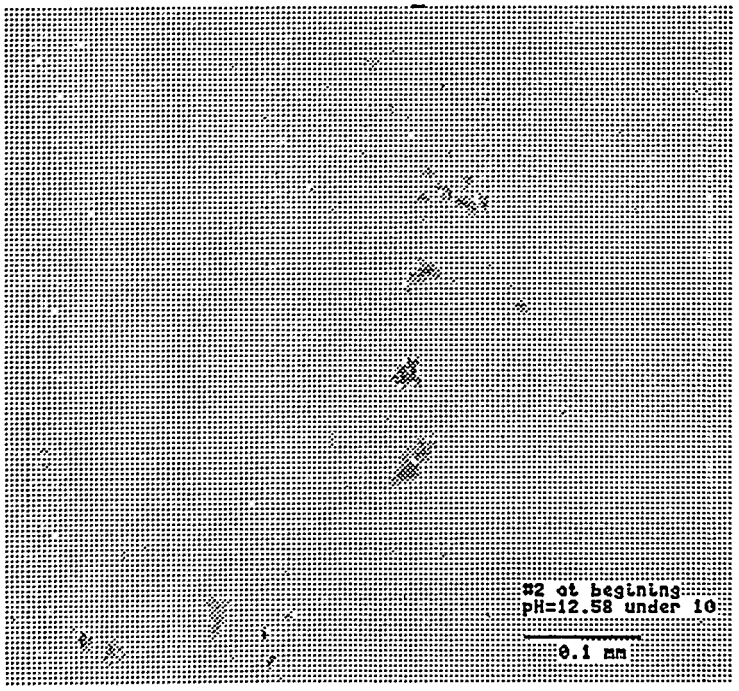

Figure 1-17. $CaCO_3$ crystal under microscope at the time that NaOH was just added (pH=12.58)

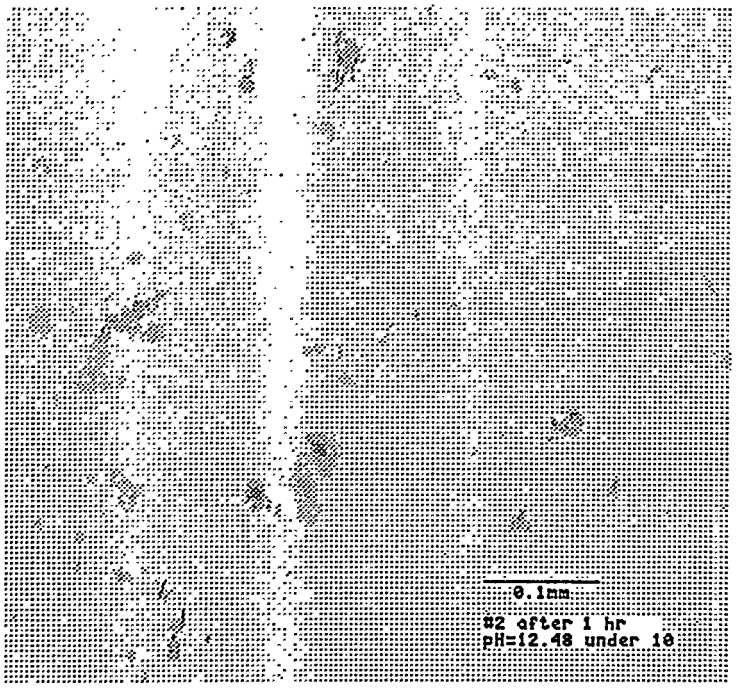

Figure 1-18. $CaCO_3$ crystal under microscope 1hr after NaOH was added

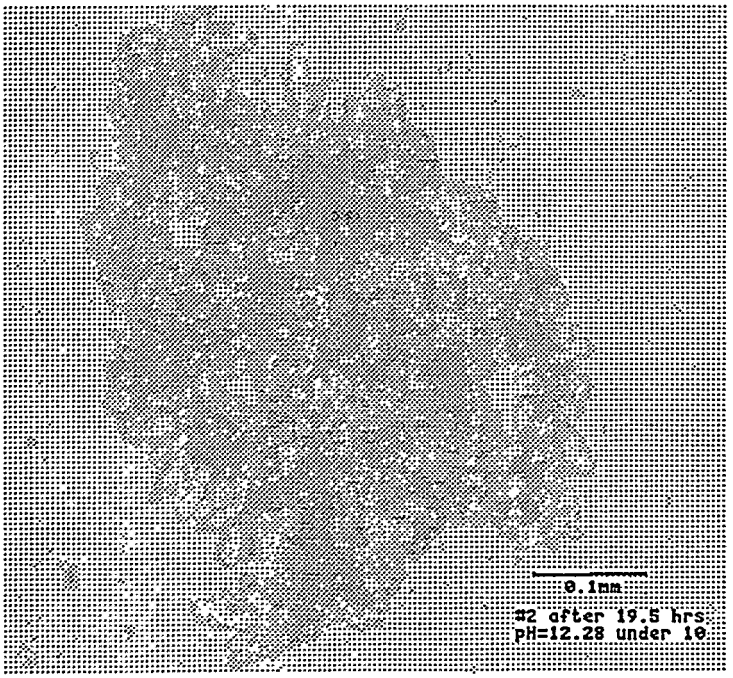

Figure 1-19. $CaCO_3$ crystal under microscope 19.5hr after NaOH was added

The $CaCO_3$ particle size was measured using a Coulter Counter particle size analyzer. In order to measure single particle sizes, an ultrasonic bath was used to break up the agglomerates into single particles. The remaining solution from the stripping experiment #25 (temperature, CaS saturation, acetic acid concentration, and CO_2 flowrate were 60°C, 30%, 0.3 N and 1 lpm respectively) was used. The pH values of the solution were adjusted to 11.54 and 11.75 by adding different amounts of NaOH solution. Single particle sizes were measured within the range of 0.8 to 25 μm. The $CaCO_3$ particle size was measured at various residence times after NaOH solution was added to determine how the particle growth changed with time. The results are shown in Figures 1-20 and 1-21. As one can see, there was no significant increase in particle growth with residence time.

The amount of precipitate in the solution was measured at different residence times to determine if the total mass of precipitate changed with residence time. The remaining solution from the stripping experiment #21 (temperature, CaS saturation, acetic acid concentration, and CO_2 flowrate were 60°C, 30%, 0.1N and 3 lpm respectively) was used. NaOH solution was added to adjust the pH to 12.03. The amount of precipitate in 75ml was measured at 1min, 10 min, 30 min and 1 hr and the data is shown in Table 1-8. It was found that the $CaCO_3$ weight increase with time was slow.

In conclusion, neither the particle growth nor the total mass increase of $CaCO_3$ particles was affected by residence time after the NaOH solution was added.

Table 1-8. The mass of precipitate in 50 ml solution (pH=12.03)

time	mass (g)
1 min	0.0047
10 min	0.0055
30 min	0.0061
1 hr	0.0070

Additional $CaCO_3$ regeneration studies were conducted in order to determine the amount of calcium recovered at different pH values. NaOH was used for adjusting pH. The remaining solution from the stripping experiment #1 (temperature, CaS saturation, acetic acid concentration, and CO_2 flowrate were 20°C, 50%, 0.1 N and 1 lpm respectively) was used and the initial Ca concentration in the solution was 4.31 g/L as $CaCO_3$. Different amounts of NaOH were added to 20ml samples of the solution, after which the precipitate was filtered and weighed. The amount of calcium remaining in the solution after the precipitate was filtered out was titrated using EDTA. The mass balance of Ca, which was derived by the summation of the amount of $CaCO_3$ that precipitated out and the amount of Ca remaining in the solution, was closed at different pH values. The results of these experiments are shown in Table 1-9 and Figure 1-21. One can see that the amount of $CaCO_3$ precipitate increases with increasing pH, from a level of about 10% recovered at a pH of ~8.0, to a level of ~45% at a pH of 13. Therefore, in order to achieve significant calcium recovery, an elevated pH is desirable.

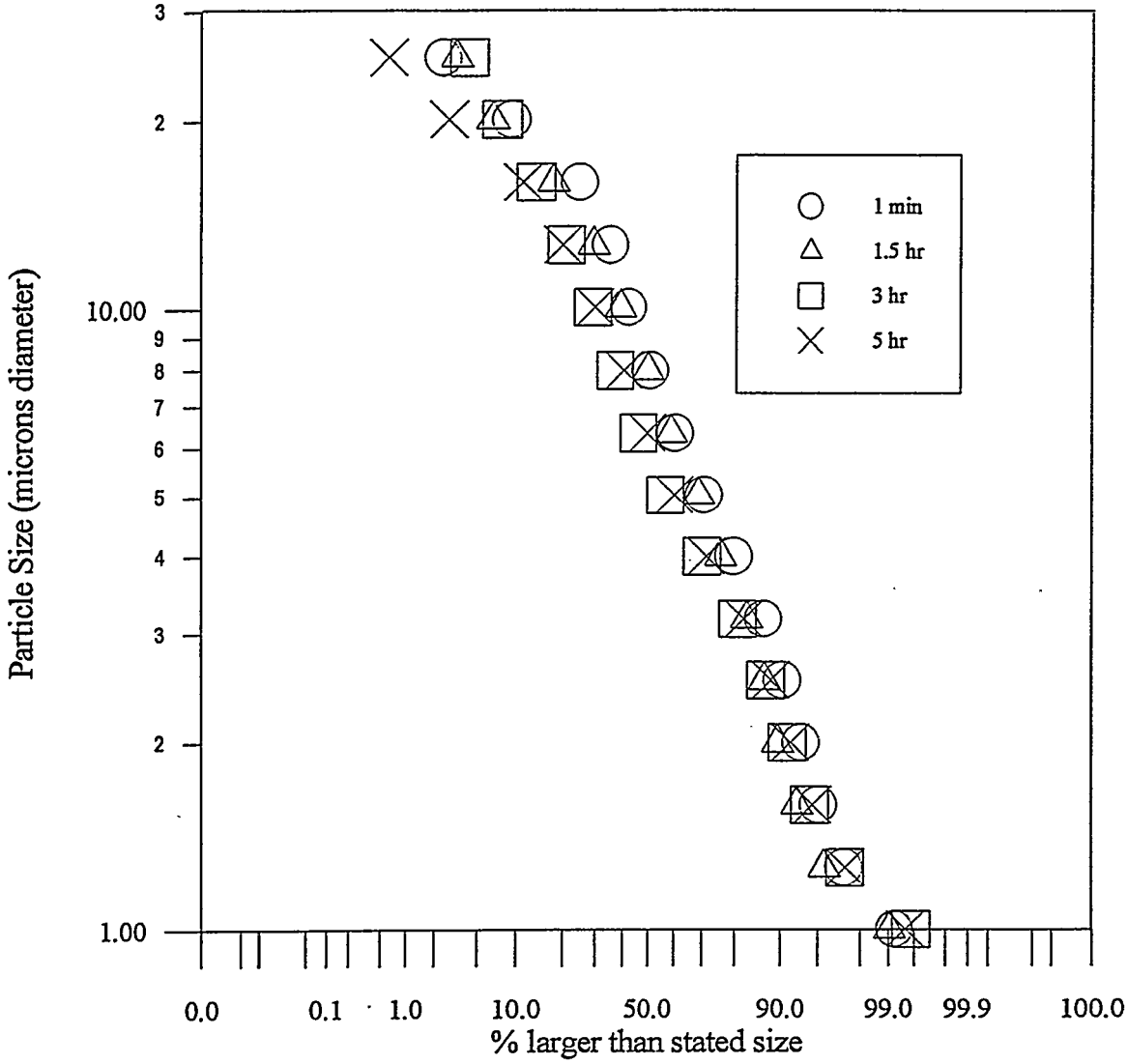

Figure 1-20. Particle Size Distribution (@ pH = 11.75)

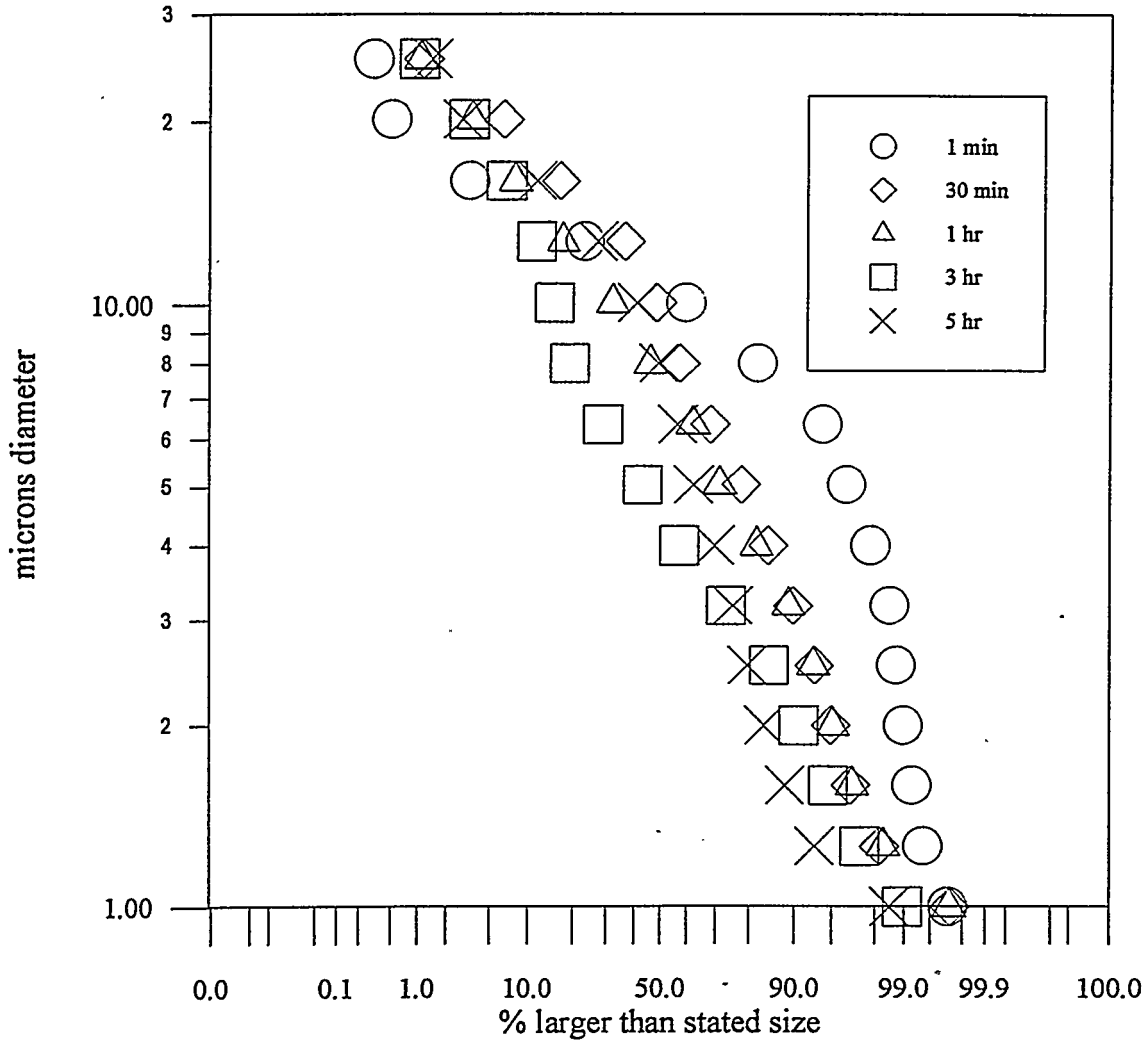

Figure 1-21. Particle Size Distribution (@ pH = 11.54)

Table 1-9. Amount of Ca Recovered at Different pH

pH	wt of precipitate (mg)	amount of Ca in the solution (mg as $CaCO_3$)	total mass of Ca in 20 ml solution (mg)	amount of Ca precipitated out (%)
8.20	7.20	76.96	84.16	8.35
9.07	20.5	59.41	79.91	23.78
9.91	21.2	66.23	87.43	24.59
11.12	26.2	56.43	82.63	30.39
12.18	38.0	53.66	91.66	44.08

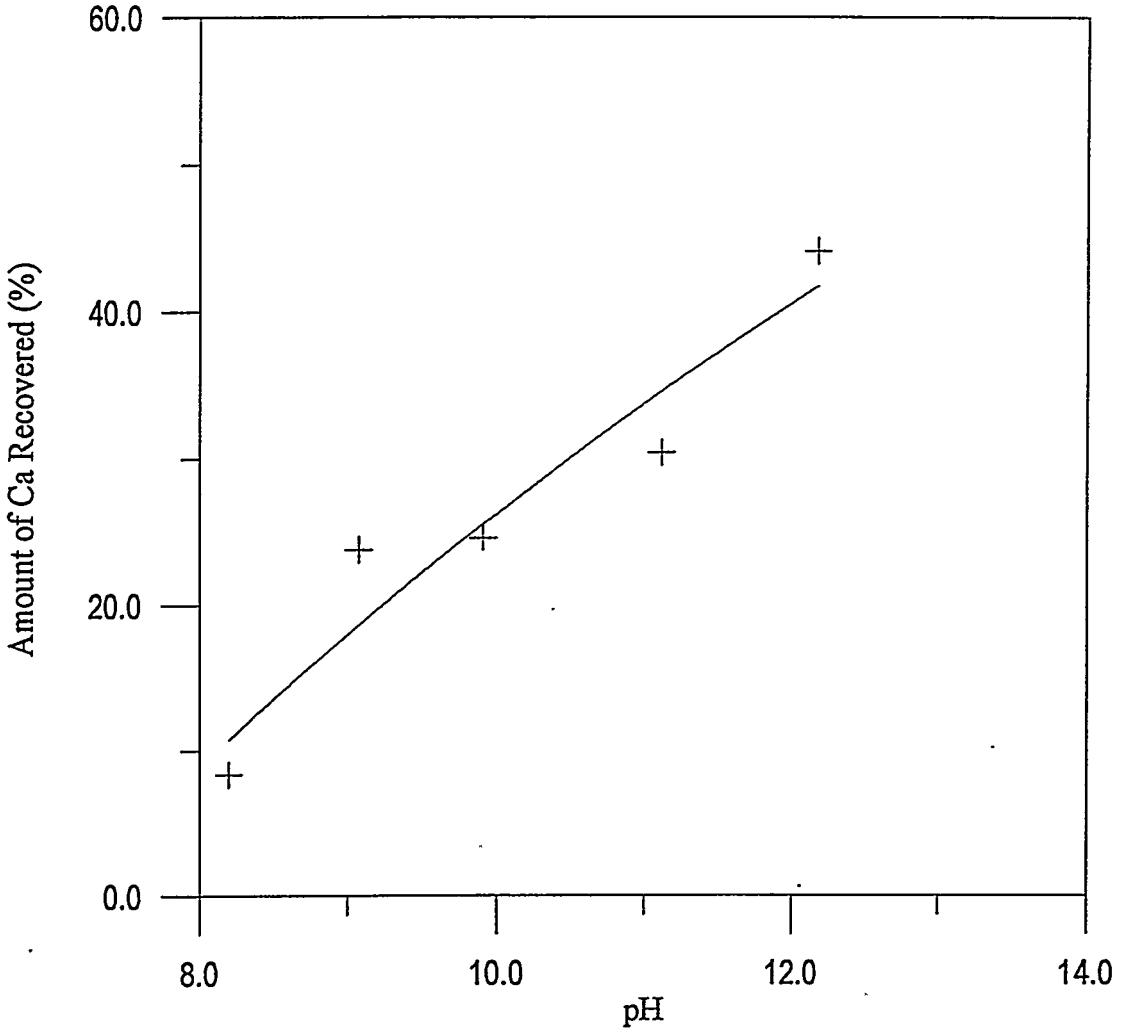

Figure 1-22. Amount of Calcium Recovered vs. pH

PHASE 2: ELEMENTAL SULFUR PRODUCTION STUDIES

Introduction / Objectives

In the first phase of this project, it has been shown that dissolving the CaS generated by the novel coal feeder in an acetic acid solution and then using CO_2 to strip out the H_2S from the solution generates a gaseous H_2S-CO_2 mixture. Phase # 2 involves passing this H_2S-CO_2 mixture through a packed bed catalytic reactor to produce elemental sulfur.

Background and Literature Review

Claus Process

Claus process is the most widely used modern process in industry for sulfur recovery. According to the estimation by Goar et al. (1986), some 90 to 95% of recovered sulfur in the world was produced by the Claus process. A typical schematic structure of the conventional Claus Process is shown in Figure 2-1. Since the Claus process was invented in 1883, a lot of modifications have been made on the commercial process which is used today, but the principal mechanisms of the process are the same as one hundred years ago.

$$2\ H_2S + 3\ O_2 \rightarrow 2\ SO_2 + 2\ H_2O \qquad \text{(Combustion Process)}$$

$$2\ H_2S + SO_2 \rightarrow 1.5\ S_2 + 2\ H_2O \qquad \text{(Claus Process)}$$

$$2\ H_2S + O_2 \rightarrow S_2 + 2\ H_2O \qquad \text{(Overall Process)}$$

Based on the above reaction equations, about one third of the H_2S needs to be burned

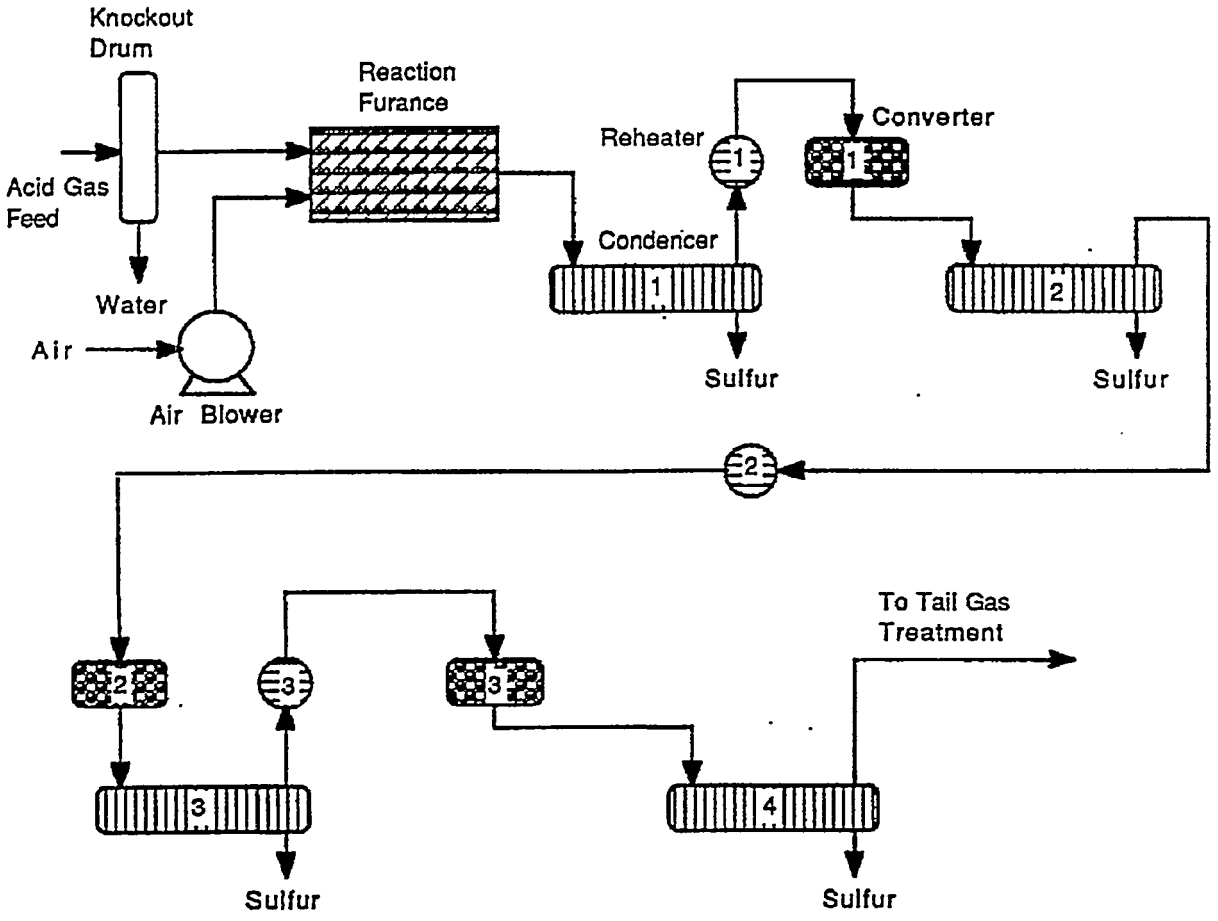

Figure 2-1. Schematic of Conventional Claus Process

in the air to form SO_2. In order to comply with the air pollution regulations, the modern Claus Process consists of a combustion stage, one to four catalytic converters, and a tail-gas clean-up unit. A detailed review of commercial developments in Claus process technology was discussed by Goar (1986).

Since there is 79% nitrogen in the air, the use of air in the Claus process requires that the inert N_2 must be treated in tail gas plant to meet the environmental regulation before it is released to the atmosphere. Tail gas treatment increases the sulfur recovery cost. About two dozens of tail gas clean-up process are reviewed by West (1984). The total recovery of sulfur has been claimed as high as 99% or greater (Goar et al., 1986). But the necessity of preventing sulfur emissions in such large systems is a very difficult task and is also very costly. By the nature of the Claus process, hydrogen can not be recovered and is finally wasted in the form of water, making the process less attractive for hydrogen economy. Because the Claus process is a highly optimized technology, it will be an outstanding revolution to the existing technology if any further development is made to reduce both the capital cost and the sulfur emissions, and simultaneously recover the elemental sulfur and hydrogen in a usable form.

Thermal Decomposition of H_2S without Catalyst

The feasibility of the production of elemental sulfur and hydrogen by decomposition of H_2S has been well established in the literature. The original purpose of this process was to produce H_2 but it has been used to produce sulfur as well.

$$H_2S \rightleftharpoons H_2 + 0.5\ S_2$$

Studies of determining the mechanism and kinetics for the H_2S decomposition have been reported by a number of researchers. Kaloidas and Papayannakos (1989) studied the kinetics of the thermal non-catalytic decomposition of H_2S. The reactions were performed at the temperature from 600 to 860°C, pressure between 1.3 to 3.0 atm. The proposed mechanism was the initial and rate-limiting step of the splitting H_2S into intermediate free-radicals. Their statistical tests indicated that their kinetic model and the experimental data agreed well with each other. They also found that α-Al_2O_3 did not act as a catalyst for H_2S decomposition in their experimental conditions.

Roth et al. (1982) carried out their experiments in the temperature range of 1965 to 2560 K, pressure between 1.8 to 2.0 bars, and H_2S concentration as low as 25 to 200 ppm for the investigation of thermal decomposition of hydrogen sulfide. The inert gas was argon (Ar). The primary reaction mechanism according to their work followed the second order kinetics:

$$H_2S + Ar \rightarrow HS + H + Ar$$
$$H_2S + H \rightarrow HS + H_2$$

Their experimental temperature was much higher than that of the common laboratory and the sulfur recovery industry requiring an expensive plasma operation.

Raymont (1975) found that H_2S could be thermally decomposed, however it was thermodynamically unfavorable below 1800 K due to the endothermic reaction mechanism. He established three different reaction systems: an empty uncatalyzed reactor, a reactor filled with blank pellets and a reactor packed with a chemically active metal catalyst. He found that certain metal catalysts had very significant effects on both hydrogen yield and reaction rate of H_2S decomposition. He also pointed out that, above 1250 K, the yields

were the same whether the reaction was catalytic or not.

Thermal Decomposition of H_2S with Catalyst

There have been several works in the efforts to increase the rate of reaction at relative lower temperatures using different catalysts. Chivers et al. (1980) found that MoS_2 was the most effective catalyst above 600°C, but WS_2 and Cr_2S_3 gave higher H_2 yields than MoS_2 below 600°C. They also found FeS, CoS, NiS, CuS, C_2S and Cu_9S_5 were not effective catalysts for the decomposition of H_2S and only a trace amount of elemental sulfur was produced in the reaction. Among the catalysts that have been tested to date, MoS_2 has been proven to be the most effective over a wide range of temperature. The catalyst properties and possible mechanisms for H_2S decomposition over MoS_2 were also described by Katsumoto et al. (1973), Kotera (1976), Mitchell (1981) and, Sugioka and Aomura (1984) over various ranges of reaction temperature and pressure.

Chivers and Lau (1985) screened the alkali metal sulfides and polysulfides group and found that sodium polysulfides were not catalytically active for H_2S decomposition. In their study, the most significant result was the discovery that Li_2S acted as a catalyst for the thermal decomposition of H_2S at 500 to 800°C. But its application was limited due to the sensitivity of Li_2S towards impurities, CO_2 and water.

Chivers and Lau (1987) continued their investigation on vanadium sulfide and mixed catalysts. The mixture of V_2S_3/Cu_9S_5 which formed Cu_3VS_4 at elevated temperatures was shown to have a higher catalytic activity than MoS_2 in a closed circulating system using a quartz reactor in the temperature range of 400 to 800°C, whereas MoS_2 was found to be a

better catalyst than V_2S_3 and V_2S_3/Cu_9S_5 in a thermal diffusion column reactor. However, the cost (per unit weight) of commercial V_2S_3 was about 30 times greater than that of MoS_2. They suggested that the catalytic mechanism of vanadium sulfide in H_2S decomposition was via a two-step process shown below:

$$2\ VS + H_2S \rightarrow V_2S_3 + H_2$$
$$V_2S_3 \rightarrow 2\ VS + S^*$$

Al-Shamma and Naman (1989 and 1990) investigated the use of V_2S_3, V_2O_5/Al_2O_3 and V_2S_3/Al_2O_3 catalysts. In the once-through flow reactor, the concentration of H_2 increased during the first 150 to 200 minutes, then it went down without reaching a steady-state value. All their experiments were carried out in the temperature range of 723 to 873 K with different vanadium oxide/alumina oxide percentages. The suggested reaction mechanism was:

$$V_2O_5 + 5\ H_2S \rightarrow V_2S_3 + 5\ H_2O + 2\ S^*$$

The subsequent reactions were the same as those by Chivers and Lau (1987). The reaction order was between zero and one, depending on combination of catalysts and reaction temperature.

Morgantown Energy Technology Center developed a direct sulfur recovery process (DSRP), which could convert either SO_2 or H_2S directly to elemental sulfur by using the coal gas and a catalyst (Gangwal et al., 1991). They claimed that the conversion could reach above 95%. The overall reactions were shown as:

$$2\ H_2 + SO_2 \rightarrow 2\ H_2O + 1/n\ S_n$$
$$2\ CO + SO_2 \rightarrow 2\ CO_2 + 1/n\ S_n$$
$$SO_2 + 3\ H_2 \rightarrow H_2S + 2\ H_2O$$
$$2\ H_2S + SO_2 \rightarrow 2\ H_2O + 3/n\ S_n$$

They also found that pressure had a significant effect on the conversion of H_2S to elemental

sulfur. Increasing reaction pressure from 1.5 to 20 atm quadrupled the sulfur recovery when the space velocity was kept at the same level. The work was focused on the conversion of dilute SO_2 to elemental sulfur.

Thermal Decomposition of H_2S while Products are Continually Removed

Even though the usage of a catalyst can increase the rate of reaction, the yield of sulfur is still limited by the equilibrium decomposition of H_2S. For this reason, some researchers have studied the ways to continually remove either H_2 and S_2 in order to shift the equilibrium to the product side and further decompose H_2S. The study of Raymont (1975) was most focused on the recovery of H_2. The use of platinum or palladium alloy membranes was suggested and a diagrammatic representation of the proposed process was also presented. Due to the unavailability of practical commercial membranes for removal of H_2 from the product stream, Banderman and Harder (1982) used a pressure swing adsorption on zeolite or carbon molecular sieves which was claimed to be competitive to the Claus process.

Oxidization of H_2S by O_2

The process of production of elemental sulfur through the oxidation of hydrogen sulfide over an activated carbon bed has been studied by several researchers (most recently Chowdury and Tollefson, 1990; Dalai et al., 1993). The apparent reaction by which the sulfur forms is:

$$2\ H_2S + O_2 \rightarrow S_2 + 2\ H_2O$$

or

$$2\ H_2S + O_2 \rightarrow 2/n\ S_n + 2\ H_2O$$

The direct conversion of H_2S to elemental sulfur with dilute oxygen at 20 atm near 635 K

was above 98 % and decreased when the pressure and the temperature were lowed (Gangwal et al., 1991). The inlet gas contained 6.46% H_2S, 3.23% O_2 and 8.14% H_2O with the balance of N_2. This method has been proven to be more effective for treating low concentration of H_2S (<10 volume %) than that used in the Claus process (Steijns and Mars, 1974; Ghosh and Tollefson, 1986).

Partial Oxidization of H_2S by CO_2

Another way of effectively decomposing the H_2S is to add oxidizing reactants such as CO_2 to react with H_2. Bowman (1991) studied the thermodynamic possibilities of reaction of H_2S with CO_2 under different reaction conditions. He divided his theoretical thermodynamic calculations into three temperature regions under various pressures. No experimental data were presented to verify the equilibrium calculations.

Liptak (1974) proposed the following reaction at a high temperature with catalysts:

$$4\ H_2S + CO_2 \rightleftharpoons 2\ S_2 + CH_4 + 2\ H_2O$$

Paushkin (1988) also proposed the following additional reaction:

$$6\ H_2S + 2\ CO_2 \rightarrow 6\ S + CH_2{=}CH_2 + 4\ H_2O$$

These reactions have been described to be potentially effective but actual reaction kinetics for various catalyst types and the effects of temperature and gas flow rate have not been well reported in the literature.

Towler et al. (1993) proposed a reaction mechanism for the production of elemental sulfur from H_2S and CO_2 as following:

$$H_2S \rightleftharpoons H_2 + 0.5\ S_2$$

$$CO_2 + H_2 \rightleftharpoons CO + H_2O$$

They proposed that the presence of CO_2 had the effect of shifting the H_2S decomposition reaction to the product side by reacting the produced H_2 with CO_2 to form CO and water via the water-gas shift reaction. The catalyst was MoS_2. However, the final H_2S conversion and sulfur yield were not conclusive, possibly due to the type of reactor for catalyst evaluation.

Based on all of these considerations, the objectives of this research are the following:

1) to perform a thermodynamic analysis in order to determine theoretically the extent of conversion, the effect of various parameters, and the possibility of formation of undesirable side-products,

2) to determine a method of preparation for the sulfided form of the Co-Mo catalyst from the oxide form in which the catalyst was purchased,

3) to test the sulfided Co-Mo catalyst to determine its feasibility in producing elemental sulfur from the H_2S-CO_2 gas mixture. This includes the design and construction of a reactor for conducting tests as well as development of an experimental procedure using the method proposed by Towler and Lynn.

Task #1 - Thermodynamic Analysis

Thermodynamic analyses for the reaction of H_2S and CO_2 were performed by using the JANAF Thermochemical Tables (DOW Chemical Company, 1971; Stull, 1971) and the STANJAN program obtained from Professor Wm. C. Reynolds (Department of Mechanical Engineering, Stanford University, Stanford, CA 94305-3030). From the findings of Kaloidas and Papayannakos (1987), S_2 was assumed to be the only elemental sulfur species present. In reality, other allotropes will exist in small amounts making these caluculations conservative. The results indicated that the following individual reactions were possible for the reaction of H_2S and CO_2:

$$2\ H_2S = 2\ H_2 + S_2 \qquad (1)$$

$$CO_2 + H_2 = CO + H_2O \qquad (2)\ \text{water-gas-shift reaction}$$

$$CO_2 + 4\ H_2 = CH_4 + 2\ H_2O \qquad (3)$$

$$CO + 3\ H_2 = CH_4 + H_2O \qquad (4)$$

At T=500°C and P=1 atm, the Gibbs free energy, the heats of reactions and the corresponding equilibrium constants for the preceding reactions are:

Reaction 1	$\Delta G = 55.48$	KJ/mol	$K=4.5\times10^{-14}$
	$\Delta H = 88.58$	KJ/mol	Endothermic
Reaction 2	$\Delta G = 10.15$	KJ/mol	$K=3.6\times10^{-3}$
	$\Delta H = 37.13$	KJ/mol	Endothermic
Reaction 3	$\Delta G = -50.21$	KJ/mol	$K=1.2\times10^{12}$
	$\Delta H = -230.14$	KJ/mol	Exothermic

Reaction 4 $\Delta G = -32.24$ KJ/mol $K=5.6x10^7$

$\Delta H = -185.21$ KJ/mol Exothermic

The ranges of the ΔH and ΔG as a function of temperature are shown in Figures 2-2 through 2-9. The rate limiting step is the decomposition of H_2S (Reaction 1). An increase in temperature would shift reactions (1) and (2) to the product sides, and shift reactions (3) and (4) to the reactant sides. An increase in pressure would shift the Reactions (3) and (4) to the product sides.

By using the STANJAN method, equilibrium calculations have been made for the decomposition of H_2S with and without CO_2. At an equilibrium state, the S_2 mole fraction is higher in the presence of CO_2 than in the absence of CO_2, indicating that CO_2 promotes the decomposition of H_2S. The H_2 mole fraction becomes lower in the presence of CO_2 since CO_2 reacts with H_2 to form CH_4, H_2O and CO. The equilibrium of H_2S decomposition is shifted to favor the formation of elemental sulfur.

Effects of Temperature and Pressure

Figure 2-10 shows the equilibrium mole fraction of H_2S as a function of temperature and pressure when the inlet ratio of H_2S to CO_2 equals 1. Because both the H_2S decomposition reaction and the water-gas shift reaction are endothermic, the H_2S mole fraction decreases as the system temperature increases. The H_2S mole fraction increases as the system pressure increases enabling the H_2S decomposition reaction to shift to the left. Figure 2-11 shows the equilibrium mole fraction of S_2 as a function of temperature and pressure.

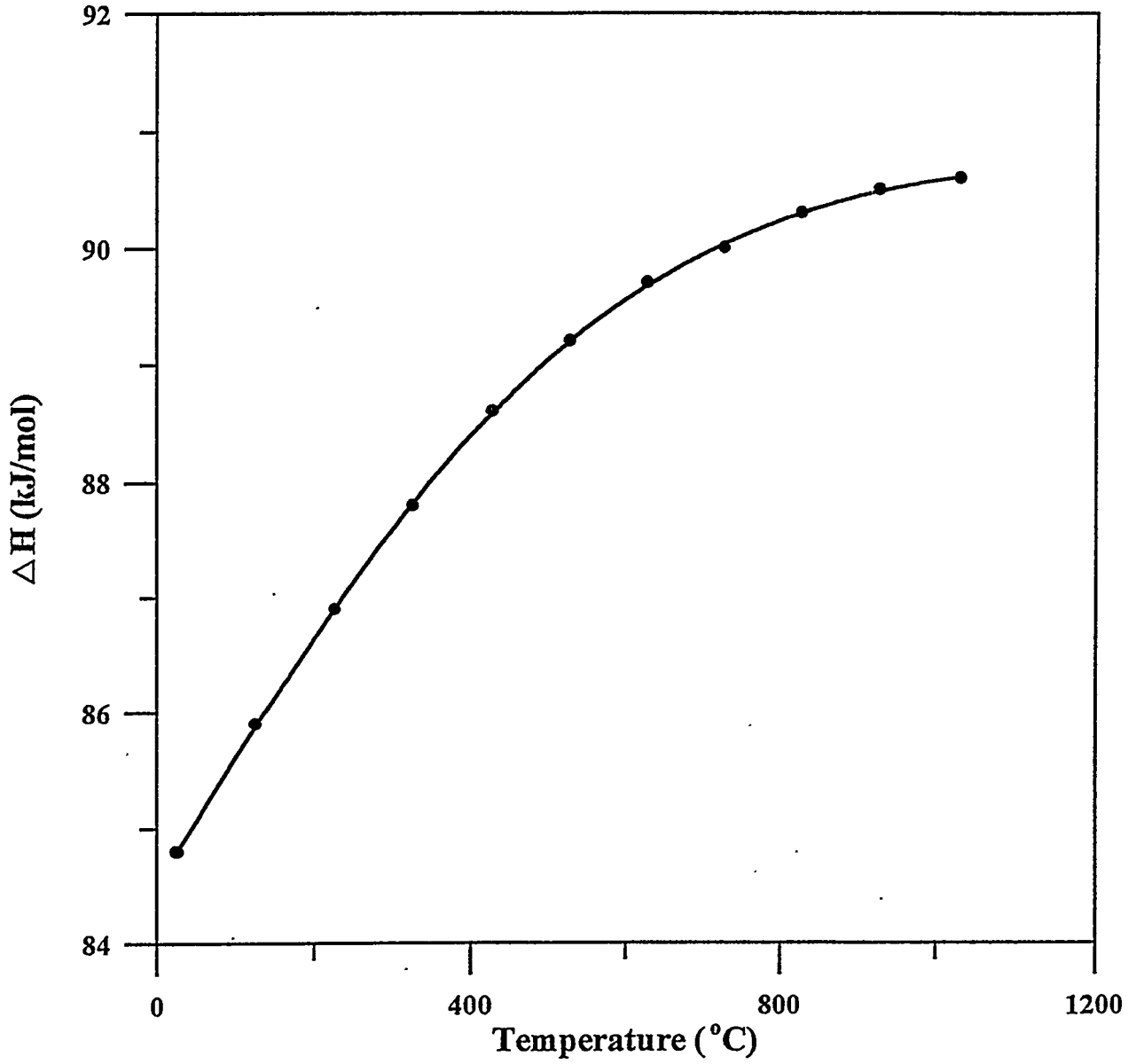

Figure 2-2. Enthalpy Change vs. Temperature For the Reaction $H_2S \rightleftharpoons H_2 + \frac{1}{2}S_2$

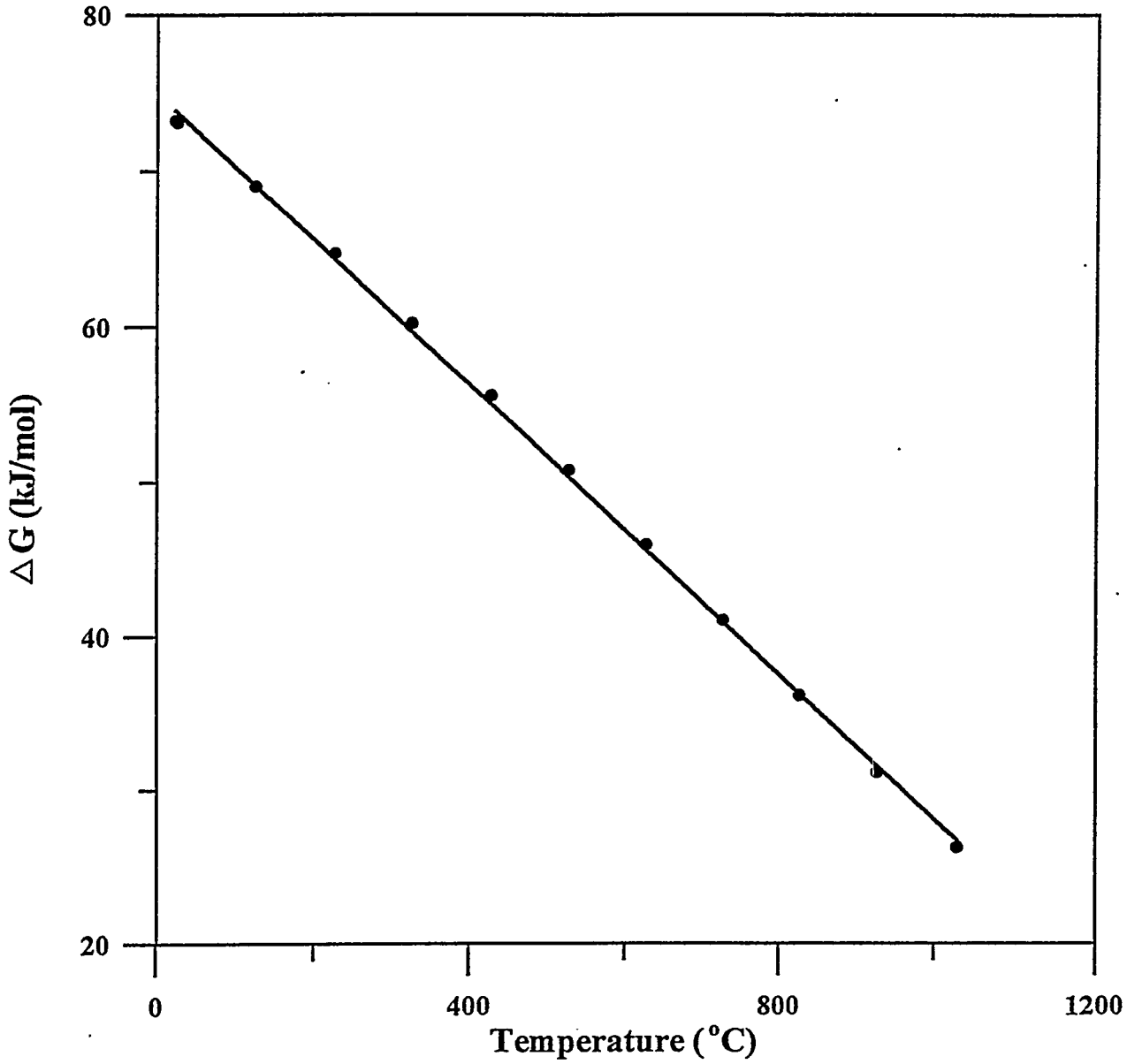

Figure 2-3. Gibbs Free Energy Change vs. Temperature For the Reaction $H_2S \rightleftharpoons H_2 + \frac{1}{2}S_2$

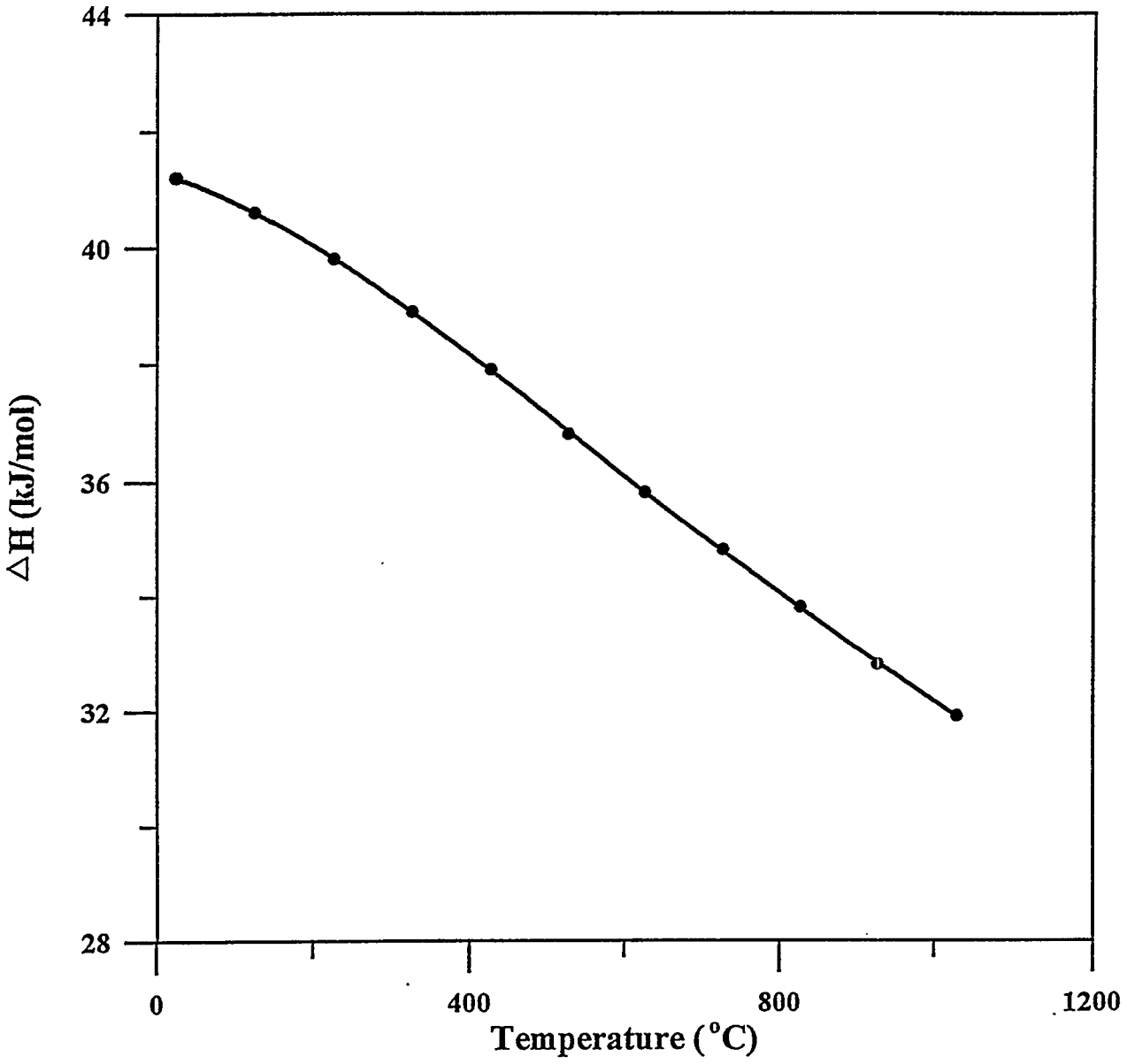

Figure 2-4. Enthalpy Change vs. Temperature For the Reaction $CO_2 + H_2 \rightleftharpoons CO + H_2O$

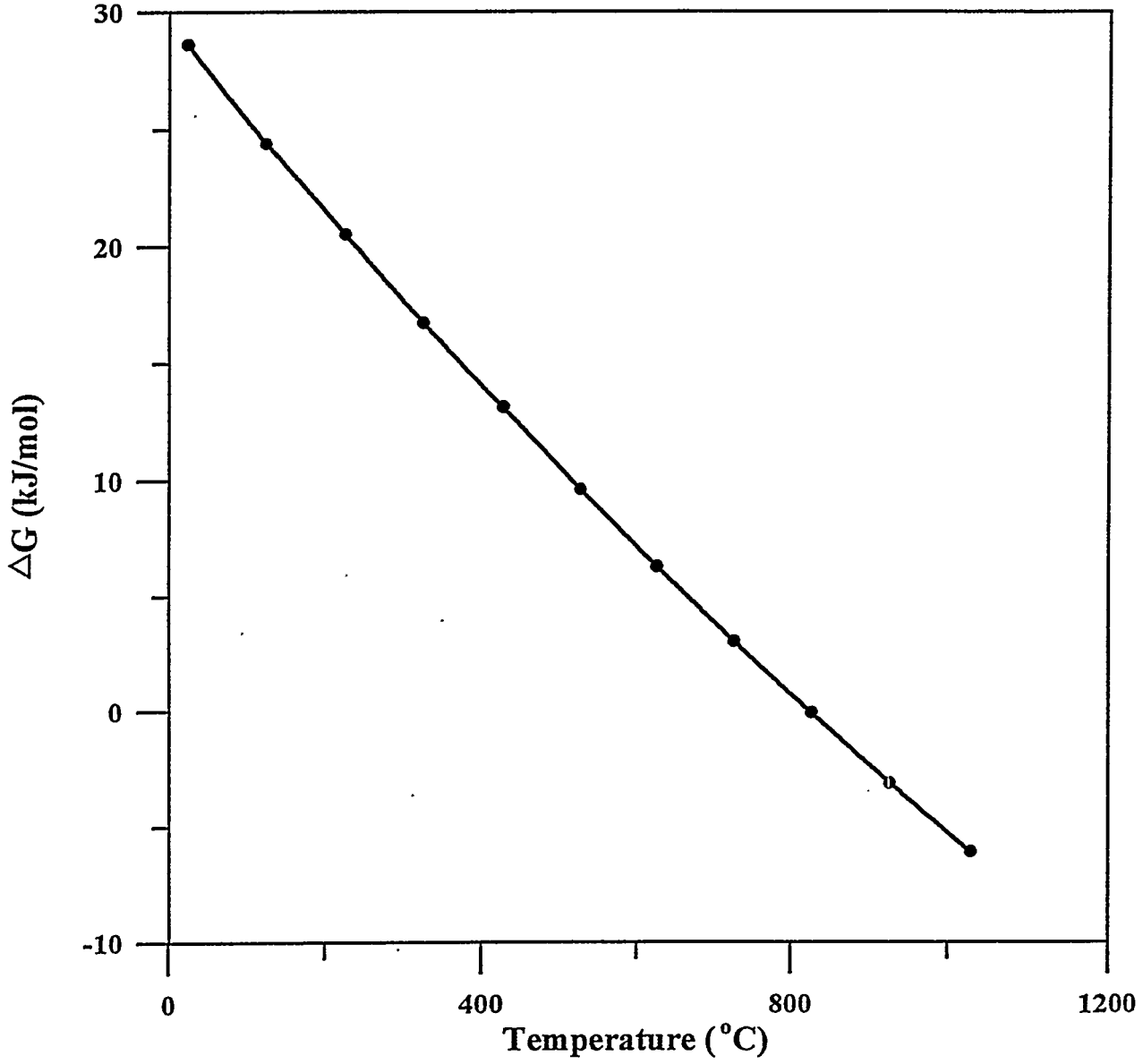

Figure 2-5. Gibbs Free Energy Change vs. Temperature For the Reaction $CO_2 + H_2 \rightleftharpoons CO + H_2O$

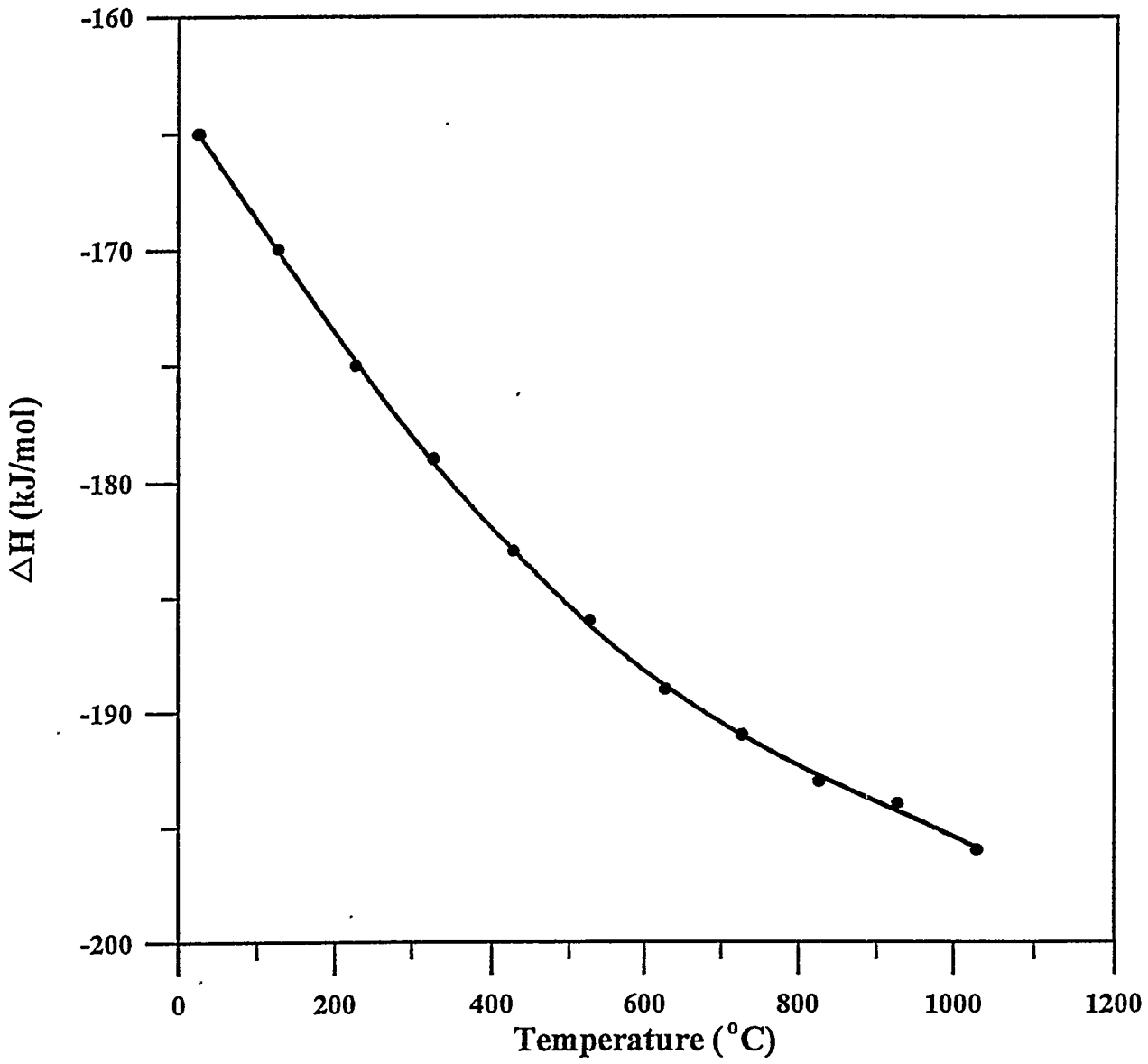

Figure 2-6. Enthalpy Change vs. Temperature For the Reaction $CO_2 + 4H_2 \rightleftharpoons CH_4 + 2H_2O$

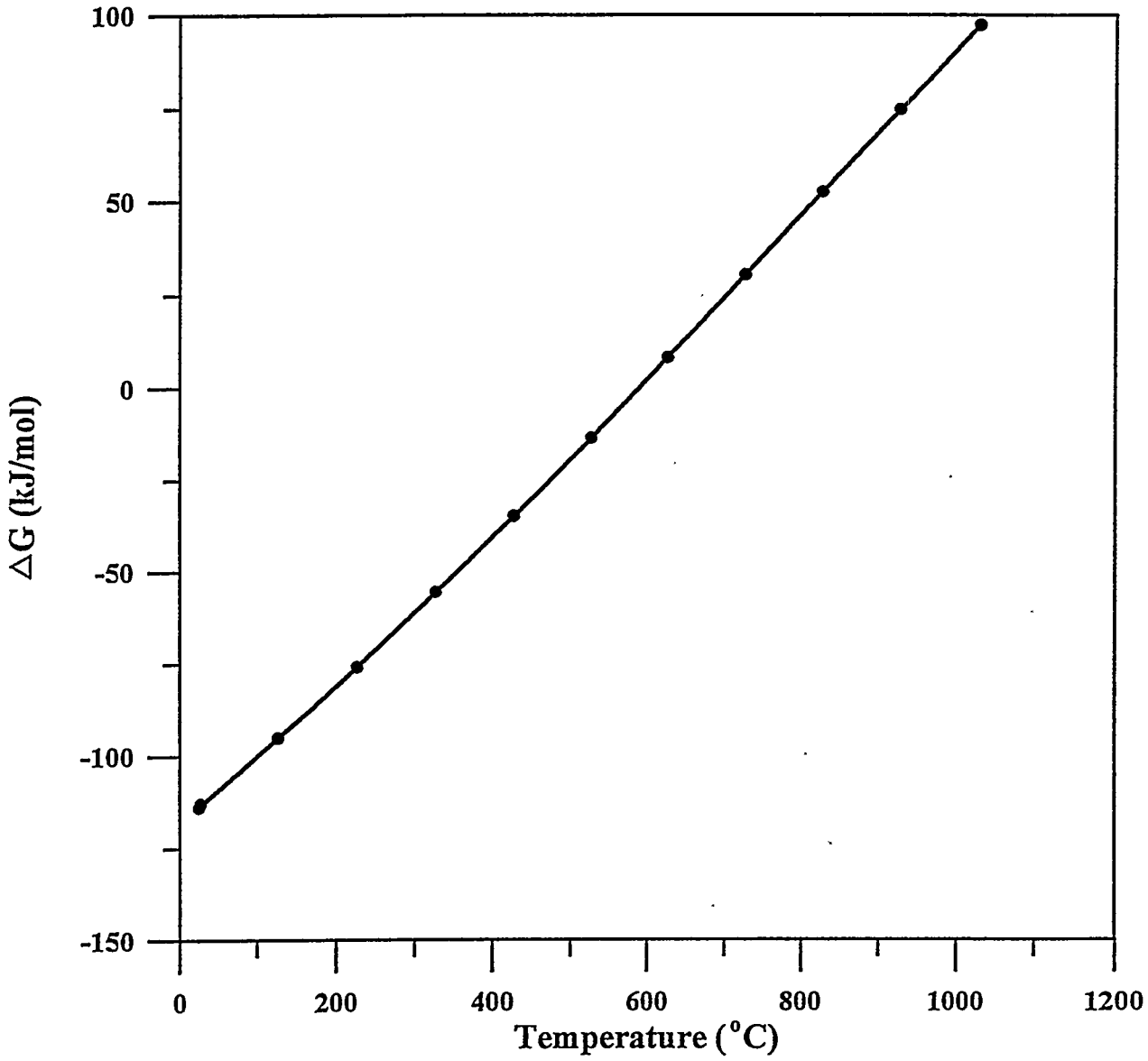

Figure 2-7. Gibbs Free Energy Change vs. Temperature For the Reaction $CO_2 + 4H_2 \rightleftharpoons CH_4 + 2H_2O$

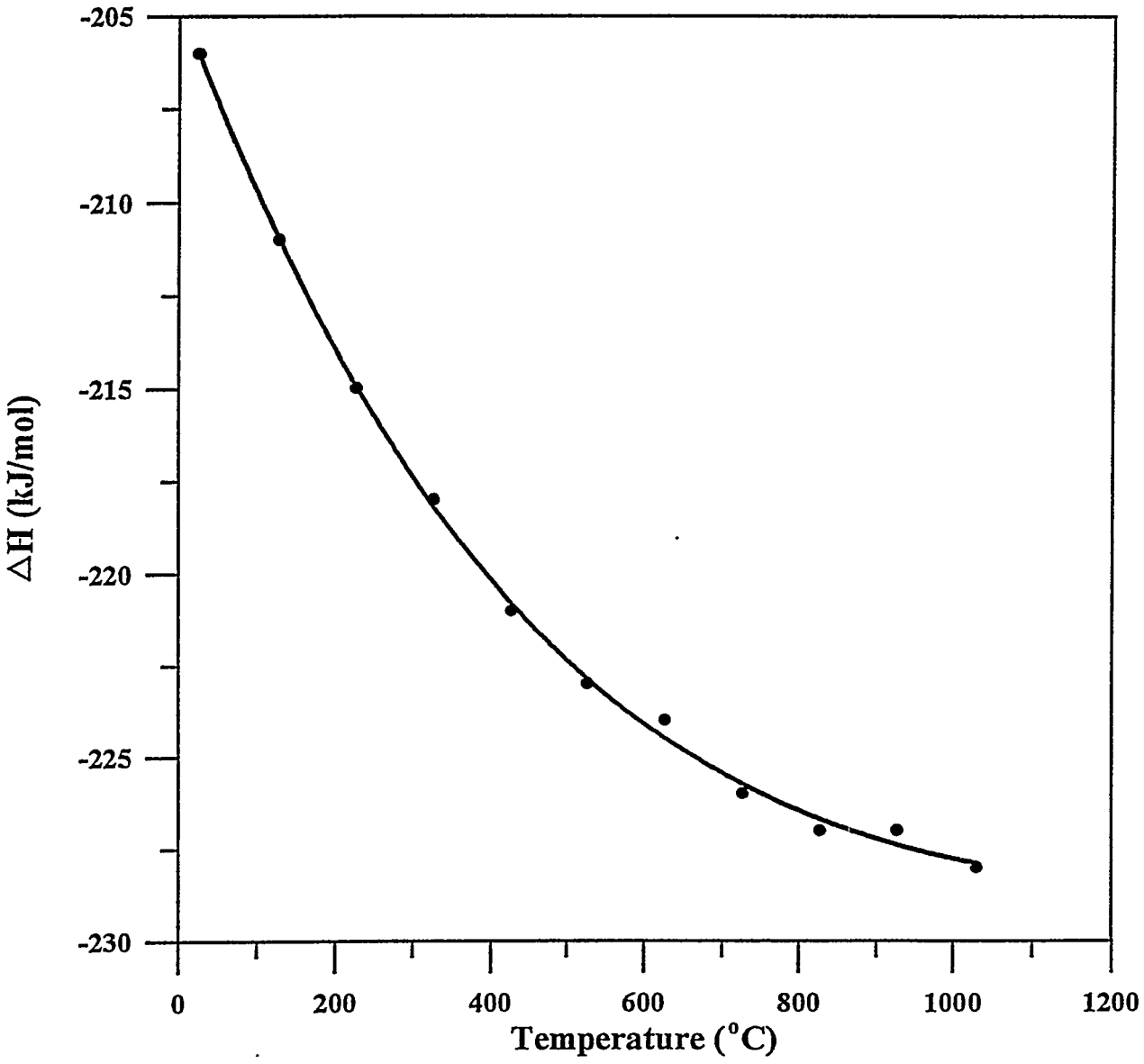

Figure 2-8. Enthalpy Change vs. Temperature For the Reaction
$CO + 3H_2 \rightleftharpoons CH_4 + H_2O$

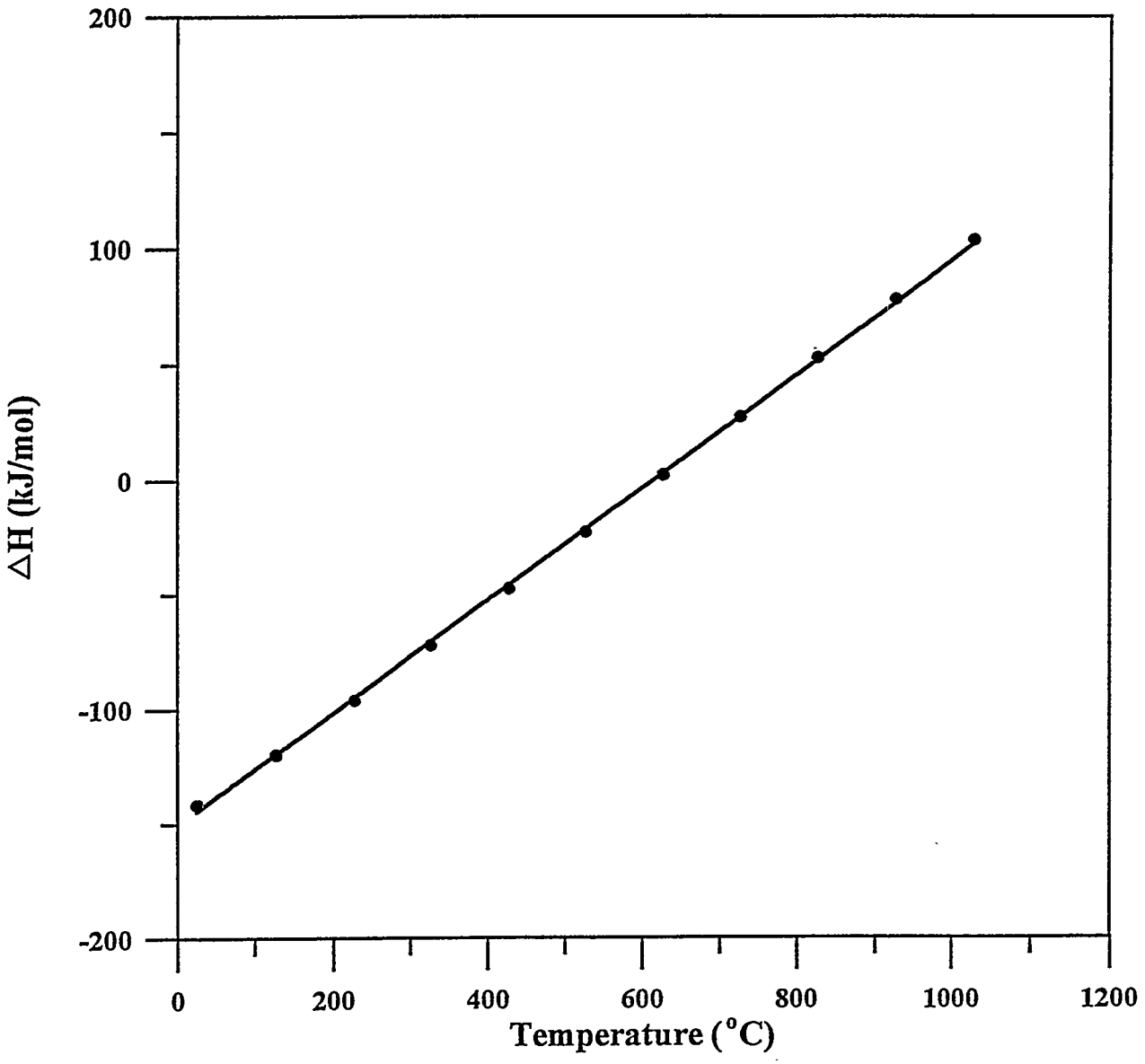

Figure 2-9. Gibbs Free Energy Change vs. Temperature For the Reaction $CO + 3H_2 \rightleftharpoons CH_4 + H_2O$

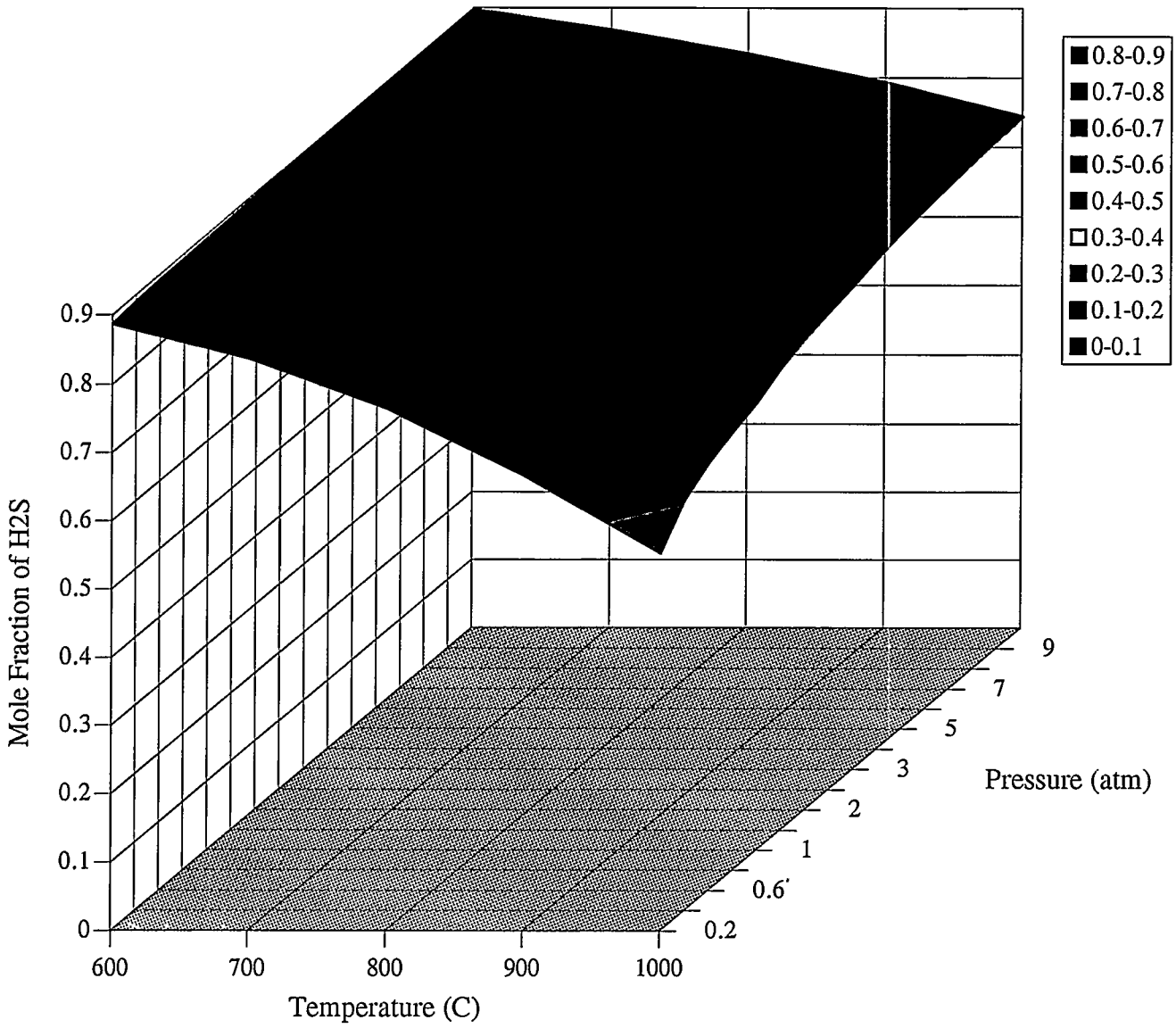

Figure 2-10. The Effect of Temperature and Pressure on the Equilibrium of H2S (H2S:CO2=1:1)

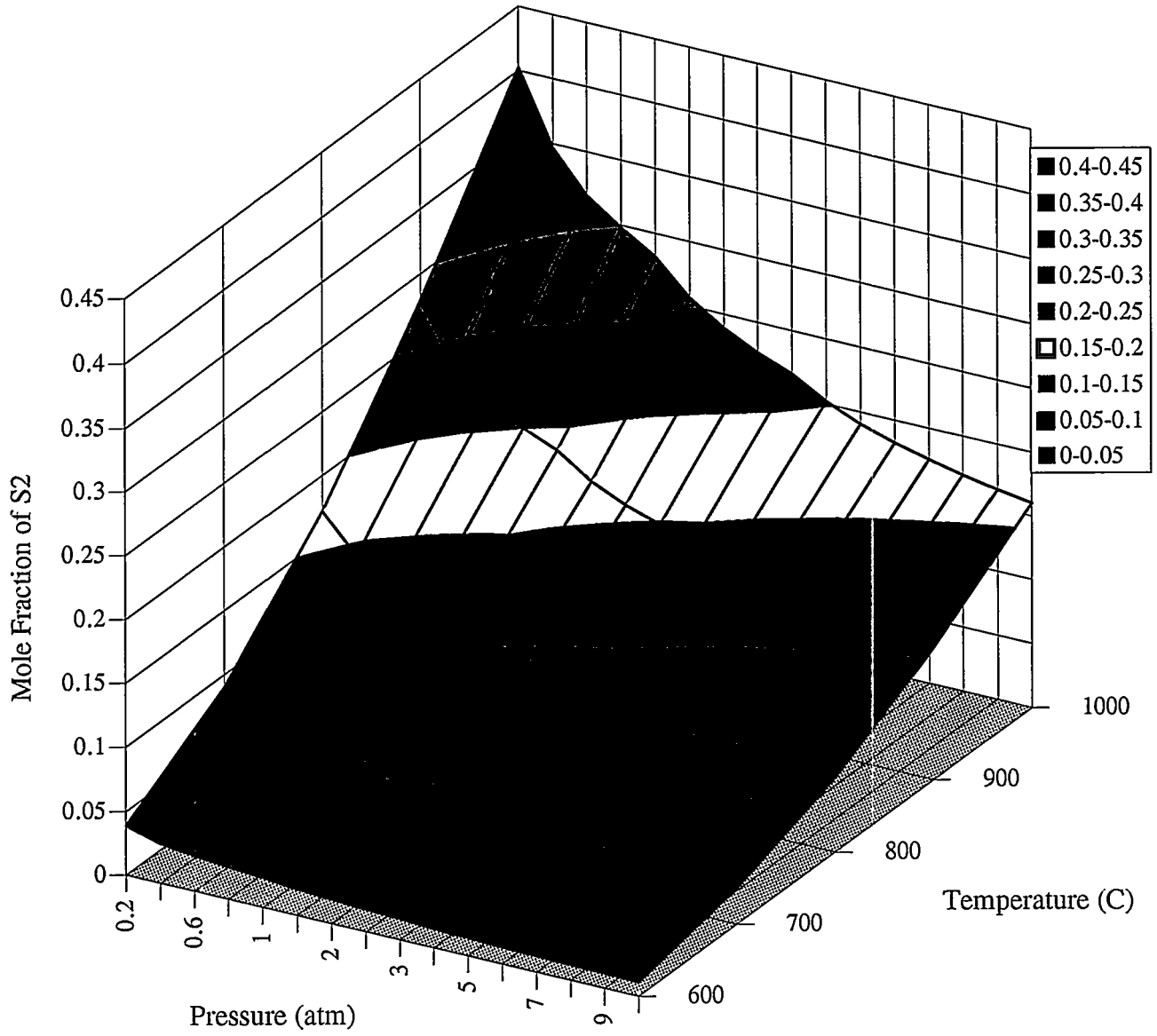

Figure 2-11. The Effect of Temperature and Pressure on the Equilibrium of S2 (H2S:CO2=1:1)

Effects of the Ratio of H_2S to CO_2

Figure 2-12 shows the equilibrium conversion of H_2S as a function of the ratio of H_2S to CO_2. A higher conversion is predicted at higher temperature and at lower ratios of H_2S to CO_2. When the ratio of H_2S to CO_2 equals 1 at a reaction temperature below 500°C, the conversion of H_2S reaches almost the same level as the case without any CO_2 present negating the beneficial effect of CO_2.

Task #2 - Catalyst Preparation

Introduction

The catalysts for this screening study was selected after a review of the literature and a consideration of the thermodynamics of the reactions involved. The choice of catalyst was made based on the fact that MoS_2 had already been claimed as an effective catalyst for the H_2S decomposition reaction. For this reason, a cobalt-molybdenum catalyst (Co-Mo) was selected as a candidate catalyst for the screening study. Additionally, the Co-Mo catalyst is used for the water-gas shift reaction (Wender, 1987) and is readily available from commercial sources. Molybdenum is also known to be catalytically active for oxidization of H_2S. Since commercial catalysts are usually supplied in the oxide form, a method of preparation was required before any commercial catalyst could be used as a catalyst for this research.

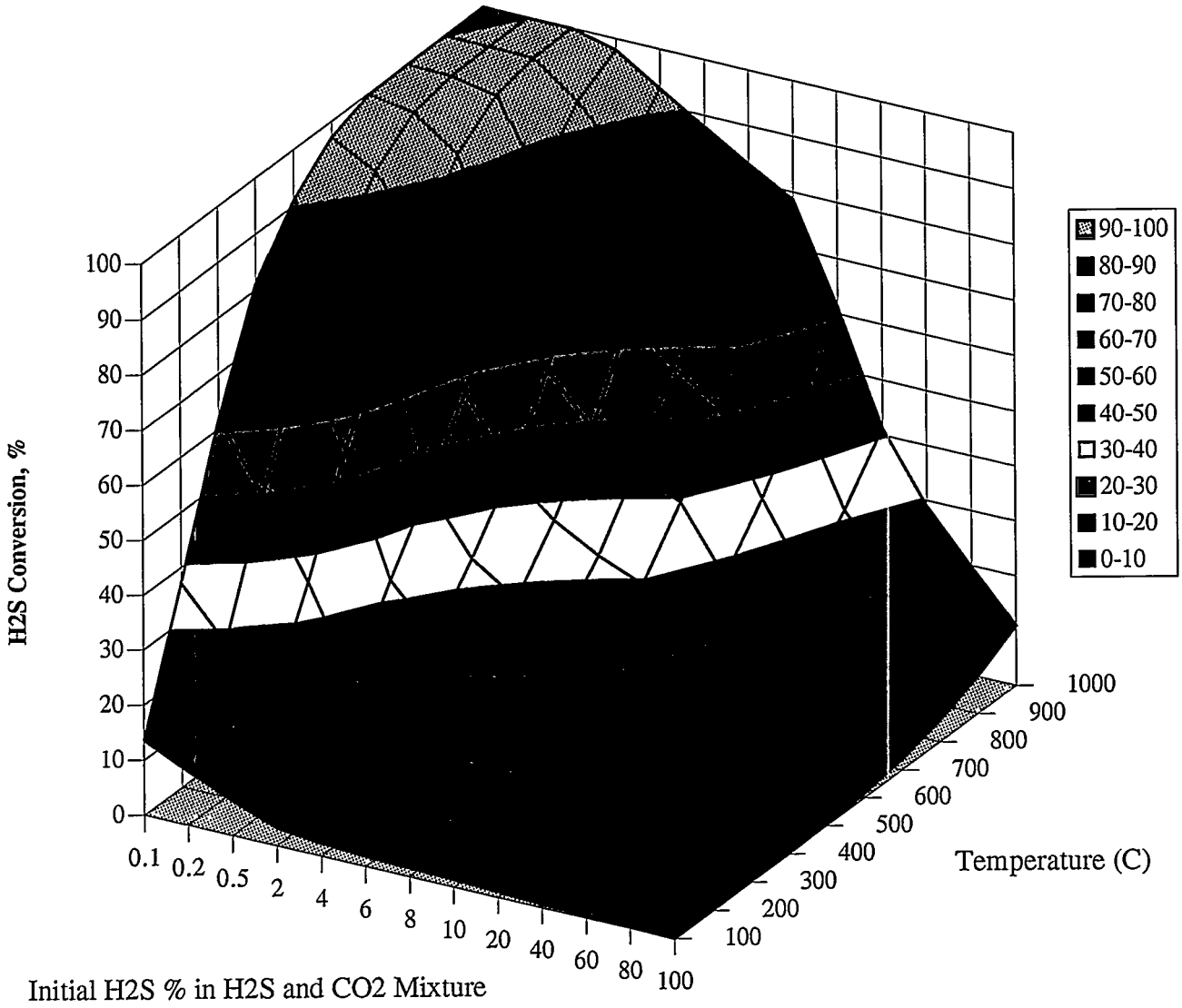

Figure 2-12. The Effect of the Initial H2S % on H2S Conversion at 1 atm

Apparatus

A thermogravimetric analyzer (Du Pont Instruments 951 TGA) was used to establish the method of preparation for the Co-Mo sulfided catalyst from the Co-Mo oxide that was obtained from the manufacturer. A schematic diagram of the TGA is shown in Figure 2-13.

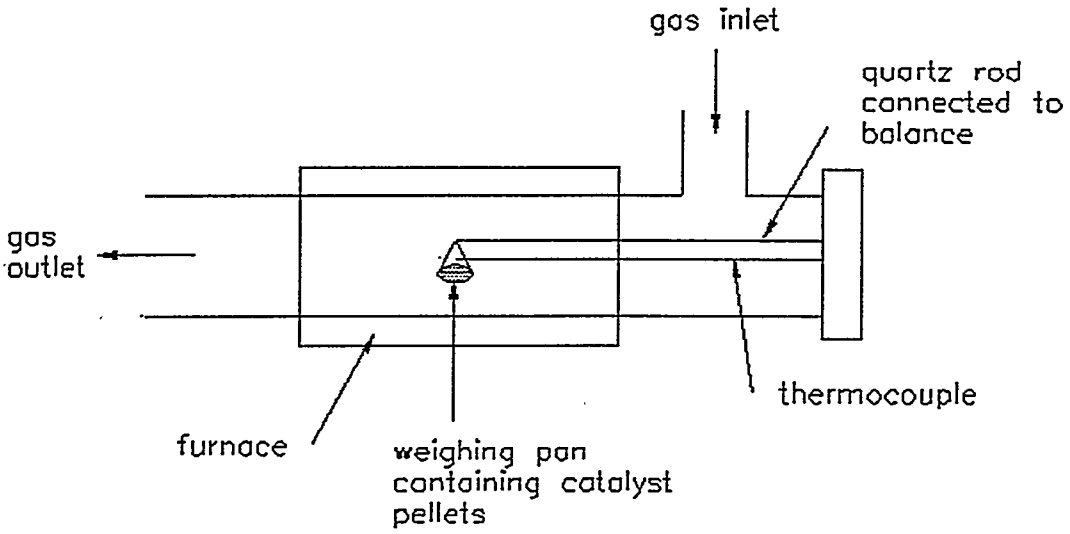

Figure 2-13. Schematic diagram of thermogravimetric analyzer.

The commercially manufactured cobalt-molybdenum catalyst (Crosfield 465, 1/20" extrudate) was obtained compliments of Crosfield Catalysts. The Co-Mo catalyst was reported to contain 5% cobalt oxide and 20% molybdenum oxide by weight with the balance

consisting of γ-alumina. Its average apparent bulk density was 41 lb/ft^3 (0.658 g/cm^3), the specific area was 255 m^2/g, and the pore volume was 0.58 cm^3/g. Sample sizes of approximately 40 mg consisting of several Co-Mo oxide catalyst pellets were used to determine to what extent they could be reduced and sulfided.

Procedure

A standard method of preparation for Co-Mo sulfide does not exist in the literature since preparation of sulfide catalysts is not usually accomplished by any standard procedure but under special conditions of preparation. In most cases, however, active sulfide catalysts can often be prepared by converting the respective oxides to sulfides. For this reason, the TGA was used to obtain a suitable method of preparation for the sulfide catalyst.

First, approximately 40 mg. of the catalyst pellets were placed on the weighing pan at the end of the balance rod in order to cover the surface of the pan. The pellets were purged under N_2 at a temperature of 200°C to remove the moisture inside the pellet pores. The purging step was stopped when the recorded weight reached a steady value. Next, the pellets were reduced using a pure flow of hydrogen at a temperature of 500°C. Once again, the H_2 flow was stopped when the weight reached a steady value. Finally, the pellets were sulfided using a pure flow of hydrogen sulfide at a temperature of 500°C. The flow was also stopped when the weight reached a steady value. For each step, the weight change and temperature above the surface of the pellets were recorded.

Work Performed / Results Obtained

The results of the thermogravimetric analysis shown in Figure 2-14 indicate that the method for catalyst preparation consists of three steps. The first step, as depicted in Figure 2-14a consists of removing the moisture content of the oxide catalyst (approximately 8-9%) by purging for a period of 1 hour under N_2 at a temperature of 200°C.

Following the catalyst purge, the next step consists of reducing the catalyst under H_2 at a temperature of 500°C. An indication that reduction is taking place is a color change from blue to black. Figure 2-14b shows that 80% reduction was achieved after 3 hours of reducing using pure H_2 and 90% reduction after 24 hours. The percent reduction was calculated on a dry catalyst basis.

Figure 2-14c shows that the sulfidation step takes place quite rapidly. Within the first five minutes, the catalyst was sulfided approximately 20%. This percentage was calculated on a dry basis and only includes the amount of catalyst that was reduced. Additional sulfidation requires a longer amount of time and is not necessary since after the catalyst is sulfided 20%, it is capable of decomposing H_2S to produce elemental sulfur. This was confirmed by the observation of condensed elemental sulfur on the reactor walls at the exit of the furnace while the sulfidation experiment was running.

In using the method of preparation obtained from the TGA results for preparing the catalyst bed in the reactor, it was important to take into consideration the difference in apparatus which implied different mass transfer conditions. In the case of the TGA, there was little or no mass transfer limitation since the bulk gas concentration surrounding the catalyst

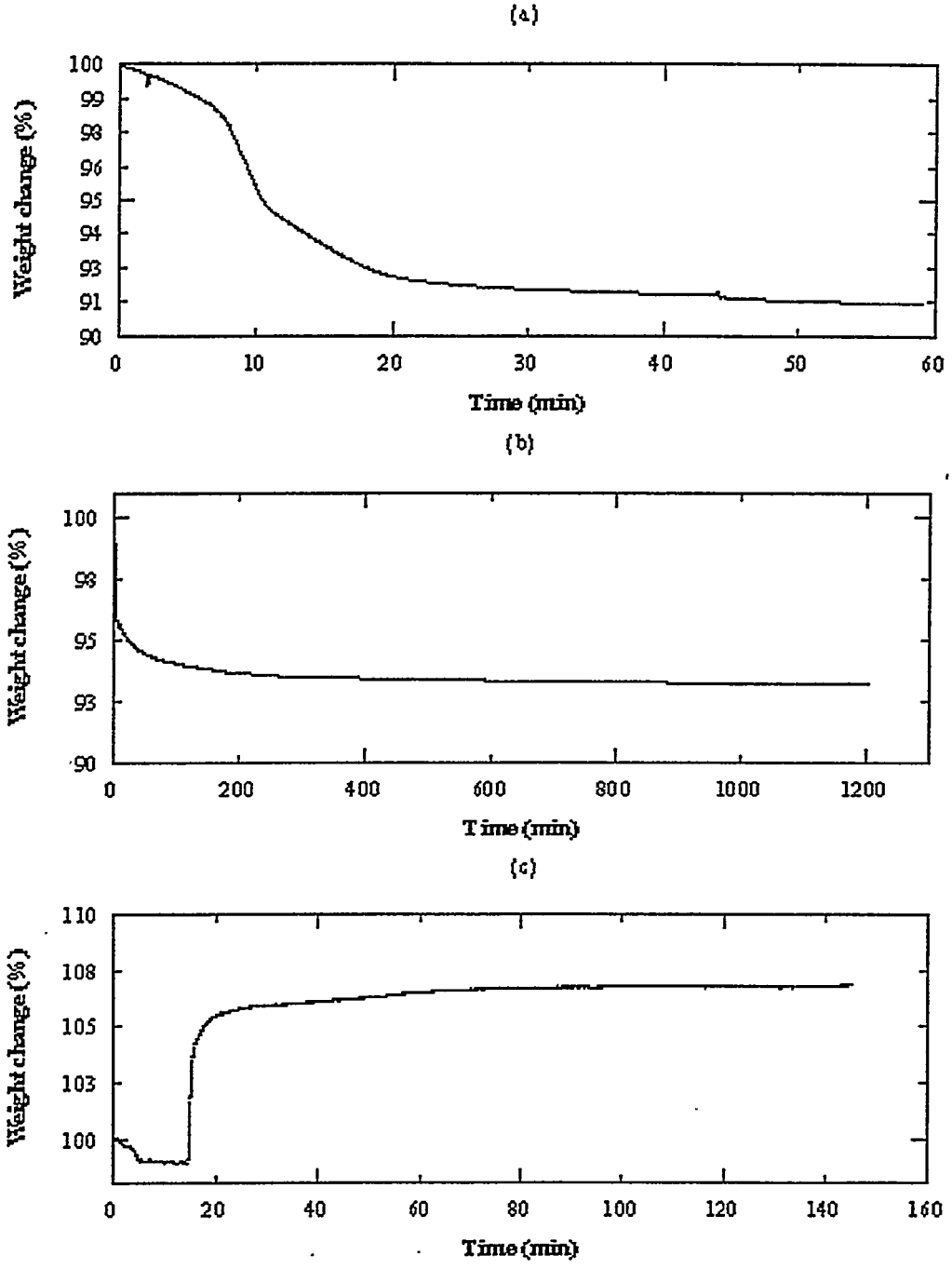

(a) Co-Mo Oxide Purge under N2, (b) Co-Mo Oxide Reduction under H2, and (c) Reduced Co-Mo Oxide Sulfidation under H2S

Figure 2-14. TGA History Plot

pellets was equal to the pure gas concentration. In the packed bed, however, mass transfer was slower due to the reduced bulk gas concentration within the voids of the bed. For both the purging and reduction steps, this difference in mass transfer conditions made little difference in the final product since the times were long enough to allow complete purging and reduction of the catalyst bed. However, since it was shown in the TGA that sulfidation takes place very rapidly, the difference in mass transfer conditions was a factor which could not have be overlooked. Therefore, the sulfidation time in the TGA could not have been used to determine the time at which to start the decomposition process after the sulfidation was complete.

It was important to know the sulfidation time in the reactor since a certain amount of the total H_2S input into the reactor was not involved with the decomposition reaction. It was assumed that during the sulfidation process, the H_2S was completely utilized for sulfidation (i.e. sulfidation and decomposition were assumed to take place in succession and not simultaneously). The time for the sulfidation process in the reactor was therefore approximated by observing the appearance of a flame at the exit of the vent tube. Since H_2S is flammable, it was assumed that the breakthrough of H_2S from the catalyst bed, as indicated by the presence of a blue flame at the exit of the vent tube, signified that the catalyst was no longer taking up any H_2S for sulfidation. From the experiments, the sulfidation time was found to be approximately 30 minutes for an H_2S flow rate of 0.2 cfh.

Task #3 - Testing of Packed Bed Catalytic Reactor

Apparatus

A schematic diagram of the experimental apparatus is shown in Figure 2-15. Flow rates of CO_2 (99.99% purity), H_2S (liq. grade, 99.5% purity), H_2 (zero grade, <1ppm impurities), and N_2 (oxygen-free grade) were controlled by calibrated rotameters. In order to obtain a mixture of the reactants, the gases were first passed through a stainless steel manifold before entering into the reactor. The bypass loop was used when the gases were being turned on in order to obtain a stabilized flow before switching the flow to the reactor. All of the tubing that came into contact with the H_2S gas was stainless steel tubing ¼" in diameter. A sampling port fitted with a septum was placed at the exit of the reactor in order to be able to withdraw samples of the product gas to be analyzed in a GC while the experiment was running. It is important to note that the condensates were not tested since these condensed in the cool end of the reactor before the sampling port.

The GC (Varian 3300) was equipped with a thermal conductivity detector and a 36' long, 1/8" diameter stainless steel column packed with a porous polymer (80/100 mesh Hayesep A) to detect CO_2, H_2S, CO, H_2, CH_4, SO_2, COS, and CS_2. The GC was calibrated using pure samples of these compounds. The temperature program used was as follows: a constant temperature of 30°C was held for 8 minutes followed by a 10°C/min. ramp up to 140°C. This temperature was held for 20 minutes after which the column was cooled back to a temperature of 30°C before injecting the next sample.

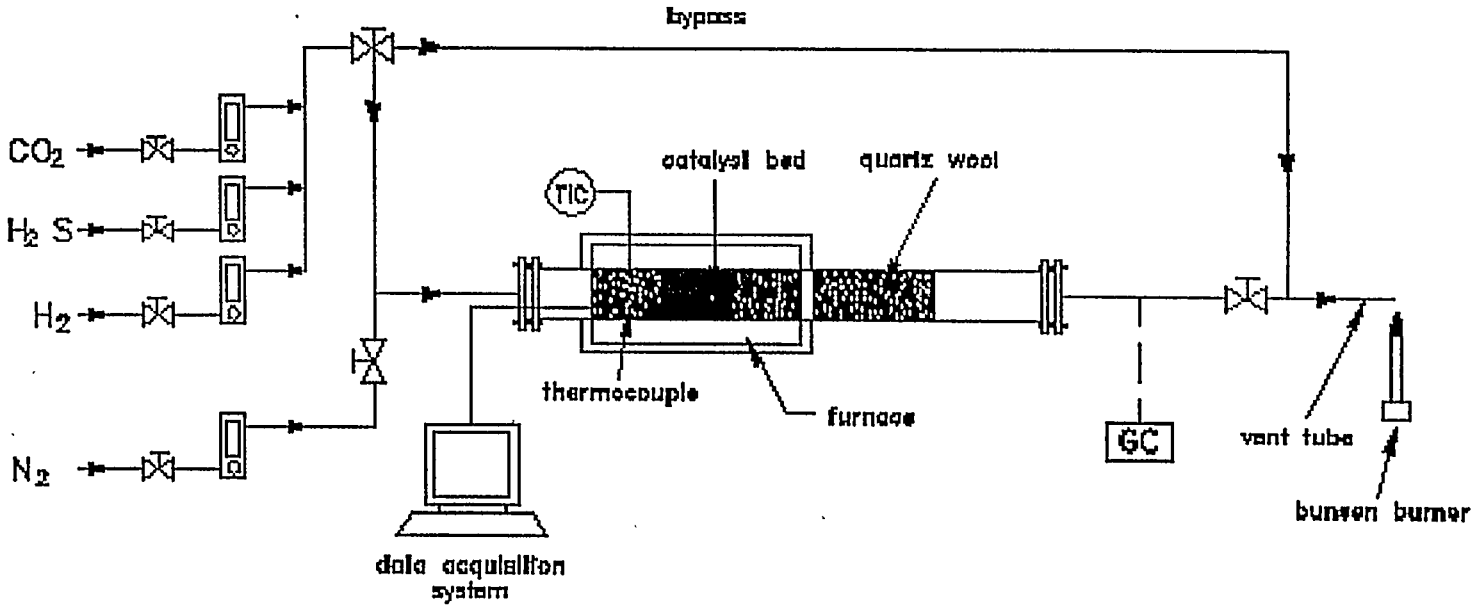

Figure 2-15. Schematic Diagram of Experimental Apparatus

The reactor consisted of a 30" long, 1" I.D. quartz tube reactor with a rubber gasket and stainless steel flange on each end. The first 12" of the reactor was heated by a horizontal tubular furnace while the rest of the length of the reactor was packed with quartz wool and exposed to ambient air. The catalyst bed was centered in the heated section of the reactor and supported on both sides by a plug of quartz wool.

In order to control and monitor the temperature inside the catalyst bed, a shielded K type Watlow thermocouple was inserted through the entrance of the reactor and positioned ¼" off the centerline and approximately half way along the length of the bed. This thermocouple was connected to a data acquisition system to record the temperature history inside the reactor. A second K type thermocouple, with an exposed junction, was used to measure the surface temperature of the reactor. It was connected to a Watlow temperature controller which turned the furnace on and off according to a set point temperature which was adjusted to obtain the desired temperature in the reactor.

For odor control, the product gases were incinerated at the exit of the reactor by a bunsen burner and vented in a fumehood.

Procedure

The reactor was packed such that one third of the reactor volume that was heated in the furnace contained the catalyst bed. This corresponded to a bed weight of approximately 45-50g. Initially, N_2 was flowed through the bed at a flow rate of 1 ft^3/hr (cfh) at a temperature of 200°C in order to purge the catalyst.

After the catalyst had been completely purged, while maintaining the N_2 flow, the cool

end of the reactor was opened to remove the moisture that had evaporated from the catalyst bed in the heated section of the reactor and condensed in the cool section. After the moisture was removed, a plug of quartz wool was placed in the reactor just at the exit of the furnace as a condenser to collect the sulfur produced. The bed was then heated to a temperature of 500°C and the H_2 passed through the reactor at a flowrate of 0.1 cfh in order to reduce the catalyst.

Once the catalyst had been reduced, flow to the reactor was stopped and the temperature was adjusted to the desired reactor temperature. One of the key considerations for sulfur-recovery systems is to operate the catalytic reactor at as low a temperature as possible that is still above the sulfur dew point. This is in order to avoid condensation of the sulfur vapor (which occurs at a temperature of 444.6°C) at lower temperatures and sintering of the catalyst at higher temperatures both of which would result in blockage of the catalyst pores and reduction of catalytic activity. Therefore, in order to neglect sintering effects as well as sulfur condensation, the experiments were carried out at temperatures of 465, 490, 515, and 575°C.

Once the desired temperature was reached in the reactor, H_2S was flowed through the reactor at a flow rate of 0.2 cfh until the catalyst was sulfided. Afterwards, while maintaining the H_2S flow, the CO_2 flow was turned on and adjusted to 0.2 cfh to obtain an equimolar reactant mixture of H_2S and CO_2. It was important to sulfide the catalyst at the same temperature that the decomposition was to take place since the decomposition took place immediately after sulfidation of the catalyst. Adjustment of the temperature after sulfidation would have resulted in a non-isothermal reaction. The reaction was run for three hours while

the data acquisition system recorded the temperature history within the catalyst bed. Sample volumes of 0.5 ml were taken at regular intervals from the reactor exit and injected into the GC for analysis. It is important to note that due to the variety in compounds that were being tested for in the GC, only a qualitative analysis could be performed. No information could be obtained on the exact composition of the products obtained since the ability of the column and the detector to detect all of the desired compounds posed significant limits on the GC's overall accuracy in predicting the exact concentration of each compound. Therefore, a qualitative analysis that was based on comparing the retention times of the peaks eluted for the gas samples to the retention times of the standards was performed.

After the experiment was over, the bed was cooled to room temperature under a flow of N_2. Then, while maintaining the N_2 flow, the cool end of the reactor was opened to remove the quartz wool plug and the sulfur that had collected on the inside walls of the reactor. This was accomplished using carbon disulfide (CS_2 - 99.95% purity) to dissolve the sulfur on the walls as well as on the quartz wool plug. The CS_2 solution containing the sulfur was collected in a beaker and the CS_2 evaporated in order to weigh the sulfur product.

Work Performed / Results Obtained

Sulfur Conversion:

The percent sulfur conversion in the packed bed catalytic reactor was calculated according to the following formula:

$$\% \ conversion = \frac{H_2S_i - H_2S_f}{H_2S_f} \ x \ 100$$

The numerator is represented by the total weight of sulfur collected and the denominator is represented by the total amount of sulfur input into the reactor minus the sulfur used to sulfide the catalyst. The denominator was calculated by multiplying the H_2S flow rate by the total time for the experiment minus the sulfidation time. The assumption was made that a negligible amount of sulfur-containing side-products was formed in the reactor.

The temperature was determined from the temperature history plot for each experiment. In each case, there was a temperature peak at the beginning of each experiment which corresponded to a change in temperature of approximately 40°C. This is probably due to the initial heat of adsorption of the reactant gases that are initially adsorbed onto the surface of the catalyst where they proceed to react. After this temperature rise, the temperature inside the reactor fell to an average constant value. This temperature was recorded as the reaction temperature for each experiment.

The experimental results for the percent conversion of H_2S to elemental sulfur with CO_2 present are shown in Figure 2-16. The experimentally determined conversions increase with temperature. Figure 2-16 also shows the equilibrium conversions as calculated from the thermodynamic analysis. However, for the temperature range tested, the experimental conversions were less than the equilibrium conversions meaning that equilibrium was never reached.

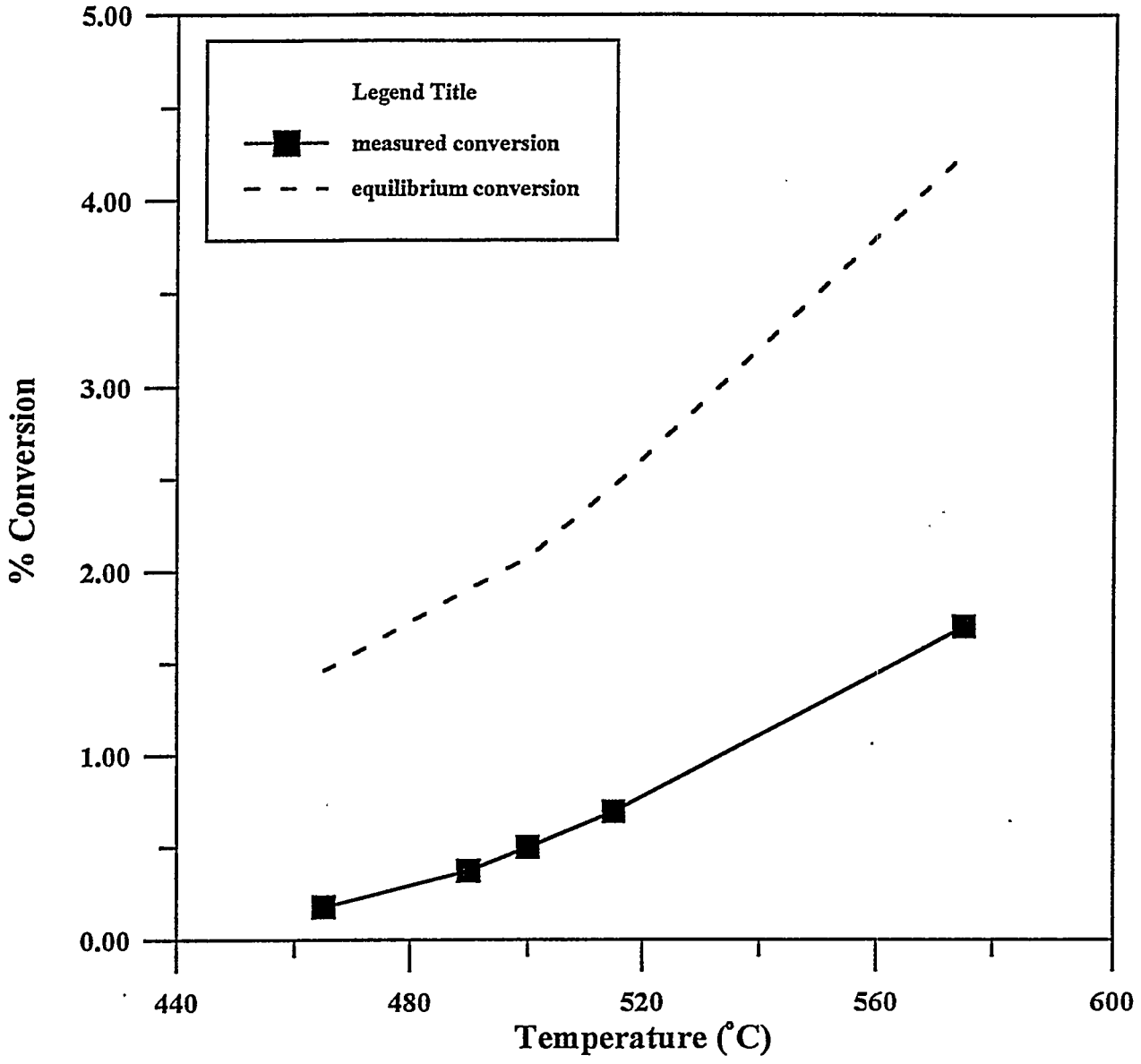

Figure 2-16. Measured vs. Equilibrium Conversion for the H_2S Decomposition Reaction with CO_2

Therefore, calculations were performed to determine the specific rate coefficient, κ, for the H_2S decomposition reaction with CO_2 at the different temperatures. The reaction order of the H_2S decomposition reaction in the presence of CO_2 was assumed to be 2nd order kinetics based on previous work by Darwent and Roberts (Darwent and Roberts, 1971) for temperatures lower than 625°C. The equation for κ, which is derived in Appendix D is as follows:

$$\kappa = \frac{F}{A(\frac{P}{RT})^2}[\frac{(2+3/2x)^2}{1-x} + \frac{9}{2}x + \frac{21}{2}\ln(1-x) - 4]$$

where x = percent conversion
F = molar flow rate of H_2S, mol/s
A = interfacial area, cm^2
P = pressure, atm.
T = temperature, °K

Figure 2-17 shows that the calculated specific rate coefficient increases with temperature. From these results, the parameters for the Arrhenius equation were calculated. Figure 2-18 shows an Arrhenius plot for the H_2S decomposition reaction with CO_2. The Arrhenius equation was found to have the following form:

$$\kappa = 3776e^{\frac{-118}{RT}}$$

where the activation energy has the units of kJ/mol.

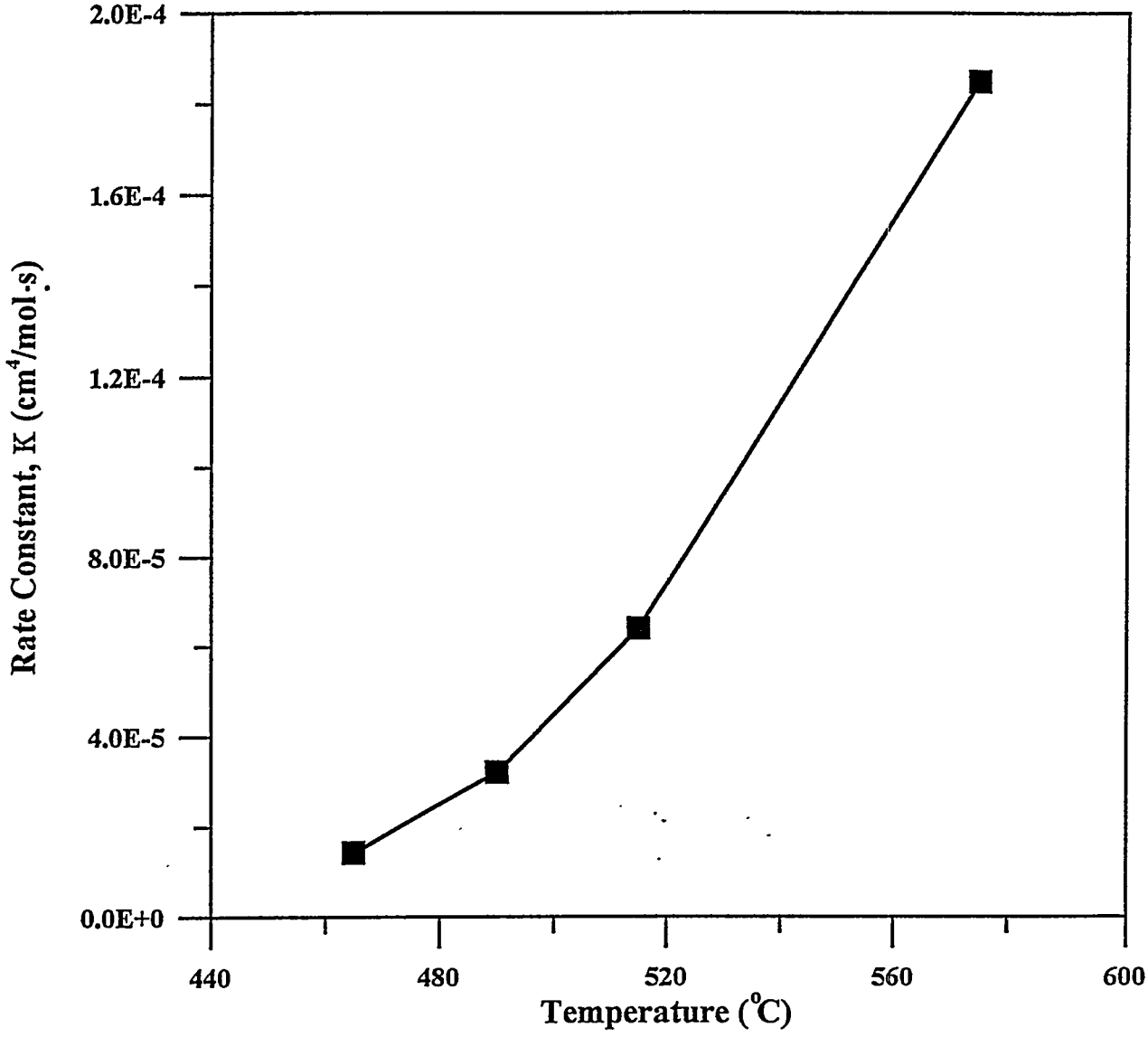

Figure 2-17. Specific Rate Coefficient for the H_2S Decomposition Reaction with CO_2

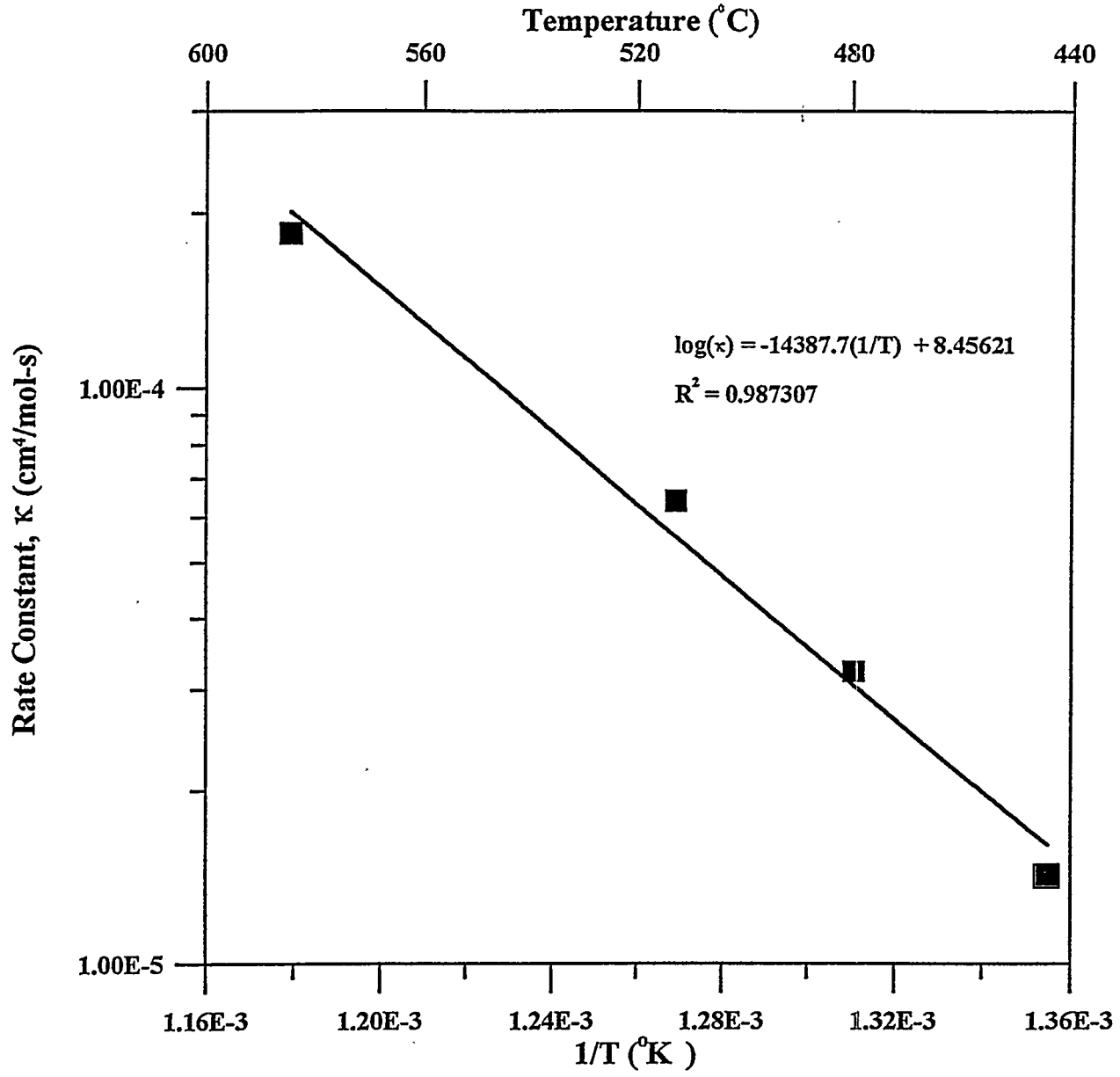

Figure 2-18. Arrhenius Plot for the H_2S Decomposition Reaction in the Presence of CO_2

Effect of CO_2:

In order to confirm the theoretical prediction that CO_2 increases the amount of H_2S decomposition, an experiment was done without CO_2. The results in Table 2-2 show that the actual experimental results confirmed the theoretical results that CO_2 increases the conversion. In addition, the percentage approach to equilibrium was calculated as the ratio of actual conversion to the average theoretical conversion and is an indication of how close the reaction approached equilibrium. One can see that the presence of CO_2 increased the reaction efficiency which signifies that the H_2S decomposition reaction was closer to equilibrium in the presence of CO_2.

This is probably an indication that the H_2S decomposition reaction is the rate-limiting step which is in agreement with Towler and Lynn's conclusion.

Table 2-2. Comparison of Equilibrium and Experimental Percent Conversion at 500°C.

	H_2S decomposition without CO_2	**H_2S decomposition with CO_2**
Experimental conversion	0.093 %	0.501 %
Equilibrium conversion	0.562 %	2.078 %
Percentage Approach to Equilibrium	16.5 %	24.1 %

Discussion on Equilibrium:

As was shown in Table 2-2, for the temperatures studied, the catalytic reactor was not

operating at equilibrium conditions. This implies that $t_e/t_r>1$, where t_e = the time required to reach equilibrium and t_r = the residence time in the catalyst bed. The residence time in the bed was calculated from the superficial velocity through the reactor and was found to be approximately 16 seconds (see Appendix E). The actual residence time would be longer due to the flow resistance as the gases pass through the catalyst bed. Therefore, in order to operate at equilibrium, either the reactor must be designed to ensure that $t_e > 16$ sec (a factor must be included to take into account the void volume of the bed through which the gases pass) or the gas flow rates must be decreased. Since it is likely that the gas flow rate would be set by the preceding process steps, the reactor would have to be designed such that $t_e < t_r$.

Results from Gas Chromatographic Analysis:

Two sets of results were obtained for the GC analysis, one for an experiment run with CO_2 and one for an experiment run without CO_2. A background run performed using air showed that N_2, O_2, and CO_2 are present due to their initial presence in the syringe that was used to draw out the gas sample. Some overlapping of the peaks occurred due to the length of time required for some of the peaks to elute, namely, H_2S and COS. However, it was possible to observe a pattern thus allowing a conclusion to be drawn about the compounds present. The similarity of the runs indicate that steady state was reached inside the reactor within the time that the experiment was allowed to run.

The results from the experiment run without CO_2 showed that H_2S and small amounts of H_2 were present in the product stream. The results from the experiment run with CO_2 show that the product stream consisted of CO_2, H_2S, CO, and COS. H_2 was not present

indicating that it was entirely used up by the water-gas shift reaction. Therefore, it may be concluded that the water-gas shift reaction is a fast reaction and not the limiting step in this process. This is in agreement with Towler.

Out of the three possible side-products that could have been formed, only COS was detected by the GC. In the thermodynamic analysis, SO_2 was not predicted to be likely to be formed so it is reasonable that it was not detected in the GC analysis.

Sampling of the products from these reactions presents an especially difficult task due to equilibrium considerations. As for COS and CS_2, one was predicted to form but only the other was detected in the GC. In the case of CS_2, it is possible that CS_2 formed in the reactor and then either condensed out since the boiling point of CS_2 is 46.3°C or decomposed before reaching the sampling port. In the case of COS, since it was not predicted to be produced in the reactor, it is possible that it formed in the gaseous product stream before reaching the sampling port. In both cases, due to the fact that the sampling port is located downstream where the gases where at at lower temperature, at least enough time is allowed to pass for the product gases to re-equilibrate at a lower temperature than what is in the reactor. It is for this reason that the results from the GC analysis cannot be compared with those listed in Table 2-1 since the temperature at which the gases were sampled is not the same as the temperature inside the reactor. Due to the complexity of the gaseous mixture, there may have been some reactions that re-equilibrated thus altering the composition of the product gas stream.

Ideally, in order to compare experimental results with those determined theoretically, it would have been necessary to sample the product gases inside the reactor. This would have been difficult since the limitations of the column used in the GC would have prevented

accurate analysis of the product gases at the temperature inside the reactor.

Due to all of these considerations, it was not possible to determine a reaction mechanism for the formation of the side-products.

PHASE 3: INTEGRATED SYSTEM DESIGN

Introduction

In the first phase, it has been shown feasible to produce a stream of H_2S gas by dissolving CaS, generated by the novel coal feeder process, in an acetic acid solution and then using CO_2 as a stripping gas. In the second phase, studies were conducted to evaluate the production of elemental sulfur by the reaction:

$$2\ H_2S \rightleftharpoons 2\ H_2 + S_2$$

$$CO_2 + H_2 \rightleftharpoons CO + H_2O$$

Catalysts such as molybdenum disulfide (MoS_2) and have been used. The above reaction has been shown to occur in the presence of MoS_2 at temperatures as low as 475°C.

The third phase consisted of combining these two systems into an integrated bench scale pilot system.

Experimental Apparatus and Procedure

The results from the previous two phases was integrated into a small scale production unit suitable for longer term studies. The diagram of the system is shown in Figure 3-1. Both the stripping and the reacting process was conducted continuously.

Calcium sulfide (CaS) was added into a mixing tank with acetic acid solution by a

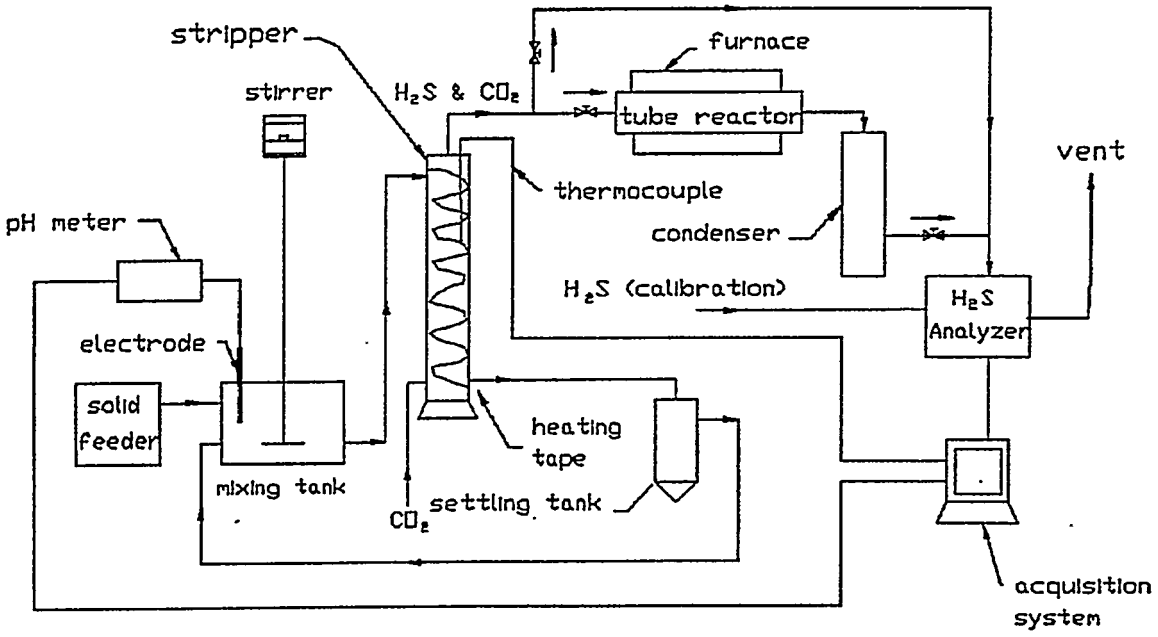

Figure 3-1. Diagram of Apparatus for Integrated System Studies

dry solid feeder and would be dissolved. The solution that came from the mixing tank was passed counter-current to the flow of CO_2 gas in a stripper to produce a gas mixture of H_2S and CO_2. The continuous stripping process was conducted to produce an effluent flow with a constant H_2S/CO_2 ratio. The stream of H_2S and CO_2 gas then entered the tube reactor at high temperature to form elemental sulfur according to the reaction above. The remaining solid in the solution was precipitated out in the settling tank and the supernate was returned to the mixing tank. The elemental sulfur formed was condensed and weighed to calculate the reaction conversion. The pH value of the solution in the mixing tank, the temperature of the stripper, and the H_2S concentration of the stream entering and exiting from the tube reactor was measured during the continuous process and recorded by the data acquisition system.

The conversion of H_2S to elemental sulfur versus reaction temperature in the tube reactor was performed. Temperature up to 950°C was applied to the tube reactor without the catalyst.

In general, the results of these integrated verification studies would provide valuable data for the design of future lager pilot systems.

Work Performed and Results Obtained

An analysis was done to determine the effect of H_2S:CO_2 ratio on the theoretical equilibrium conversion at 950°C using the Stanjan program. Figure 3-2 shows the variation in the percent conversion with the percent H_2S in CO_2 at atmospheric pressure. The amount of S_8 was not take into account because at 950°C S_2 is the predominant sulfur species.

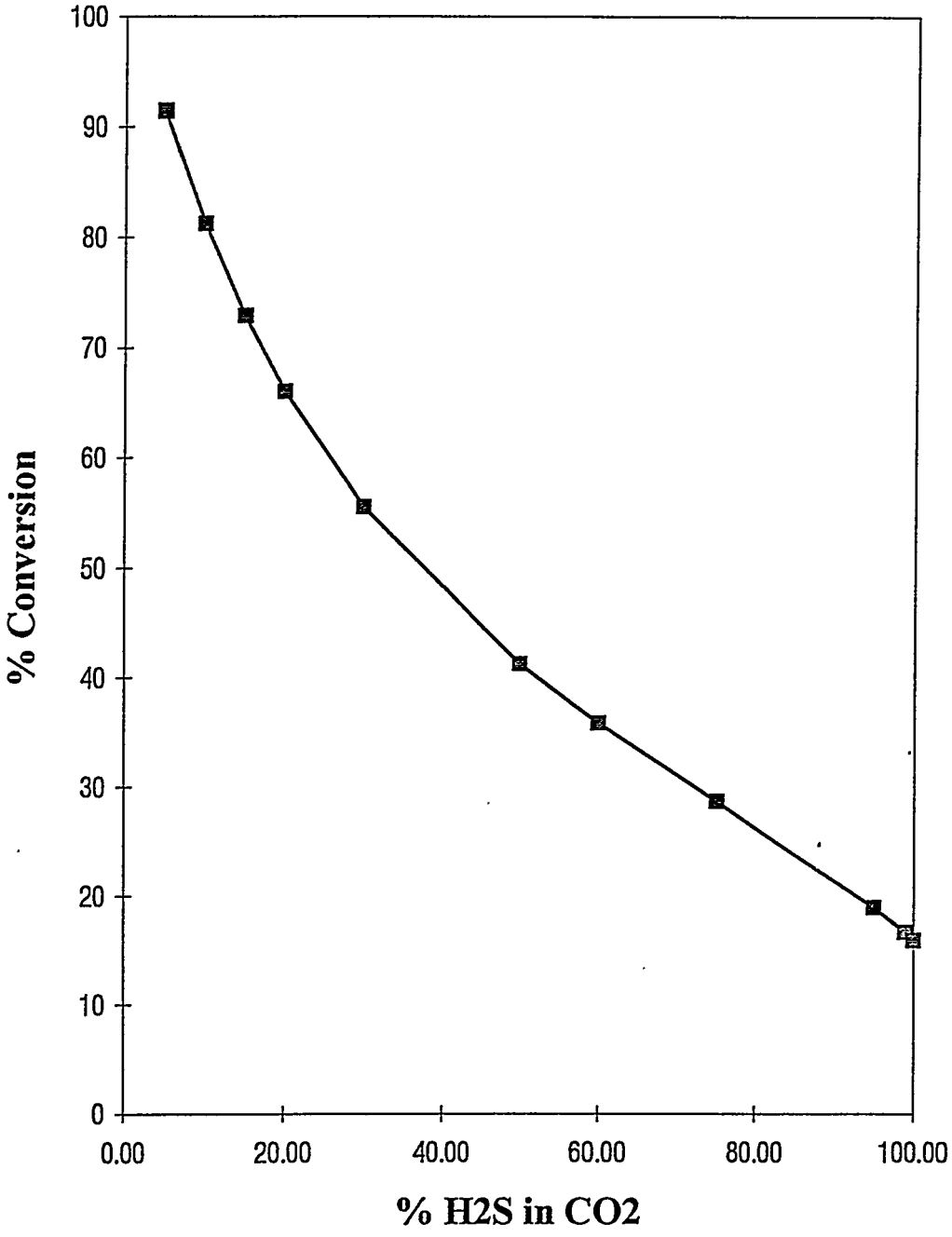

Figure 3-2. Effect of H_2S:CO_2 Ratio @ 950°C

Two sets of experiments were conducted. The continuous stripping process were conducted to produce an effluent flow with a constant H_2S/CO_2 ratio. 0.3, 0.5, 1.0, 1.5 and lpm CO_2 flowrates were used to stripping H_2S out of the solution while keeping the liquid flow rate as a constant, 170 lpm. H_2S concentration from the stripper was controlled to be around 5% or 10% in CO_2 by adjusting the feed rate of CaS. The gas mixture of H_2S and CO_2 then passed through the tube reactor at 950°C without catalyst to form elemental sulfur. The conversion of H_2S to elemental sulfur was calculated by measuring the weights of elemental sulfur collected by sulfur condensers. The results of the experiments are shown in Table 3-1 and Figure 3-3. One can see that the conversion decreases with increasing gas flowrate (or, conversion increases with increasing gas residence time) as would be expected.

Table 3-1. The conversion of H_2S to elemental sulfur at 950°C

CO_2 flowrate (lpm)		0.3	0.5	1.0	1.5	2.0
residence time in the reactor (sec)		54.0	32.5	16.3	10.8	8.1
conversion (%)	5% H_2S in CO_2	39.7	33.9	23.9	7.4	6.1
	10% H_2S in CO_2	51.1	47.0	39.5	-	37.7

Comparing Fig. 3-2 with Fig. 3-3, one can see that for the CO_2 flow rate range tested, the actual conversion was less than the theoretical conversion meaning that the equilibrium was never reached.

Another experiment was conducted at 700°C with Co-Mo catalyst in the tube reactor in order to evaluate the effect of the catalyst on conversion. The liquid flow rate, CO_2 flow

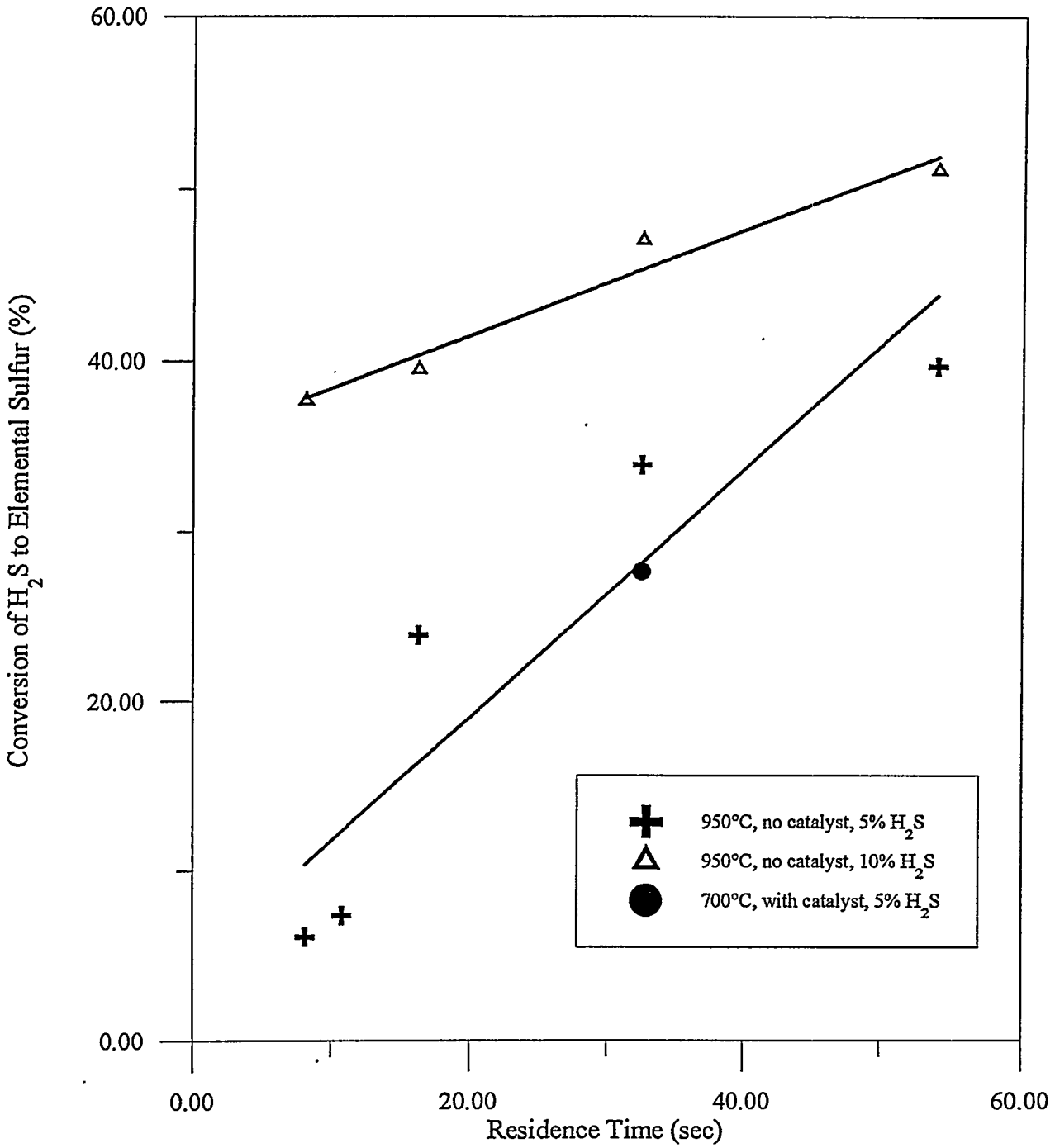

Figure 3-3. Conversion vs. Residence Time

rate and the feed in H_2S concentration were 170 lpm, 0.5 lpm and 5% respectively. The conversion under these operating condition was 27.6%. The theoretical equilibrium conversion at 700°C is 52.38% which means that equilibrium was not reached. This result indicates the importance of the catalyst in promoting conversion at a lower temperature. This result is compared to the data for no catalyst shown in Figure 3-3. As can be seen, the conversion with the Co-Mo catalyst at 700°C is similar to that found (and represented by a linear relationship in Figure 3-3) at 950°C where no catalyst was used.

CONCLUSIONS

The results from this work can be summarized as follows:

Phase #1: Basic Studies

Task 1: CaS Solubility Studies

Solubility of CaS in acetic acid solutions with different concentrations at different temperatures were measured. Solubility of CaS in acetic acid increases with increasing both the acid concentration and the solution temperature.

Task 2: H_2S Stripping Studies

Stripping experiments were conducted in a batch stripping column. A mathematical model was derived to calculate mass transfer coefficients at different stripper operating conditions. These conditions include acid concentration, liquid temperature and CO_2 flow rate. CO_2 can strip as much as 95% of the H_2S out of solution, depending on the conditions. The mass transfer coefficient increases with increasing CO_2 flow rate. The effect of acid concentration and stripper temperature on the mass transfer coefficient is not obvious. The theoretically calculated mass transfer coefficient was compared with the experimental measured data, and the agreement was found to be reasonable.

Task 3: $CaCO_3$ Regeneration Studies

The liquid solution from the stripper outlet was investigated in terms of regenerating $CaCO_3$. Particle formation and growth as a function of residence time and pH were measured by a Coulter Counter Particle Size Analyzer and observed under a microscope. An analysis of the amount of Calcium recovered versus pH was performed. These results indicate that

adjusting pH of the resulting solution.may not be an effective way to precipitate a substantial amount of $CaCO_3$ after stripping

Phase #2: Elemental Sulfur Production Studies

A thorough review of the literature concerning the production of elemental sulfur was performed. An experimental investigation was performed at different operating conditions for the reaction:

$$2\ H_2S \rightleftharpoons 2\ H_2 + S_2$$

$$CO_2 + H_2 \rightleftharpoons CO + H_2O$$

The following three separate tasks were performed.

Task 1: Thermodynamic Analysis

The theoretical equilibrium conversions were calculated using the Stanjan program. The analysis was done to determine the effect of three different parameters: temperature, pressure, and H_2S:CO_2 ratio.

Task 2: Catalyst Preparation

A suitable method of preparation for Co-Mo sulfide catalyst was obtained using a thermogravimetric analyzer.

Task 3: Testing of Packed Bed Catalytic Reactor

Experiments were conducted in the tube reactor packed with Co-Mo catalyst. The results show that higher sulfur conversions can be obtained by using an equimolar mixture of H_2S and CO_2 instead of H_2S alone. The results also show that sulfur conversion increases with increasing temperature. These conclusions can be summarized as:

(1) It was experimentally found that the Co-Mo sulphided catalyst was a good candidate

for the decomposition of H_2S to elemental sulfur. In the presence of CO_2, the conversion of H_2S to elemental sulfur increased significantly. The experimental values were reasonably close to the thermodynamic equilibrium limits.

(2) It was experimentally demonstrated that the present catalytic process produced a significant amount of sulfur, CO and H_2. The H_2S conversion level of about 4% was still lower than the industrial interest at the present experimental temperature of 550°C, requiring a recycle and/or two reaction zones.

Phase #3: Integrated System Design

The results from the previous two phases were integrated into a small scale production unit suitable for long term studies. Both the stripping and the reacting process were conducted continuously. The results showed that the conversion of H_2S to elemental sulfur decreases with decreasing gas residence time. The presence of a sulfided Co-Mo catalyst improved conversion at temperatures of 700°C to those levels measured at temparatures of 950°C without a catalyst.

While the results of this project indicate that the impact of the water-gas shift reaction on hydrogen sulfide decomposition is very positive, additional consideration and experimentation is needed in order to develop a method for the continuous formation and removal of elemental sulfur. The temperature limitations imposed by the use of effective catalysts means that the reactions must be carried out at temperatures below the sintering point, generally <600°C. At these temperatures, the reactions are limited by equilibrium considerations. Therefore, a multi-stage seperation method, or recycling system would be beneficial.

REFERENCES

Al-Shamma, L. M. and S. A. Naman, "Kinetic Study for Thermal Production of Hydrogen from H_2S by Heterogeneous Catalysis of Vanadium Sulfide in a Flow System." *Int. J. Hydrogen Energy*, vol. 14, no. 3, 173-179 (1989).

Al-Shamma, L. M. and S. A. Naman, "The Production and Separation of Hydrogen and Sulfur from Thermal Decomposition of Hydrogen Sulfide over Vanadium Oxide/Sulfide Catalysts." *Int. J. Hydrogen Energy*, vol. 15, no. 1, 1-5 (1990).

Bowman, M.G., Thermochemical Cycle for Splitting Hydrogen Sulfide, U.S. Patent Document 4,999,178, Mar. 12 1991.

Chivers, T., J. B. Hyne and C. Lau, "The Thermal Decomposition of Hydrogen sulfide over Transition Metal Sulfides." *Int. J. Hydrogen Energy*, vol. 5, 499-506 (1980).

Chivers, T. and C. Lau, "The Thermal Decomposition of Hydrogen sulfide over Alkali Metal Sulfides and Polysulfides." *Int. J. Hydrogen Energy*, vol. 10, no. 1, 21-25 (1985).

Chivers, T. and C. Lau, "The Thermal Decomposition of Hydrogen sulfide over Vanadium and Molybdenum Sulfides Catalysts in Quartz and Thermal Diffusion Column Reactors." *Int. J. Hydrogen Energy*, vol. 12, no. 4, 235-243 (1987).

Chowdury, A. I. and Eric L. Tollefson, "Catalyst Modification and Process Design Considerations for the Oxidation of Low Concentrations of Hydrogen Sulfide in the Natural Gas." *Can. J Chem. Eng.*, vol 68, 449-454, June (1990).

Dalai, Ajay K., Amitabha Majumdar, Aminul Chowdury and Eric L. Tollefson, "The Effects of Pressure and Temperature on the Catalytic Oxidation of Hydrogen Sulfide in Natural Gas and Regeneration of the Catalyst to Recover the Sulfur Produced." *Can. J Chem. Eng.*, vol 71, 75- 82, Feb. (1993).

Darwent, B. de B. and R. Roberts, "The Photochemical and Thermal Decomposition of

DOW Chemical Company, Thermal Research Laboratory, JANAF Thermochemical Tables, U.S. National Bureau of Standards, Washington, (1971).

Gamson, B.W. and R.H. Elkins, "Sulfur from Hydrogen Sulfide", *Chem. Eng. Prog.*, Vol.49, No.4, pp. 203-215, (1953).

Gangwal, S. K., W. J. McMichael and T. P. Dorchak, "The Direct Sulfur Recovery Process." *Environmental Progress*, vol. 10, no. 3, 186-191 (1991).

George, Z.M., "Kinetics of Cobalt-Molybdate-Catalyzed Reactions of SO_2 with H_2S and COS and the Hydrolysis of COS", *J.Catalysis*, Vol. 32, pp. 261-271, (1974).

Ghosh, Tushar K. and Eric L. Tollefson, "A Continuous Process for Recovery of Sulfur from Natural Gas Containing Low Concentrations of Hydrogen Sulfide." *Can. J. Chem. Eng.*, vol. 64, 960-968, Dec. (1986).

Goar, B. G., Goar, Allison & Associates Inc., "Sulfur Recovery Technology." *Energy Progress*, vol. 6, no. 2, 71-75 (1986).

Hasatani, M., Yuzawa, M., Yashima, I. "Desulfurization of Hot Fuel Gases Produced from Low-Grade Solid Fuels with Calcium Oxide Pellets." Kagaku Kogaku Ronbunshu, 9 (2), 166-171 (1983).

"Hydrogen Sulfide", *Proc. R. Soc. Ser. A*, Vol.216, p. 344, (1953).

Kaloidas, V. E. and N. G. Papayannakos, "Kinetics of Thermal, Non-Catalytic Decomposition of Hydrogen Sulfide." *Chemical Engineering Science*, vol 44, no. 11, 2493-2500 (1989).

Kaloidas, V. and N.G. Papayannakos, "Hydrogen Production from the Decomposition of Hydrogen Sulfide. Equilibrium Studies on the System $H_2S/H_2/S_i$, (i=1,...,8) in the Gas Phase", *Int. J. Hydrogen Energy*, Vol.12, No.6, pp. 403-409, (1987).

Katsumoto, Masayuki, Kazuo Fueki and Takashi Mukaibo, "An Investigation of the Gas-solid Interface Reaction." *Bulletin of the Chemical Society of Japan*, vol. 46, 3641-3644 (1973).

Kotera, Y., "The Thermochemical Hydrogen Program at N.C.L.I." *International Journal of Hydrogen Energy*, vol. 1, 219-220 (1976).

Liptak, B.G., Environmental Engineers' Handbook: Vol. II: Air Pollution, Chilton Book Company, Radner, PA, p. 998, (1974).

Mitchell, P.C.H., "Sulphide Catalysts: Characterization and Reactions Including Hydrodesulfurization" In: Catalysis Volume 4, The Royal Society of Chemistry, London, p. 176, (1981)

Paushkin, Ya. M., "Synthesis of Organic Compounds on the Basis of the Inorganic Compounds CO_2, H_2O, and H_2S." *Doklady Chemical Technology*, 61-66, Jan.-June (1988).

Perry, R.H. and D. Green, Perry's Chemical Engineers' Handbook, 6th ed., McGraw Hill Book Company, New York, (1984).

Rau, H., T.R.N. Kutty, and J.R.F. Guedes de Carvalho, "Thermodynamics of Sulfur Vapour", *J. Chem. Thermodynamics*, Vol.5, pp. 833-844, (1973).

Raymont, M. E. D., "Make Hydrogen from Hydrogen Sulfide." *Hydrocarbon Processing*, vol. 54, no. 7, 139-142 (1975).

Rendall, W.A., M.E. Moir, and J. Szarka, Removal of Hydrogen Sulfide from Gaseous Mixture and its Use in Manufacture of Sulfur, British UK Patent Document 2,248,444, Apr. 8 1992.

Roth, P, R. Löhr and U. Barner, "Thermal Decomposition of Hydrogen Sulfide at Low Concentrations." *Combustion and Flame*, vol. 45, 273-285 (1982).

Sheldon, R.A., Chemicals from Synthesis Gas: Catalytic Reactions of CO and H_2, D. Reidel Publishing Company, Dordrecht, Holland, (1983).

Steijns, M. and P. Mars, "The role of Sulfur Trapped in Micropores in the Catalytic Partial Oxidation of Hydrogen Sulfide with Oxygen.", *Journal of Catalysis*, vol. 35, 11-17 (1974).

Stull, D. R. and H. Prophet et al., *JANAF Thermochemical Tables.* Second Edition, Office of Standard Reference Data, National Bureau of Standards, Washington, D. C., June (1971).

Sugioka, M. and K. Aomura, "A Possible Mechanism for Catalytic Decomposition of Hydrogen Sulfide over Molybdenum Disulfide." *Int. J. Hydrogen Energy*, vol. 9, no. 11, 891-894 (1984).

Towler, G.P., Synthesis and Development of Processes for the Recovery of Sulfur from Acid Gases, Ph.D. Thesis, University of California, Berkeley, (1993).

Weisser, O. and S. Landa, Sulphide Catalysts, Their Properties and Applications, Academia-Publishing House, Prague, Czechoslovakia, p. 25, (1973).

Wender, I., "Catalysis in the Conversion of Synthesis Gas to Chemicals" In: Chemicals from Coal: New Processes, Critical Reports on Applied Chemistry, Vol.14, Society of Chemical Industry, John Wiley & Sons, Chichester, Great Britain, (1987).

West, J. R., "Sulfur Recovery." *Kiri-Othmer Encyclopedia of Chemical Technology*, 3rd edition, Editor: Martin Grayson et al., vol. 22, 276-289, Wiley, New York (1984).

Ya. M., "Synthesis of Organic Compounds on the Basis of the Inorganic Compounds CO_2, H_2O, and H_2S", *Doklady Chemical Technology*, pp. 61-66, Jan-Jun (1986).

APPENDICES

Appendix A: Measured Data Versus Model Predictions for the H_2S Stripping Experiments

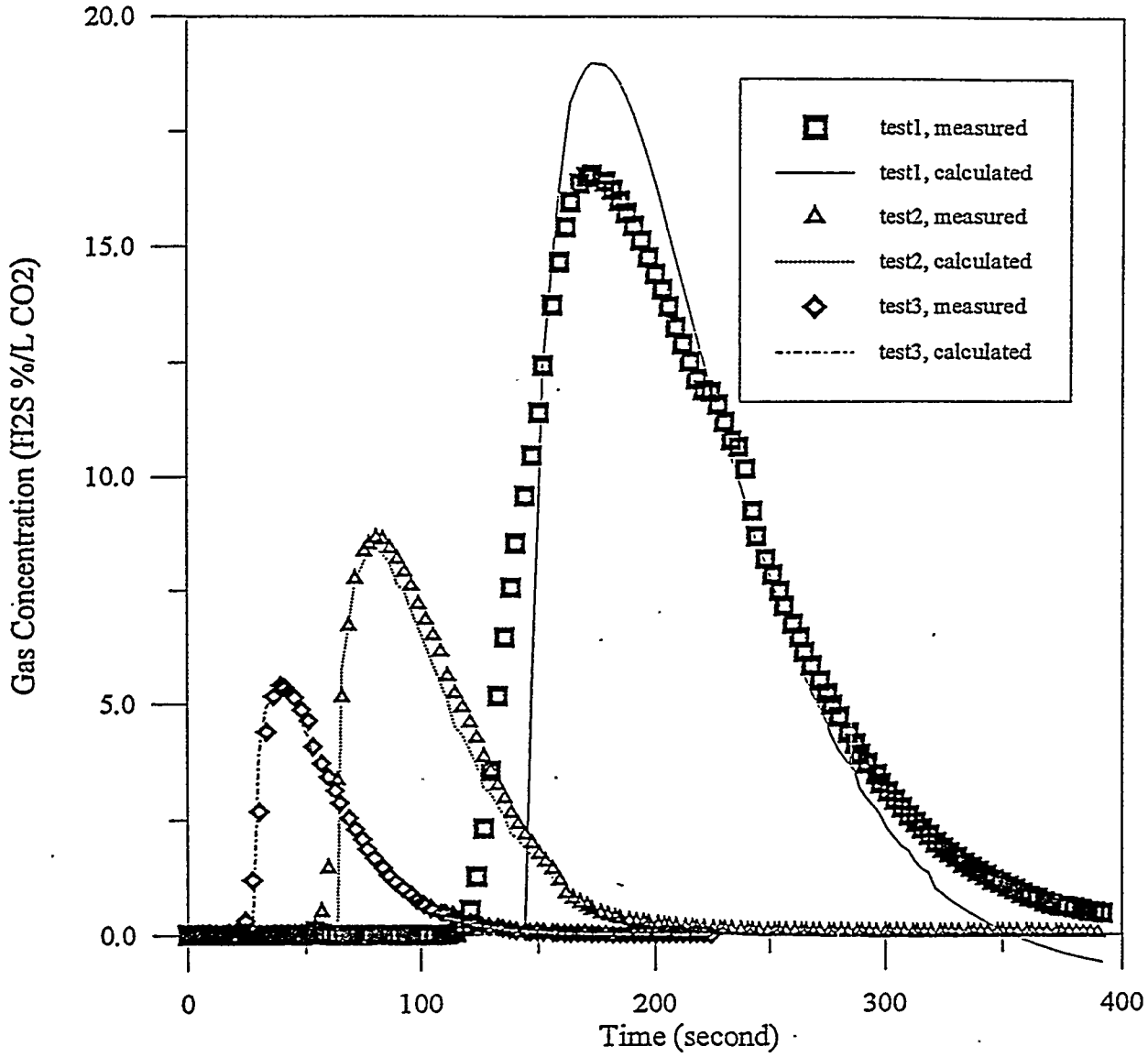

Measured vs Calculated H_2S Concentration
(for test 1 to 3)

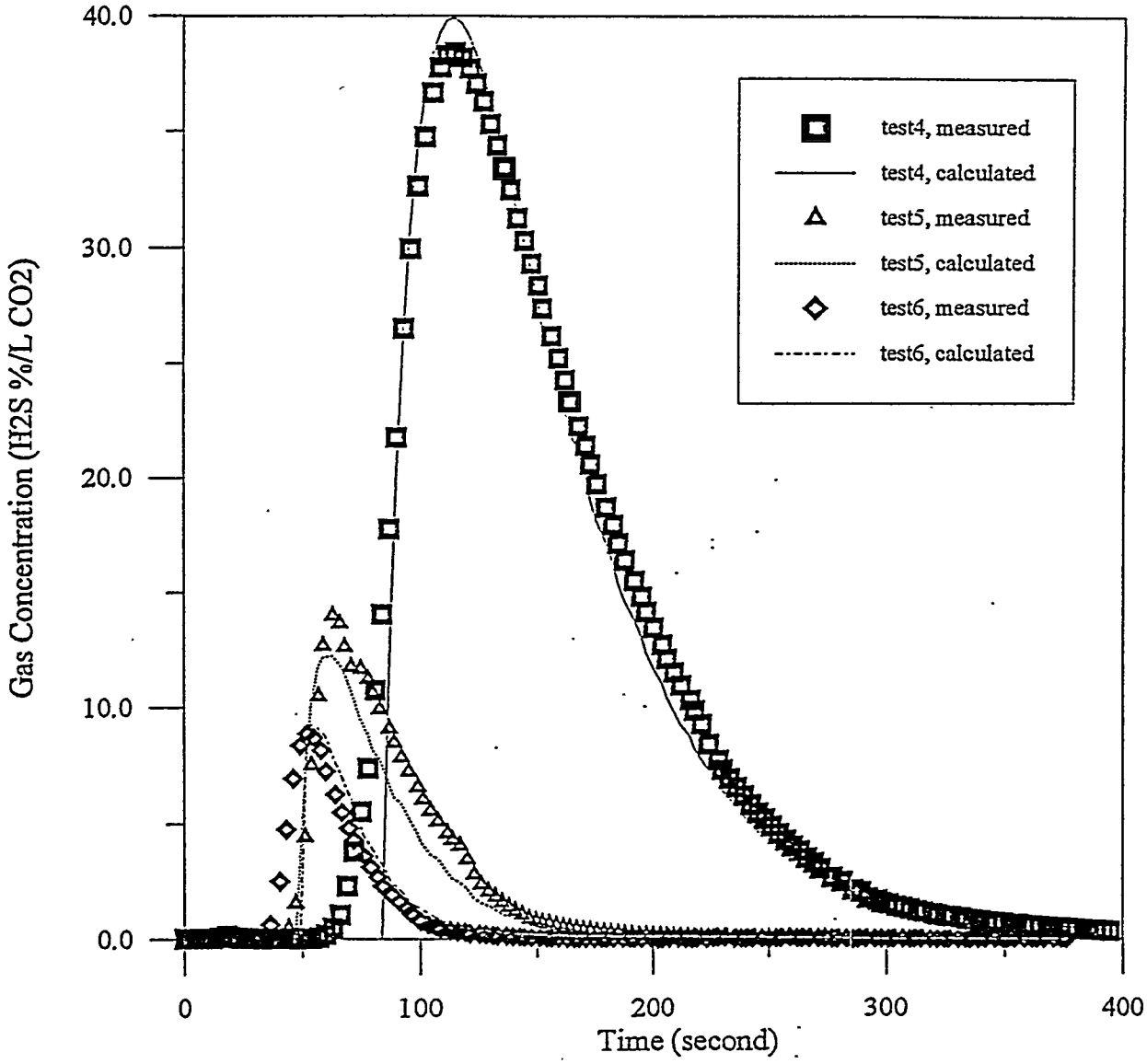

Measured vs Calculated H_2S Concentration
(for test 4 to 6)

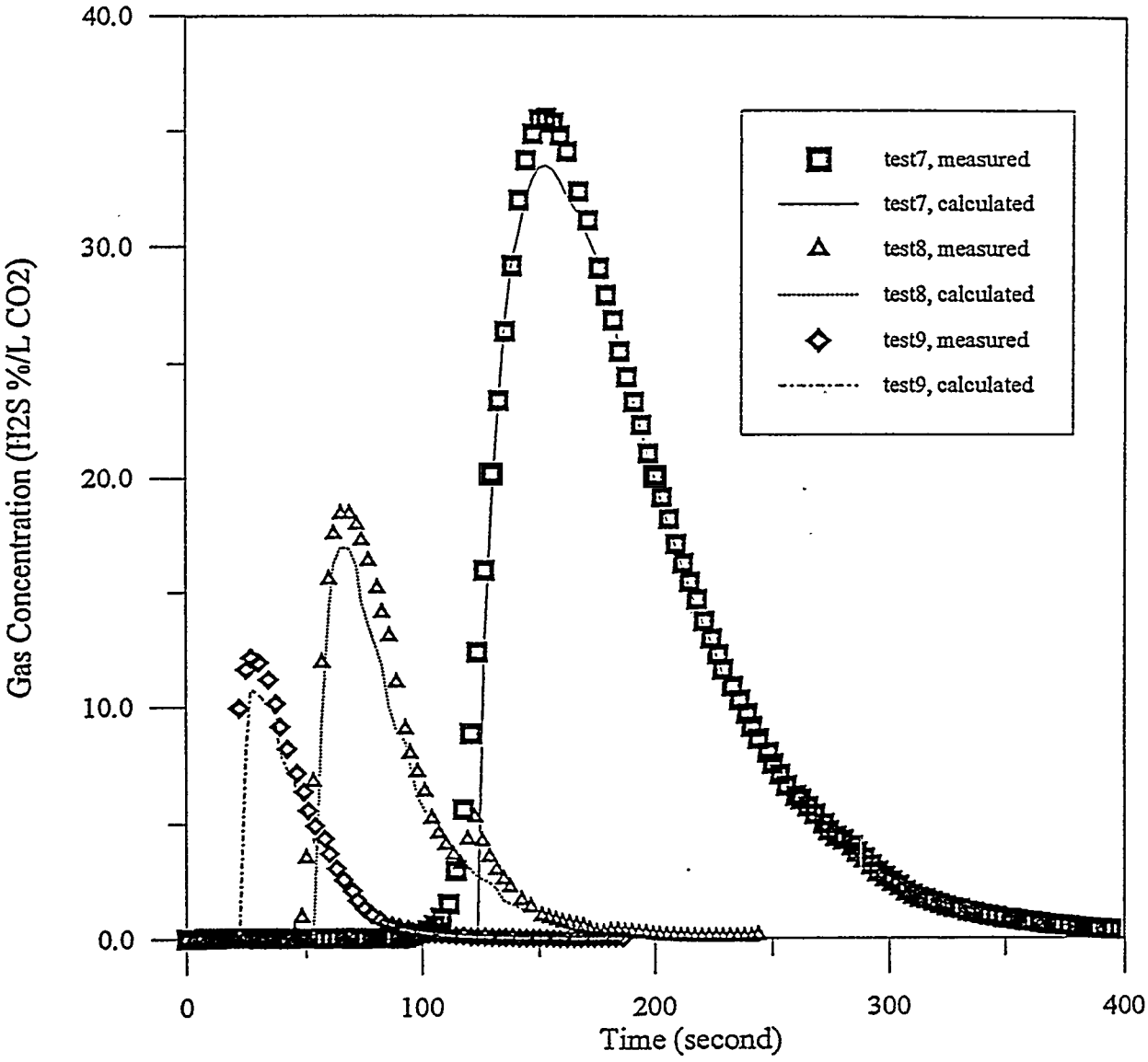

Measured vs Calculated H_2S Concentration
(for test 7 to 9)

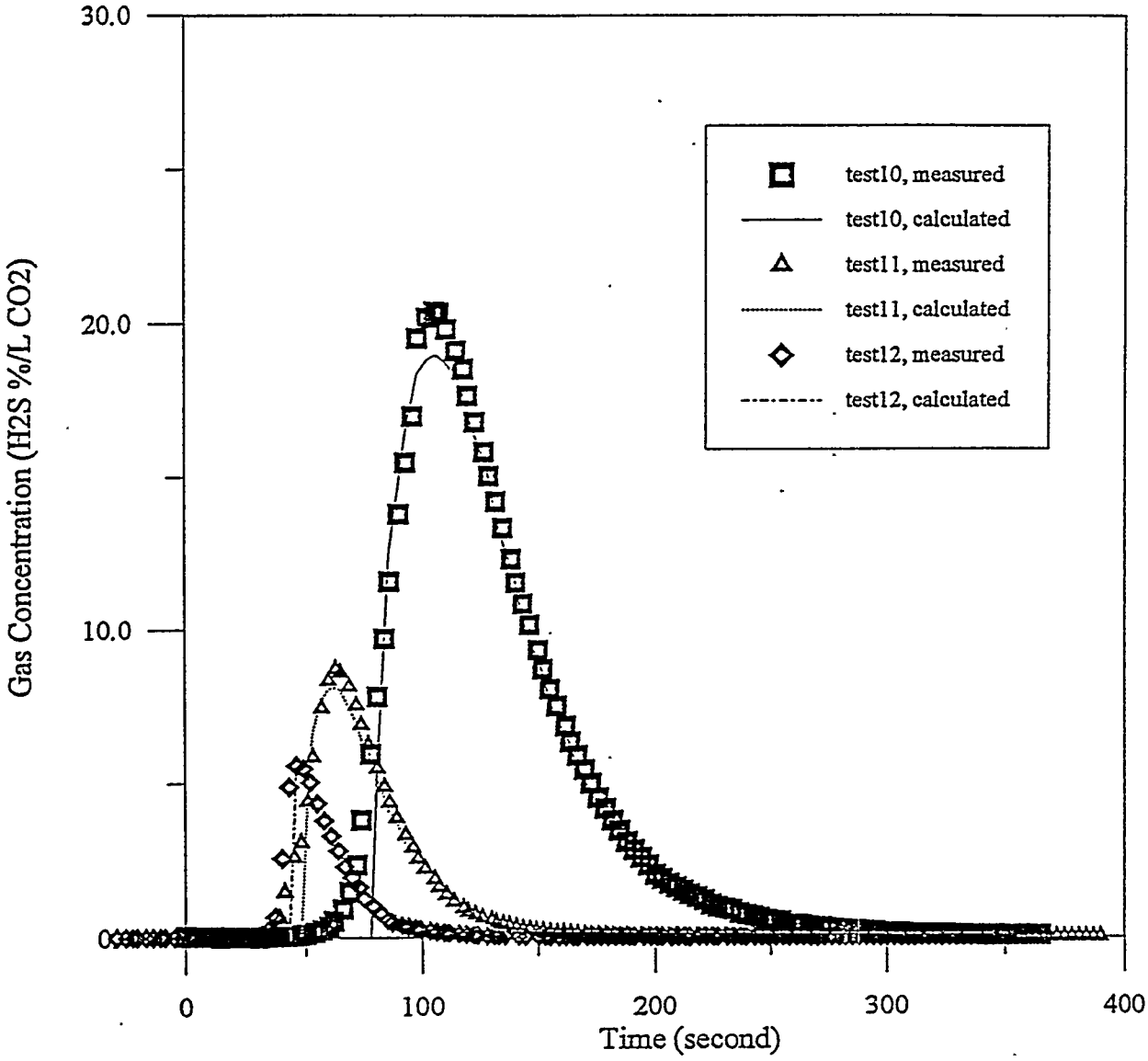

Measured vs Calculated H_2S Concentration
(for test 10 to 12)

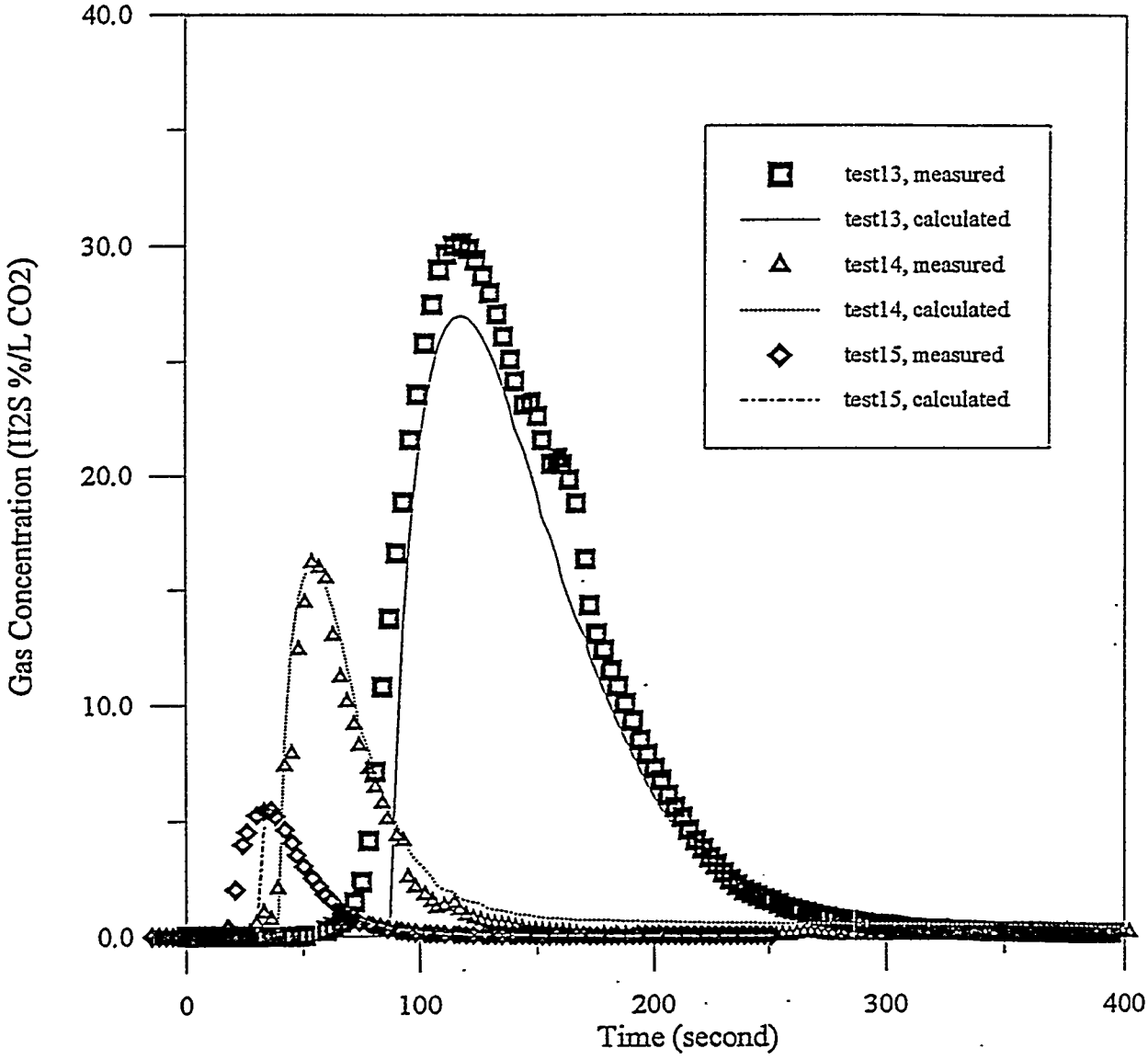

Measured vs Calculated H_2S Concentration
(for test 13 to 15)

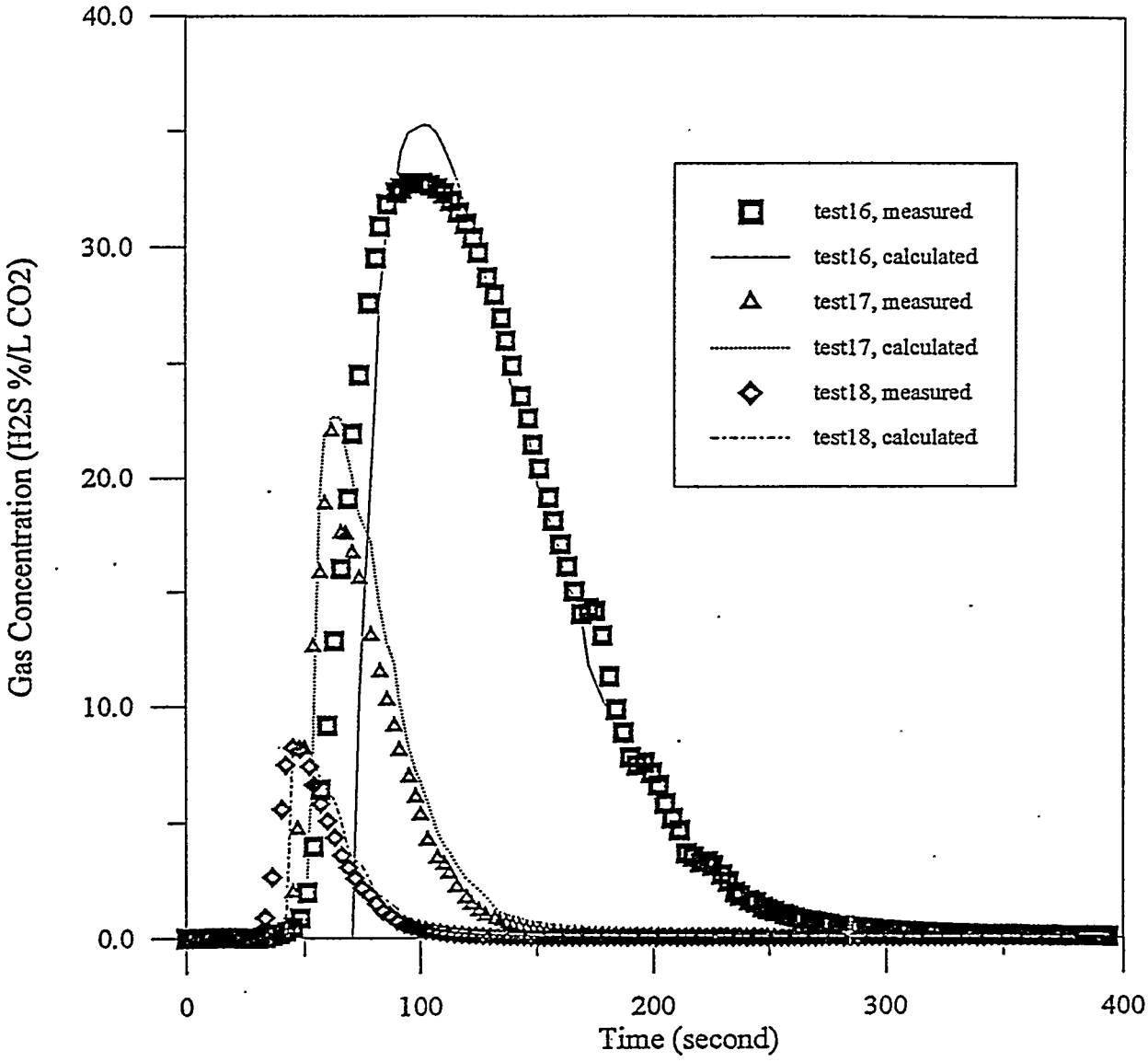

Measured vs Calculated H_2S Concentration
(for test 16 to 18)

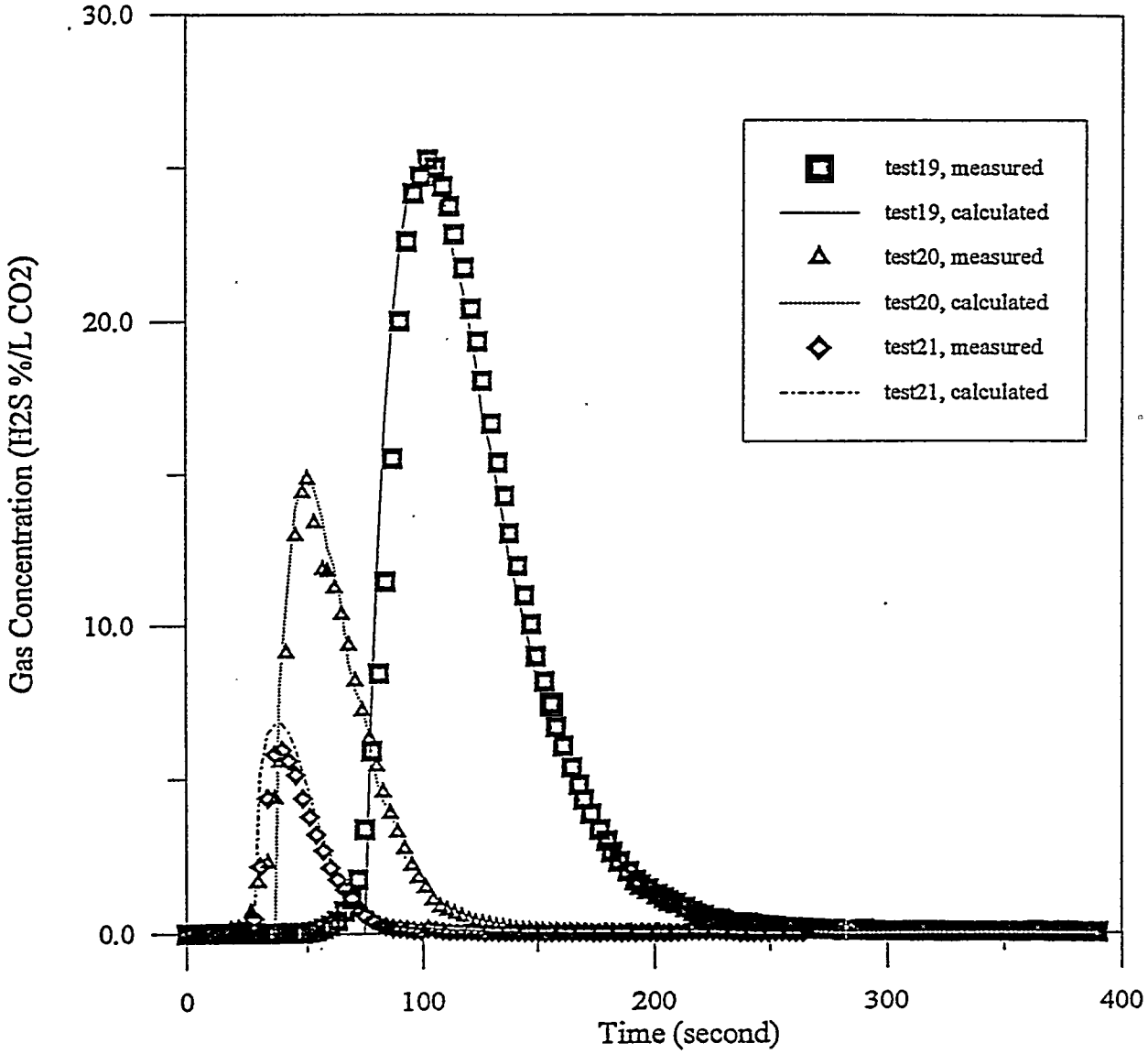

Measured vs Calculated H_2S Concentration
(for test 19 to 21)

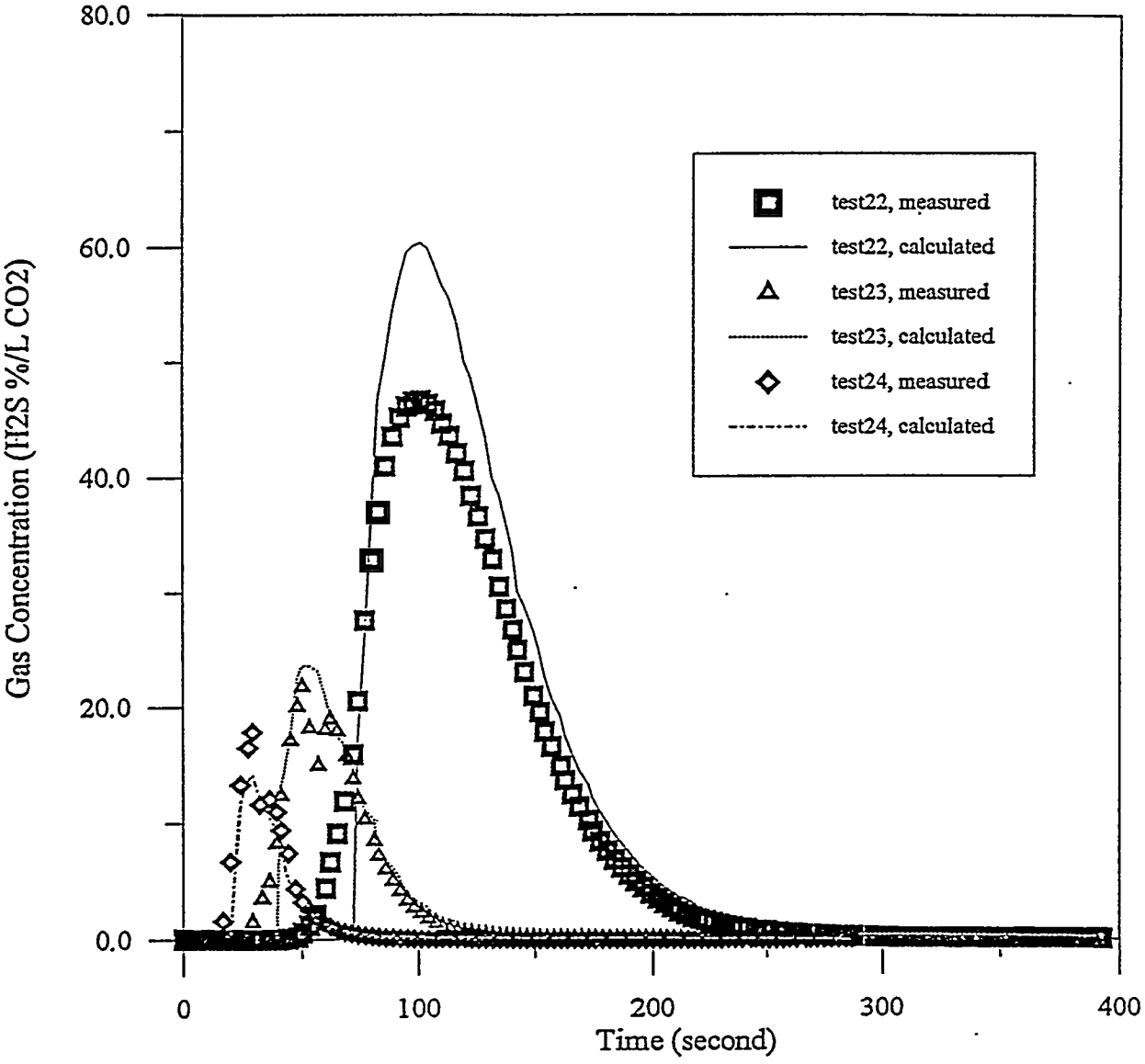

Measured vs Calculated H_2S Concentration
(for test 22 to 24)

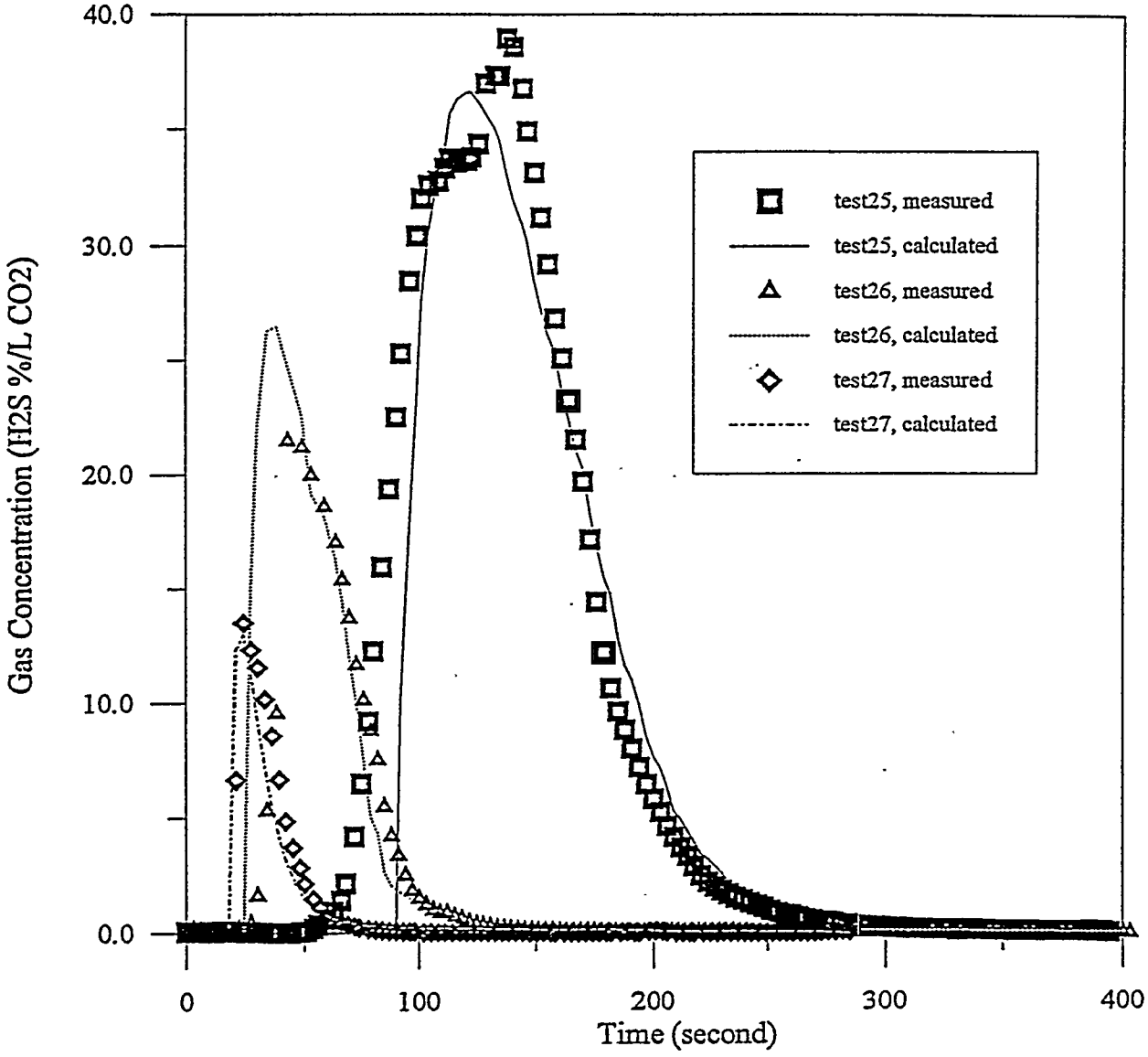

Measured vs Calculated H_2S Concentration
(for test 25 to 27)

Appendix B: Phase 1 Experimental Data; Calculation of Bubble Size; Calculation of Equilibrium Constants and Sulfur Mass Balance.

Solubility of CaS in CH_3COOH

Temperatur 20°C

Time	N	vol %	ml CH_3COOH in 50 ml of DI water	wt of CaS put in (gm)	wt of pan + filter paper		CaS dissolved (mg/50ml)	solubility (mg/100 ml)	pH
					initial	final			
11:05 - 11:50	0.05	0.29	0.15	0.2127	41.4567	-	-	-	11.30
12:10 - 12:40	0.1	0.57	0.29	0.6296	44.8925	45.3675	0.1546	0.3092	11.30
12:50 - 1:40	0.2	1.14	0.57	0.908	50.1795	50.5336	0.5539	1.1078	11.20
2:00 - 2:35	0.3	1.72	0.86	0.9616	46.8863	47.0147	0.8332	1.6664	8.30
2:35 - 3:05	0.4	2.29	1.15	1.0149	39.6831	39.8142	0.8838	1.7676	7.70
3:05 - 3.35	0.5	2.86	1.43	1.0589	43.1868	43.3582	0.8875	1.7750	7.12
3:50 - 4:20	0.7	4.01	2.01	1.2713	41.4294	41.709	0.9917	1.9834	5.95
4:20 - 4:50	1.0	5.72	2.86	1.3016	44.9462	45.2904	0.9574	1.9148	4.78
4:50 - 5:25	1.5	8.59	4.3	1.5631	39.6828	39.9899	1.2560	2.5120	4.65
5:35 - 6:10	2.0	11.45	5.73	1.7991	50.1817	50.6022	1.3786	2.7572	3.19

Solubility of CaS in CH_3COOH

Temperatur 40°C

Time	N	vol %	ml CH_3COOH in 50 ml of DI water	wt of CaS put in (gm)	wt of pan + filter paper		CaS dissolved (mg/50ml)	solubility (mg/100 ml)	pH
					initial	final			
11:25 - 12:00	0.05	0.29	0.15	0.3529	39.7080	39.8999	0.1610	0.3220	11.52
12:00 - 12:30	0.1	0.57	0.29	0.8184	43.1867	43.7030	0.3021	0.6042	11.52
12:35 - 1:15	0.2	1.14	0.57	1.0468	50.2028	50.7231	0.5265	1.0530	11.22
1:20 - 1:55	0.3	1.72	0.86	1.1311	46.8853	47.2419	0.7745	1.5490	9.28
1:55 -2:35	0.4	2.29	1.15	1.1827	41.4557	41.5832	1.0552	2.1104	8.66
2:35 - 3:05	0.5	2.86	1.43	1.2839	44.9733	45.2309	1.0263	2.0526	8.54
3:05 - 3:35	0.7	4.01	2.01	1.5154	39.7033	40.0169	1.2018	2.4036	7.78
3:45 - 4:20	1.0	5.72	2.86	2.1999	43.1917	43.7077	1.6839	3.3678	7.01
4:20 - 4:50	1.5	8.59	4.3	2.5211	50.2018	50.7547	1.9682	3.9364	5.41
5:00 - 5:30	2.0	11.45	5.73	3.6414	46.8665	47.4078	3.1001	6.2002	4.42

Solubility of CaS in CH_3COOH

Temperatur 60°C

Time	N	vol %	ml CH_3COOH in 50 ml of DI water	wt of CaS put in (gm)	wt of pan + filter paper		CaS dissolved (mg/50ml)	solubility (mg/100 ml)	pH
					initial	final			
10:50 -11:20	0.05	0.29	0.15	0.452	39.7177	40.001	0.1687	0.3374	11.19
11:20 - 11:50	0.1	0.57	0.29	0.8043	43.1935	43.7136	0.2842	0.5684	11.28
11:50 - 12:30	0.2	1.14	0.57	1.0963	50.2699	50.7915	0.5747	1.1494	11.19
12:30 -1:00	0.3	1.72	0.86	1.135	46.8884	47.202	0.8214	1.6428	10.06
1:05 - 1:35	0.4	2.29	1.15	1.2846	41.4496	41.6829	1.0513	2.1026	9.34
1:40 -2:10	0.5	2.86	1.43	1.4023	44.984	45.252	1.1343	2.2686	8.68
2:10 - 2:45	0.7	4.01	2.01	2.0715	39.708	40.1249	1.6546	3.3092	8.02
2:50 - 3:30	1.0	5.72	2.86	2.6473	43.1951	43.9067	1.9357	3.8714	8.35
3:35 - 4:05	1.5	8.59	4.3	3.189	50.273	50.9925	2.4695	4.9390	7.99
4:10 - 4:40	2.0	11.45	5.73	3.6356	46.8849	47.1565	3.3640	6.7280	7.82

TASK #2

Calculation of bubble size (CO2 in CH3COOH solution)

$$D_B^3 = \frac{6\ D\ \sigma}{g\ (\rho_l - \rho_g)}$$

(from Perry's Chemical Engineers' Handbook P18-68)

Where,

D_B - bubble diameter;

D - orifice diameter;

σ - the interfacial tension of the gas-liquid film;

ρ_l - the density of the liquid;

ρ_g - the density of the gas.

Surface tension of acetic acid at 30°C (from CRC Handbook of Chemistry and Physics)

wt% 1.00 f (mN/m) 68

density of CO2 gas @0°C, 1 atm: 0.1235 lb/ft^3

density of acetic acid solution (gm/cm^3)

	0%	2%	5%	10%	15%	20%
20°C	0.9982	1.0012	1.0055	1.0125	1.0195	1.0263
40°C	0.9922	0.9946	0.9982	1.0042	1.0099	1.0153

1 gm/cm^3 was used as the density of acetic acid solution

unit converstion

1 lb/ft^3 = 16.92 kg/m^3

g = 9.81 m/s^2

mN/m = 10^{-3} kg m/s^2/m=10^{-3} kg/s^2

$$D_B^3 = \frac{6\ D\ \sigma}{g\ (\rho_l - \rho_g)} = \frac{6\times75\times10^{-6}m\times68\times10^{-3}kg/s^2}{9.81m/s^2\ (10^3kg/m^3 - 0.1235\times16.02kg/m^3)}$$

$$D_B = 1.46 \times 10^{-3}\ \text{m} = 0.146\ \text{cm}$$

Calculation of equilibium constants (K_1, K_2) for chemical ractions:

$H2S \rightleftarrows HS^- + H^+ \ (K_1)$

$HS^- \rightleftarrows S^{2-} + H^+ \ (K_2)$

Calculation of K_1

	$H2S \rightleftarrows$	HS^- +	$H^+ \ (K_1)$
ΔGf^0 (kJ/mol)	-27.87	12.05	0
ΔH_f^0 (kJ/mol)	-39.75	-17.6	0

$$\Delta G^0 = (\sum v_i \ \Delta G^0_{f,i})_{products} - (\sum v_i \ \Delta G^0_{f,i})_{reactants}$$
$$= 12.05 + 27.87 = 39.92$$

$$\Delta H^0 = (\sum v_i \ \Delta H^0_{f,i})_{products} - (\sum v_i \ \Delta H^0_{f,i})_{reactants}$$
$$= -17.6 + 39.75 = 22.15$$

$-RT \ln K = \Delta G^0 \qquad R = 8.31 \times 10^{-3}$ kJ/K mol

$-8.31 \times 10^{-3} \times 298 \ \ln K_1^0 = 39.92$

$K_1^0 = 9.98 \times 10^{-8}$

$$\ln \frac{K^0}{K} = \frac{\Delta H^0}{R} \left(\frac{1}{T} - \frac{1}{T^0}\right)$$

$$\ln \frac{9.98 \times 10^{-8}}{K} = \frac{22.15}{8.31 \times 10^{-3}} \left(\frac{1}{T} - \frac{1}{298}\right)$$

20°C T = 293 K $\qquad K_{1,20} = 8.57 \times 10^{-8}$

40°C T = 313 K $\qquad K_{1,40} = 1.53 \times 10^{-7}$

60°C T = 333 K $\qquad K_{1,60} = 2.56 \times 10^{-7}$

Calculation of K_2

	HS^-	$\rightleftarrows$	S^{2-}	+	H^+ (K_2)
$_{\Delta}G_f^0$ (kJ/mol)	12.05		85.8		0
ΔH_f^0 (kJ/mol)	-17.6		33.0		0

$$\Delta G^0 = (\sum v_i \Delta G^0_{f,i})_{products} - (\sum v_i \Delta G^0_{f,i})_{reactants}$$
$$= 85.8 - 12.05 = 73.75$$

$$\Delta H^0 = (\sum v_i \Delta H^0_{f,i})_{products} - (\sum v_i \Delta H^0_{f,i})_{reactants}$$
$$= 33.0 + 17.6 = 50.6$$

$$-RT \ln K_2 = \Delta G^0$$

$$K_2^0 = 1.16 \times 10^{-13}$$

$$\ln \frac{K^0}{K} = \frac{50.6}{8.31 \times 10^{-3}} \left(\frac{1}{T} - \frac{1}{298}\right)$$

20°C	T = 293 K	$K_{2,20} = 8.22 \times 10^{-14}$
40°C	T = 313 K	$K_{2,40} = 3.10 \times 10^{-13}$
60°C	T = 333 K	$K_{2,60} = 9.97 \times 10^{-13}$

The overall Mass Balance of Sulfur

Overall Mass Balance of Sulfur

Stripping Experiment #	1	2	3	4	5	6	7	8	9
CaS added (gm)	0.9326	0.9354	0.9361	1.832	1.0892	1.0984	1.3923	1.3954	1.3948
S added (mg)	414.49	415.73	416.04	814.22	484.09	488.18	618.80	620.18	619.91
S stripped out (in the form of H2S, mg)	395.95	472.91	459	874.1	608.2	603.2	691.57	756	754.32
Remaining Sulfur in the solution (gm)	0.0106	0.0041	0.0054	0.0251	0.0035	0.0075	0.0043	0.0013	
Error (%)	-1.91534	14.73942	11.62269	10.43668	26.36109	25.09787	12.45475	22.11015	21.68196

Stripping Experiment #	10	11	12	13	14	15	16	17	18
CaS added (gm)	0.559	0.5589	0.5599	1.0994	1.0992	1.0942	1.3957	1.396	1.3901
S added (mg)	248.44	248.40	248.84	488.62	488.53	486.31	620.31	620.44	617.82
S stripped out (in the form of H2S, mg)	296.84	310.31	302.4	559.8	515.45	545.3	700.36	626.4	472.1
Remaining Sulfur in the solution (gm)				0.0134	0.0043	0.00562	0.0242	0.0242	
Error (%)	19.47943	24.92351	21.5217	17.30944	6.389874	13.28551	16.8059	4.860315	-23.5864

Stripping Experiment #	19	20	21	22	23	24	25	26	27
CaS added (gm)	0.9115	0.9344	0.9363	1.8281	1.8253	1.0982	1.3911	1.3941	1.3928
S added (mg)	405.11	415.29	416.13	812.49	811.24	488.09	618.27	619.60	619.02
S stripped out (in the form of H2S, mg)	403.5	437.8	286.8	709.2	667.6	672.8	640.1	599.7	476.8
Remaining Sulfur in the solution (gm)									
Error (%)	-0.3977	5.420591	-31.0798	-12.7127	-17.7067	37.84374	3.531378	-3.21175	-22.9753

PHASE 3

Calculation of Residence Time in Reactor

inner diameter of reactor: 1-1/4" (3.17 cm)

length of reactor l = 13.5" (34.29cm)

cross-section area of reactor A $= 1/4\ \pi\ d^2$

$= 1/4\ \pi \times 3.17^2 = 7.89\ cm^2$

CO_2 flow rate F (lpm)

velocity v = F/A

residence time in the reactor t = l/v

F (lpm)	0.3	0.5	1.0	1.5	2.0
v (cm/min)	38.0	63.4	126.7	190.1	253.5
t (sec)	54.0	32.5	16.3	10.8	8.1

Appendix C: Calculation of Theoretical Conversion

$$H_2S \quad \Leftrightarrow \quad H_2 \quad + \quad \tfrac{1}{2}\, S_2$$

$$H_2S_i - x \qquad x \qquad \tfrac{1}{2}\, x$$

$$CO_2 \quad + \quad H_2 \quad \Leftrightarrow \quad H_2O \quad + \quad CO$$

$$(CO_2)_i - y \qquad x - y \qquad y \qquad y$$

total # of moles $= H_2S_i - x + x + \tfrac{1}{2}\, x + (CO_2)_i - y + x - y + y + y$

$$= H_2S_i + (CO_2)_i + 3/2\, x$$

$$H_2S \text{ mole fraction} = y_{H_2S} = \frac{H_2S_i - x}{H_2S_i + CO_{2_i} + 3/2x}$$

solving for x:

$$x = \frac{H_2S_i - y_{H_2S}(H_2S_i + CO_{2_i})}{1 + 3/2\, y_{H_2S}}$$

for stoichiometric ratios of H_2S:CO_2, the equation becomes:

$$x = \frac{1 - 2y_{H_2S}}{1 + 3/2\, y_{H_2S}}$$

Appendix D: Derivation of Equation for Specific Rate Coefficient

General rate equation:

$$r = -\kappa\left(\frac{P}{RT}\right)^2\left(\frac{1-x}{2+3/2x}\right)^2$$

Substituting r into the design equation for a plug flow reactor gives:

$$\frac{A}{F} = \frac{aV}{F} = -\int \frac{dx}{-\kappa\left(\frac{P}{RT}\right)^2\left(\frac{1-x}{2+3/2x}\right)^2}$$

$$\frac{A}{F} = \frac{1}{\kappa\left(\frac{P}{RT}\right)^2}\int\left(\frac{2+3/2x}{1-x}\right)^2 dx$$

$$\kappa = \frac{F}{A\left(\frac{P}{RT}\right)^2}\int\left(\frac{2+3/2x}{1-x}\right)^2 dx$$

$$\int \frac{(a+bx)^m}{(a'+b'x)^n}dx = -\frac{1}{(n-1)b'}\left[\frac{(a+bx)^m}{(a'+b'x)^{n-1}} - mb\int\frac{(a+bx)^{m-1}}{(a'+b'x)^{n-1}}dx\right]$$

$$\int \frac{(a+bx)}{(a'+b'x)}dx = \frac{bx}{b'} + \frac{ab'-a'b}{(b')^2}\ln(a'+b'x)$$

Therefore,

$$\int \frac{(2+3/2x)^2}{(1-x)^2}dx = \frac{(2+3/2x)^2}{(1-x)} - 3\int \frac{(2+3/2x)}{(1-x)}dx$$

$$= \frac{(2+3/2x)^2}{(1-x)} - 3[-\frac{3}{2}x - \frac{7}{2}\ln(1-x)]$$

$$= [\frac{(2+3/2x)^2}{(1-x)} + \frac{9}{2}x + \frac{21}{2}\ln(1-x)]$$

implementing the limits from 0 --> x to the above equation gives:

$$= \frac{(2+3/2x)^2}{1-x} + \frac{9}{2}x + \frac{21}{2}\ln(1-x) - 4$$

Therefore,

$$\kappa = \frac{F}{A(\frac{P}{RT})^2}[\frac{(2+3/2x)^2}{1-x} + \frac{9}{2} + \frac{21}{2}\ln(1-x) - 4]$$

In performing the above calculations, the following assumptions were made:

- the amount of sulfur-containing side products was negligible therefore the sulfur contained in the H_2S was converted only to elemental sulfur
- the sulfur product formed consisted entirely of S_2
- the gases were ideal

- the reactor was isothermal

- the reactor was a plug flow reactor

- the reactor was operating at steady state

- the H_2S decomposition reaction was a second order reaction

- neither the reduction nor the sulfidation changed the surface area of the catalyst

Appendix E: Calculation of Retention Time in Catalyst Bed

H_2S flow rate:0.2 cfh

CO_2 flow rate:0.2 cfh

inner diameter of reactor:1 in.

length of catalyst bed:4 in.

Total volumetric flow rate = 0.4 cfh

Cross-sectional area of reactor = $\prod r^2$

= $\prod (0.5 \text{ in})^2$

= 0.785 in^2

$$\frac{0.4 ft^3}{hr} \times \frac{1\ hr}{3600\ s.} \times \left(\frac{12 inches}{ft}\right)^3 \times \frac{1}{(0.785')^2} = 0.24 inch/s.$$

$$\frac{4 inches}{0.24 inch/s.} = 16 \text{sec. } retention\ time$$